AN ABSTRACT OF THE THESIS OF

Luca A. Adelfio for the degree of Master of Science in Water Resources Science presented on April 21, 2016

Title: Geomorphic and Climatic Controls on Water Temperature and Streambed Scour, Copper River Delta, Alaska: Implications for Understanding Climate Change Impacts to the Pacific Salmon Egg Incubation Environment

Abstract approved:

_____

Steven M. Wondzell

Pacific salmon (*Oncorhynchus* spp.) face numerous challenges associated with climate change. Most research has emphasized the potential effects of elevated summer water temperatures; however, climatic changes are also projected to significantly alter incubation and rearing habitats during the late autumn, winter, and spring months ("the incubation period"). Along the southern coast of Alaska, projected climatic changes include increases in the frequency of above freezing winter temperatures and reductions in low elevation snowpack. These changes are expected to impact the hydrology of salmon streams by increasing both water temperatures and the magnitude and frequency of winter floods.

Projected increases in water temperature may accelerate embryo development, impacting juvenile viability. More powerful and more frequent winter floods could reduce the survival of salmon eggs by increasing streambed scour. Here, I investigate climatic and geomorphic controls of water temperature and potential scour depth at salmon spawning and rearing sites on the Copper River Delta, a large coastal foreland in Southcentral Alaska.

In chapter 2, I utilized surface water temperature data collected at 18 sites to test the abilities of regression models to project year-round water temperature metrics based on catchment characteristics (elevation, slope, area, percent lake area) and air-water

temperature correlations. Considerable variability in water temperature was observed on spatial and temporal scales. Both temperature maxima and the frequency of freezing conditions were positively correlated with percent lake area and negatively correlated with catchment elevation and slope. Sites with upwelling groundwater and sites with high-relief, high elevation catchments exhibited lower thermal sensitivity and water temperatures are anticipated to be less impacted by projected climatic changes.

In chapter 3, I utilized surface and streambed water temperature data collected at 8 spawning sites to compare water temperatures during incubation periods under climatological mean ("severe winter") and anomalously warm ("mild winter") conditions. I also collected stream stage and channel geometry data at a subset of 3 sites and calculated streambed scour at bankfull discharge. The magnitude and seasonality of accumulated thermal units (^{o}C/day) (ATU) within spawning gravels varied significantly between severe and mild winters at shallow flowpath sites, but not at upwelling groundwater sites. When seasonal snow and ice was absent, increases in spring ATU at shallow flowpath sites were particularly significant. Modelled mean scour depths varied from 3 to 72 cm, suggesting the impacts of scour on egg mortality will be variable across the landscape. I conclude that the impacts of projected climatic changes are likely to vary in magnitude across the Copper River Delta, even at small spatial scales, due to heterogeneity in climatic and geomorphic controls.

Geomorphic and Climatic Controls on Water Temperature and Streambed Scour, Copper River Delta, Alaska: Implications for Understanding Climate Change Impacts to the Pacific Salmon Egg Incubation Environment

by

Luca A. Adelfio

A THESIS

submitted to

Oregon State University

in partial fulfillment of

the requirements for the

degree of

Master of Science

Presented April 21, 2016

Commencement June 2016

Master of Science thesis of Luca A. Adelfio presented on April 21, 2016

APPROVED:

Major Professor, representing Water Resources Science

Director of the Water Resources Graduate Program

Dean of the Graduate School

I understand that my thesis will become part of the permanent collection of Oregon State University libraries. My signature below authorizes release of my thesis to any reader upon request.

Luca A. Adelfio, Author

ACKNOWLEDGEMENTS

I greatly appreciate the support provided by my colleagues at the Chugach National Forest, Cordova Ranger District. D. Kuntzsch, K. Hodges, R. Skorkowsky, and T. Tanner afforded me a flexible work schedule while I attended classes. A. Morin, S. Meade, R. Ertz, A. Gottshall, A. Lorenz, and A. Morse provided critical assistance in the field. The Corvallis Forestry Sciences Lab became a home away from home. Thank you B. Hansen and K. Christiansen for helping me feel welcome and for assisting me with logistics. Collaborating with my fantastic committee was one of the most rewarding parts of graduate school. This project would not have been possible without Gordie Reeves' leadership, hard work, and boundless energy. Nate Mantua provided valuable guidance both in the field and in front of the computer. I cannot imagine a better advisor than Steve Wondzell. I am very fortunate to consider him both a mentor and a friend. Finally, thank you Chantel for unwavering love and support throughout this process.

TABLE OF CONTENTS

TABLE OF CONTENTS (Continued)

LIST OF FIGURES

LIST OF FIGURES (Continued)

Figure Page

LIST OF FIGURES (Continued)

Figure Page

LIST OF TABLES

LIST OF TABLES (Continued)

Table Page

LIST OF APPENDIX FIGURES

LIST OF APPENDIX TABLES

1 An Introduction to the Geomorphology, Climatology, and Hydrology of the Copper River Delta, Alaska

1.1 Water Temperature and Salmon- An Overview

Water temperature drives many biological processes, including salmon egg incubation rates. Pacific salmon (*Oncorhynchus* spp.) eggs incubate within a matrix of benthic substrates (hereafter "the shallow streambed"). In most environments, Pacific salmon embryos incubate throughout the autumn (ON) and winter (DJF) months, ensuring juveniles emerged from the gravel during the spring (MAM) when food resources are increasing in abundance. Incubation duration is sensitive to small changes in temperature. Even 1-3°C increases in incubation period water temperature may shorten development times by weeks or even months [*Murray and McPhail*, 1988; *Beacham and Murray*, 1990]. Thus, an increase in mean shallow streambed temperature may accelerate emergence timing, potentially impacting juvenile viability [*Shepard et al.*, 1986; *Leppi et al.*, 2014].

Surface air temperatures across the native North American range of Pacific Salmon are projected to increase by 3-5°C within the next 60 years, based on mid-range emissions scenarios [*Romero-Lankao et al.*, 2014; *Shanley and Albert*, 2014; *University of Alaska*, 2015]. Quantifying the relationship between atmospheric conditions and water temperature is critical to assess how climate change will impact salmon spawning and rearing success [*Mote et al.*, 2003; *Mantua et al.*, 2010].

The sensitivity of water temperature to atmospheric conditions is largely controlled by topography, discharge, and water exchanges through the streambed [*Poole and Berman*, 2001; *Caissie*, 2006; *Wawrzyniak et al.*, 2013]. On catchment and regional scales, these factors are governed by geomorphology, which can exhibit considerable spatial heterogeneity. Consequently, water temperature exhibits significant variability, particularly in landscapes with complex flowpaths and multiple water sources [*Kelleher et al.*, 2012].

Innovative studies [e.g. *Mantua et al.*, 2010; *Lisi et al.*, 2013, 2015; *Fellman et al.*, 2014] have increased our understanding of how water temperatures in salmon-producing

catchments are impacted by interactions between climate and geomorphology. These studies, however, have largely focused on surface water temperature data collected during the summer. More research is needed to assess the sensitivity of shallow streambed temperatures to atmospheric conditions during the incubation period [*Zimmerman and Finn*, 2012], particularly in regions with complex geomorphology.

To this end, I collected and analyzed year-round surface water and shallow streambed temperature data at known salmon spawning sites in the Copper River Delta Region, a spatially heterogeneous landform in Southcentral Alaska.

This chapter provides an introduction to what is known about water sources and flowpaths in the study area. Water sources, residence times, and flowpaths are controlled by climate and geomorphology, so this chapter first introduces the study site and describe former and active geomorphologic processes. Next, this chapter describes present-day hydrology and climate at the study area, introduce potential impacts of climate change on water temperatures, and conclude with study questions.

1.2 The Copper River Delta

The Copper River Delta (CRD) extends along 80 km of Gulf of Alaska coastline, adjacent to the southern piedmont of the Chugach Mountains (Figure 1.1). The CRD is protected as "critical habitat" for fish and wildlife and is reputed to be the largest wetland on the Pacific Rim of North America [*Thilenius*, 1990b; *Bryant*, 1992; *Boggs*, 2000]. The CRD supports healthy runs of coho and sockeye salmon that are critically important to the economy, culture, and ecology of the region [*Christensen*, 2000].

The CRD includes both marine and subaerial (above eustatic sea level) habitats. In the marine environment, the CRD is characterized by extensive tidal flats, barrier islands, and an actively prograding delta front [*Reimnitz*, 1966; *Galloway*, 1976]. The substrate is primarily sand and silt and is too finely textured to be utilized by spawning salmon. The subaerial deltaic plain is utilized by Pacific salmon and will be the focus of this chapter.

The subaerial deltaic plain grades into the Chugach piedmont. Surficial geology in the piedmont is primarily composed of sedimentary rocks (Orca Group) with localized

granodiorite intrusions [*Reimnitz*, 1966; *Winkler et al.*, 1992]. These layers are underlain with basalts of the late Paleocene or early Eocene age [*Winkler et al.*, 1992]. Peak elevations in the southern piedmont are around 2,300 m. The soil mantle is composed of shallow till or peat on the hillslopes. Deposits of colluvium and glaciofluvial drift are present in the valleys. The largest valleys are high-relief (1,500 m on average) and glaciated [*Barclay et al.*, 2013]. Five valley glaciers ("the proximal glaciers") terminate on the CRD between 50 and 120 m in elevation (Table 1.1).

Deposition from these proximal glaciers covers much of the 1,000 km^2 subaerial deltaic plain, and this portion of the CRD effectively functions as a low-relief glacial foreland. The substrates are a heterogeneous mix of coarse glacigenic sand and gravel and fine organic materials in abundant peatlands and marshes [*Reimnitz*, 1966; *Galloway*, 1976]. Below the piedmont glacial valleys, thick layers of gravels enable phreatic storage and provide excellent spawning habitat for salmon.

The CRD is a Holocene landform, the 450 km^3 deltaic pile has formed entirely during the last 10,000 years. The deltaic pile is largely composed of glaciofluvial sand and silt and has an average thickness of 180 m [*Reimnitz*, 1966]. It is actively prograding seaward today [*Jaeger et al.*, 1998]. The structure and morphology of this feature are controlled by 1) the supply of glacigenic sediments distributed by the Copper River and proximal glaciers [*Reimnitz*, 1966; *Barclay et al.*, 2013], 2) reworking in the high energy marine environment [*Galloway*, 1976], and 3) tectonic activity [*Plafker*, 1990].

1.2.1 Glacigenic Sediments from the Copper River

The Copper River has the second highest mean annual discharge (1625 m^3s^{-1}) [*Brabets*, 1997] and the highest mean annual suspended-sediment load (70 million tons) in Alaska [*Milliman and Meade*, 1983; *Jaeger et al.*, 1998], despite having the state's sixth largest catchment area (62,960 km^2). The Copper River distributes disproportionate quantities of meltwater and sediment due primarily to seasonal ablation and erosion associated with glacial activity [*Kargel et al.*, 2014].

The Copper River catchment is flanked by the Alaska Range and the Wrangell St. Elias, Chugach, and Talkeetna Mountains. Peak elevations exceed 4,000 m and 18% of the

catchment is glaciated [*Kargel et al.*, 2014]. The combination of high-relief terrain and abundant snowfall maintains wet-based glaciers which move relatively rapidly and generate atypically large quantities of sediment [*Jaeger et al.*, 1998; *Kargel et al.*, 2014].

The sediment transported to the CRD by the Copper River is primarily fine sand and silt [*Jaeger et al.*, 1998]. These materials compose the deltaic platform, however, the surficial geology of the subaerial CRD includes coarser sand and gravel from the proximal glaciers [*Barclay et al.*, 2013] as well as finer organic materials due to vegetative growth and succession [*Reimnitz*, 1966].

1.2.2 Marine Reworking

Glacigenic sediments from the Copper River are re-distributed by tidal action, westerly longshore currents, and large storms, resulting in the CRD's long and asymmetric (relative to the river mouth) shape [*Galloway*, 1976]. Tidal range in Orca Inlet (near Cordova) averages 3.5 m but can exceed 6.5 m during the highest spring tides. Westerly longshore currents are powered by prevailing winds over the Gulf of Alaska and transport Copper River sediments as far as 100 km west of the river mouth [*Jaeger et al.*, 1998]. Storms are common over the Gulf of Alaska, particularly during the fall, winter, and spring months, and are characterized by high winds and large swell that greatly impacts the CRD deltaic front [*Galloway*, 1976]. Marine reworking of the deltaic sediments smoothed the formerly irregular and steep coastline, enabling the proximal glacier outwashes to grade over the subaerial CRD [*Reimnitz*, 1966].

1.2.3 *Tectonics*

The Copper River catchment is located near the Aleutian subduction zone, a seismically active thrust fault boundary [*Grantz et al.*, 1964]. Tectonic processes at this fault are responsible for the orogenic mountain ranges present in coastal Alaska. Similar to other tectonically-active regions, these mountains have high erosion and sediment production rates [*Jaeger et al.*, 1998].

Subduction zone earthquakes have impacted sedimentation on the CRD directly and indirectly. Direct impacts include landslides that have deposited colluvial materials in piedmont valleys and the adjacent outwash plain [*Tuthill and Laird*, 1966; *Waller*, 1966]

and co-seismic tsunamis and seiches that re-distributed sediments in the marine environment [*Reimnitz*, 1966]. Mega-thrust earthquakes indirectly impact sedimentation on the CRD by elevating the land surface relative to sea level.

Plafker [1990] used sediment cores from the subaerial CRD to identify nine co-seismic uplift events in the last 5,600 years. Each event resulted in a 0.8 m to 2.4 m uplift with recurrence intervals of a 300-950 years. On the low-relief CRD, these sudden shifts in surface elevation greatly reduced the extent of tidal influence, resulting in major vegetation and land surface changes. The most recent event occurred in 1964 and will be discussed further in section *1.3.4*.

Tectonic ("crustal") subsidence averages 7 mm yr^{-1} between co-seismic uplift events [*Plafker*, 1990]. As a result, the CRD experiences net submergence over time. Buried marsh and tidal flat deposits are present 8-20 m below the surface of the subaerial CRD near the Scott and Sheridan glacial outwashes [*Reimnitz*, 1966], providing record of submergence events and contributing to subsurface heterogeneity. Stumps and freshwater marsh materials were also buried in situ across the subaerial CRD [*Tarr and Martin*, 1914; *Reimnitz*, 1966; *Plafker*, 1990], adding further complexity to subsurface water flowpaths.

Co-seismic uplift and gradual inter-seismic subsidence greatly influence geomorphic processes on the seaward fringe of the subaerial delta while glacial processes are dominant on the foreland [*Barclay et al.*, 2013], including in the habitats where salmon spawning occurs. Here, surficial processes that govern subsurface flowpaths have been heavily influenced by the Pleistocene and Holocene advances of proximal glaciers.

1.2.4 *Pleistocene Glaciation*

The Copper River has bisected the Chugach Mountains and discharged directly into the Gulf of Alaska for approximately the last 10,000 years. During the prior 50,000 years, however, the Chugach Mountains were more heavily glaciated and the river's corridor through the Chugach range was filled with 750 m of ice [*Reimnitz*, 1966], effectively damming most of the Copper River's catchment and forming the 9,000 km^2 proglacial Lake Atna [*Wiedmer et al.*, 2010]. The present-day location of the CRD was covered with 500 m of ice [*Tarr and Martin*, 1914]. Eustatic sea level was over 100 m below current levels and

the glaciers likely extended at least 20 km beyond the present-day barrier islands [*Reimnitz*, 1966].

1.2.5 *Holocene Glaciation*

Glaciers have generally retreated during the Holocene, enabling Lake Atna to drain down the Copper River's corridor through the Chugach Range; however, periodic Holocene glacial advances have been documented in the study area and globally. Barclay et al. [2013] documented glacial advance and retreat on the subaerial CRD during the last 2,000 years. Their reconstruction of Sheridan Glacier's late Holocene activity is one of the most complete records worldwide of glacial activity during the last 2,000 years. Sheridan Glacier has advanced four times during the late Holocene (530s to 640s, 1240s to 1280s, 1510s to 1700s and 1810s to 1860s). The last three advances were during the Little Ice Age. The last two advances were also recorded at Scott, Sherman, and Saddlebag glaciers.

The Little Ice Age advances played an important role in shaping the surficial geology of the subaerial CRD. The glaciers pushed moraines as they advanced. The moraines forced melt water to move laterally across the outwash plain, spreading glaciofluvial material ("drift") over nearly the entire subaerial CRD [*Barclay et al.*, 2013]. Unlike the morainal tills, drift is generally well-sorted, creating layers of coarse substrates that are well-drained and layers of finer substrates that are poorly-drained. On the CRD, the poorly-drained regions promote peat-formation while the well-drained regions enable phreatic water storage. The well-drained regions tend to be located directly down-valley from piedmont glaciers where the drift materials are thickest [*Galloway*, 1976].

1.2.6 Driftless Area

There is a small driftless area on the CRD, between the Saddlebag and Sheridan glaciers [*Tarr and Martin*, 1914; *Reimnitz*, 1966]. Due to glacial geometry, this area remained largely unglaciated during the Pleistocene and the Holocene, as evidenced by the presence of "seastacks" (also referred to locally as "haystacks"), which are vertical rock formations that were shaped by waves, not by ice. Coarse glacial drift is absent around these seastacks, the land surface elevation is low, and tidal influence extended all the way to the piedmont before the 1964 co-seismic uplift. As a result, the surficial materials are

fine-grained marine sediments that are poorly drained. Angular gravel is present where high energy piedmont streams intersect the CRD and coho salmon spawn in these areas, but water flowpaths are likely different than in the outwash gravels, adding further heterogeneity to present-day hydrologic processes.

1.3 *Hydrology and Climate*

The study region includes most of the subaerial CRD and the adjacent piedmont front and is defined as the 2950 km^2 area within 15 National Hydrography Dataset (NHD, www.usgs.gov) HUC 12 catchments (Table 1.2). Catchment elevations range from sea level to over 1700 m and over 1000 m of relief is typical. Catchment geometries are not uniform and mean catchment elevations ranges from 19 m to over 600 m (Figure 1.2).

Land Cover

Based on NHD figures, lakes and pond coverage ranges from 0 to 19% and ice coverage ranges from 0 to 17% of the HUC unit land areas (Table 1.2). NHD stream layers are incomplete for this region, but small streams are numerous in the piedmont and on the glacial outwash. Glacial meltwater distributaries cross the CRD and discharge into tidal sloughs on the lowest reaches of the subaerial CRD.

Perennial snow and ice is prevalent in the large glacial valleys and is present above 1100 m elsewhere. Two general types of lakes are present in the study area 1) proglacial lakes located between glacial ice and Little Ice Age moraines and 2) clear-water lakes that form along lateral outwash margins between piedmont slopes and outwash materials. Ponds are prevalent in both the uplifted marsh region and in the driftless area. Ponds are also present on the outwash plain in locations where beavers (*Castor canadensis*) are present [*Cooper*, 2007].

National Land Cover (www.mrlc.gov) data indicate human developments within the study region are limited except for residential development along Eyak Lake and River, government and commercial infrastructure at the Mudhole Smith Airport ("the airport"), paved highway between the airport and Cordova, and <100 km of gravel roads elsewhere.

Woody wetlands, shrub/scrub, and evergreen forests cover most land surfaces (Table 1.3). Barren bedrock surfaces are prevalent above 1000 m.

Surficial geology is characterized by bedrock and till on piedmont slopes, colluvium and drift in unglaciated piedmont valleys, drift and till on the outwash plain, and marine sediments on the uplifted marsh (Figure 1.3 and Table 1.4).

1.3.1 Climate

The climate is cool and wet and is characterized as maritime. Based on 1980-2010 climate records, the monthly average maximum air temperatures ranges from 16 °C (August) to 1 °C (January) and the monthly average minimum air temperatures ranges from 8 °C (July) to -5 °C (January) (Figure 1.4). Measureable precipitation occurs 220 days per year. Annual precipitation averages 235 cm per year at the airport (13 m above sea level), but considerably more precipitation is likely to accumulate in localized areas and at higher elevations. Monthly precipitation at the airport ranges from 13 cm (June) to 34 cm (September) (Figure 1.5) and precipitation may fall as rain any day of the year. Snowfall is also common from October until May (Figure 1.6) and normal snowfall exceeds 250 cm per year. A shallow (<30 cm) snowpack is usually present at sea level from November until May [*Reimnitz*, 1966] while deeper snowpacks (>3m) accumulate in the mountains and persist throughout the summer months [*Kargel et al.*, 2014].

Cold and dry continental air masses periodically influence the study area during the late fall, winter, and early spring months. Temperatures below -20 °C have been recorded most days between early November and late March (Figure 4). These influences are particularly pronounced down valley from the Copper River Canyon, where a local gap wind transports cold interior air onto the CRD due to gravity- and pressure gradient-induced air flows [*Reimnitz*, 1966]. The pressure difference is due to prevailing high pressure north of the Chugach Mountains and low pressure over the Gulf of Alaska. Along the Copper River, winds in excess of 150 km hr^{-1} have been recorded during the fall, winter, and spring months [*Reimnitz*, 1966]. In addition to transporting cool interior air, these winds redistribute snow and sand and have created a large dunes where the Copper River

bisects the CRD, adding further complexity to the region's geomorphology [*Reimnitz*, 1966; *Galloway*, 1976].

1.3.2 *Streamflow*

The US Geological Survey (USGS) maintains two gage sites on the CRD, Copper River at Million Dollar Bridge (station ID 15214000) and Glacier River Tributary (station ID 15215900). Data are also available for two inactive USGS sites, Middle Arm Eyak Lake (station ID 15216003) and Power Creek (station ID 15216000). This section will not incorporate Copper River discharges but will introduce data from the three other sites that are more representative of the study streams (Table 1.5). Middle Arm Eyak Lake and Power Creek are both salmon spawning areas that are used as study sites in this project. Glacier River Tributary is located in a piedmont catchment adjacent to Sheridan Glacier. Although this site is not utilized by spawning salmon, the hydrograph is likely comparable to nearby piedmont streams that do provide spawning habitat.

Annual discharge increases exponentially with catchment area due to the positive correlation between catchment area, elevation, and total precipitation. Stream discharge is lowest in the late winter and early spring (JFM) in all three streams. The seasonality of maximum discharges varies with watershed size and elevation.

Power Creek has the largest and highest elevation catchment with rain, snow, and glacier melt water sources. The mean annual specific discharge was 0.49 mm hr^{-1} during the period of record. Mean monthly discharge ranges from 1.36 m^3s^{-1} (March) to 15.0 m^3s^{-1} (July). Snow and ice melt contribute to high late summer discharge rates. Peak discharges occur when early autumn storms coincide with snow and ice melt (September and October). Peak discharges exceeded 28 $m^3 s^{-1}$ each year of record and a maximum peak runoff of over 170 $m^3 s^{-1}$ (11.55 mm hr^{-1}) was recorded in September, 1993.

Middle Arm Eyak Lake is a steep piedmont catchment with rain and snow melt water sources. The gage record is short (2 years), but indicates monthly discharge ranges from 0.27 $m^3 s^{-1}$ (January) to 2.4 $m^3 s^{-1}$ (August). Mean annual specific discharge was 0.56 mm hr^{-1} during the period of record. Peak discharge was recorded in August 1993 and exceeded 28 $m^3 s^{-1}$ (13.44 mm hr^{-1}).

Glacier River Tributary is also a piedmont catchment with rain and snow melt water sources. After 4 years of record, mean discharge ranges from 0.11 $m^3 s^{-1}$ (March) to 1.0 $m^3 s^{-1}$ (September) and mean annual specific discharge is 0.31 mm hr^{-1}. Peak daily discharge occurred on September 16, 2012 and exceeded 6.3 $m^3 s^{-1}$ (4.00 mm hr^{-1}). USGS also monitors water temperatures at this site. Mean monthly water temperatures are lowest in March (0.7°C) and highest in August (7.5°C).

1.3.3 *Groundwater*

A 52 m deep well at the airport provides a glimpse into subsurface layering within the outwash gravels between Sheridan and Sherman Glaciers. Drill log records indicate interbedded silt, sand, gravel, and organic material between 3 and 20 m below the surface [*Dorava and Sokup*, 1994], suggesting heterogeneous hydraulic conductivity.

Alaska Department of Highways (ADOT) performed test borings on the CRD in 1963-1964, near the location of the present day Copper River Highway [*Reimnitz*, 1966]. Test borings were also performed in 1914 during railroad construction. These borings indicate that glaciofluvial gravels are prevalent in the upper layers of the subaerial CRD. Isolated logs indicate previous forest cover. Reimnitz [1966] reported ADOT borehole samples (n=30) had an average water content of 29.4%. The relatively low water content may be due to co-seismic compaction. Grain densities are 2.7 to 2.8 g cm^{-3} [*Reimnitz*, 1966].

Borings also indicate a widespread layer of dense silty sand between 8 and 17 m below present-day sea level. This layer is likely an old tidal flat and extends from Eyak Lake to the Copper River along the mountain front [*Reimnitz*, 1966]. Thus, this elevation is likely the basement of unconfined aquifers on the subaerial CRD.

1.3.4 *Impacts of the 1964 Earthquake*

The magnitude 9.2 "Good Friday" earthquake occurred on March 27, 1964 [*Grantz et al.*, 1964]. Co-seismic uplift on the CRD was measured between 1.8 and 3.4 m relative to tide line, but changes to the tidal prism likely add uncertainty to these measurements [*Reimnitz*, 1966; *Plafker*, 1990]. The uplift elevated the lowest reaches of the subaerial CRD above tidal influence ("the uplifted marsh"). The formerly *carex*-dominated salt marshes are now freshwater wetlands [*Thilenius*, 1990a]. Particle sizes are small and hydraulic

conductivity is low due to the organic marsh deposits [*Bryant*, 1992]. While the uplifted marsh is important habitat for birds and other wildlife, it is not suitable for spawning salmon.

Groundwater within the glacial foreland was affected by the earthquake. Co-seismic settling reduced pore space, forcing groundwater laden with sand and silt to flow to the surface [*Reimnitz*, 1966], but the extent of these impacts is unknown. The City of Cordova reported no noticeable effects to four city water supply wells in a 43 m thick deposit of glacial drift between Eyak Lake and Orca Inlet [*Waller*, 1966]. Eyak Lake, which recharges the aquifer, was uplifted 3 m, preventing saltwater intrusion. Artesian pressure in the aquifer fluctuates with the tides. Post-earthquake measurements (1964) indicated the tide and groundwater level were out of sync by 6 hours (e.g. groundwater pressure was low when the tide was high) [*Waller*, 1966].

The earthquake triggered widespread avalanching, rockfalls, and rockslides which transferred colluvium to piedmont valleys and the glacial foreland [*Reimnitz*, 1966; *Waller*, 1966]. One well-documented landslide during the 1964 earthquake deposited 78 $x10^6$ tons of rock onto the ablation zone of Sherman Glacier [*Tuthill and Laird*, 1966]. These materials are likely still reducing ablation rates today.

The 1964 earthquake provided a unique opportunity to observe the hydrologic impacts of a large tectonic disturbance. The impacts of previous disturbances (tectonic, marine, climatic, and glacial) to the CRD have been extrapolated from the geologic record. The sum of this evidence suggests that punctuated disturbances have played a critical role in the morphology of catchments on the subaerial CRD. Heterogeneity in catchment geometry, geology, and land cover likely results in catchment-scale differences in water sources and flowpaths, creating a hydrologically diverse landscape.

Despite these catchment-scale differences, Pacific Salmon, particularly Coho, spawn broadly across the CRD. Here and elsewhere across the Pacific Rim, salmon have exhibited a general ability to adapt to changing landscapes and climate conditions on geologic timescales [*Benda et al.*, 1992; *Smith et al.*, 2001; *Mote et al.*, 2003]; however, salmon have not exhibited resilience to anthropogenic disturbances [*Bisson et al.*, 2009; *Waples et al.*, 2009].

1.3.5 Climate Change Projections

Climate models project mean monthly air temperatures along the Gulf of Alaska coastline to increase 3-5°C by 2080, based on mid-range emissions scenarios (Figure 1.7) [*Romero-Lankao et al.*, 2014; *University of Alaska*, 2015]. The greatest magnitude of changes are anticipated during the winter (DJF) [*Hall*, 1988; *Romero-Lankao et al.*, 2014]. Mean DJF monthly air temperatures are projected to surpass the freezing point, greatly reducing low elevation snowpack and seasonal ice cover on waterways [*McAfee et al.*, 2014]. Meltwater from seasonal snow and ice is an important water source that contributes to discharge and significantly cools water temperatures throughout summer (JJAS) [*Kyle and Brabets*, 2001; *Neal et al.*, 2002; *Lisi et al.*, 2015] and recent research has also begun to shed light on the significance of these projected hydrologic changes during the salmon incubation period (Oct-May).

Warming autumn (ON), winter (DJF), and spring (MAM) air temperatures will likely impact the hydrology of the incubation environment in coastal Alaska by increasing both water temperature and the magnitude and frequency of winter freshets [*Leppi et al.*, 2014; *Shanley and Albert*, 2014; *Wobus et al.*, 2015].

These hydrologic changes are anticipated to influence the development and survival of salmon embryos, which incubate in the shallow streambed environment over the winter months. Increases in water temperature may accelerate embryo development, potentially impacting viability [*Holtby*, 1988; *Murray and McPhail*, 1988; *Braun et al.*, 2013]. Peak discharge was correlated with Coho salmon egg mortality at Carnation Creek, BC, likely due to increased scour [*Holtby and Healey*, 1986]. More powerful and more frequent winter freshets could reduce the survival of embryos by increasing streambed scour [*Battin et al.*, 2007; *Goode et al.*, 2013]. Fall-spawning Coho Salmon (*O. kisutch*) are expected to be particularly sensitive to these changes [*Bryant*, 2009; *Shanley and Albert*, 2014] and egg-to-fry survival is projected to be the most heavily impacted life stage [*Leppi et al.*, 2014]. However, the significance of these impacts are likely to exhibit spatial variation from catchment to sub-reach scales, particularly in landscapes with complex geomorphology [*Montgomery et al.*, 1999; *Shanley and Albert*, 2014; *Wobus et al.*, 2015].

1.4 Study Questions

In order to better understand changing conditions within Pacific salmon incubation habitats, the U.S.D.A. Forest Service (USFS) is monitoring surface (stream) water temperature year-round at 20 salmon spawning locations in 19 catchments across the CRD. Streambed water temperatures are monitored year-round at 15 of these sites in 14 catchments (Appendix A). To augment this dataset, I collected stage, discharge, and channel geometry data at a subset of 3 sites.

For this thesis, I utilized these data to assess spatial variability in salmon habitats across the CRD and to elucidate potential climate change impacts to the incubation environment. The next two chapters will be structured as independent journal articles and will address these questions:

Chapter 2:

Can simple regression models accurately project water temperatures across a landscape with spatially heterogeneous water flowpaths? Can a regression model developed under historically normal climate conditions accurately hindcast water temperatures during an anomalously warm year when low-elevation snowpack was absent?

Chapter 3:

How does winter severity impact accumulated thermal units in salmon incubation habitats? Do mild winter conditions increase streambed scour risk at salmon spawning areas on the CRD?

1.5 Figures

Figure 1.1 Copper River Delta Study Region, Southcentral Alaska.

Table 1.1 Geometry and terminus characteristics for the five glaciers that terminate on the CRD.

Proximal Glaciers to the CRD						
Name	Geometry		Terminus Description			
	Length (km)	Area (km^2)	Latitude	Longitude	Elevation (m)	Type
Martin River	44	349	60.47	-144.25	100	Lake
Scott	24	167	60.61	-145.38	110	Land
Sheridan	24	60	60.51	-145.35	50	Lake
Sherman	13	58	60.54	-145.21	120	Land
Saddlebag	8	8	60.48	-145.1	85	Lake

Table 1.2 National Hydrography Dataset zone statistics and waterbody areas for the study region.

HUC Zone Statistics								NHD Waterbody	
HUC12	NAME	km^2	meters					km^2	
		AREA	MIN	MAX	RANGE	MEAN	S.D.	Lake & Pond	Ice Mass
190201041707	Alaganik Slough-Frontal Gulf of Alaska	377.9	0	908	908	19	72	12.8	0.0
190201041704	Mirror Slough-Frontal Gulf of Alaska	253.2	-1	941	943	32	101	4.3	0.0
190201041703	Martin River Slough	118.9	-1	1037	1038	202	227	1.9	0.0
190201041603	Power Creek	54.1	16	1468	1452	620	314	0.0	6.4
190201041304	190201041304	159.7	10	1558	1548	145	232	0.6	1.6
190201041302	Goat Mountain	51.7	18	1329	1311	243	301	0.1	0.5
190201041503	Glacier River-Sheridan River	121.5	0	1145	1145	111	188	7.1	10.6
190201041305	Sheep Creek	97.6	8	1284	1276	194	259	0.6	0.4
190201041705	Outlet Copper River-Frontal Gulf of Alaska	847.5	0	1547	1547	36	124	8.2	16.4
190201041406	Outlet Martin River	83.9	5	787	782	94	144	4.5	0.0
190201041405	Martin Lake	80.2	27	971	945	211	186	8.3	0.0
190201041604	Eyak Lake	54.1	1	960	959	230	215	10.2	0.0
190201041605	Eyak River-Frontal Gulf of Alaska	425.7	0	1466	1466	157	270	12.9	3.0
190201041404	Headwaters Martin River	160.7	36	1702	1666	282	303	8.8	16.1
190201041706	Salmon Creek	63.6	1	1292	1291	395	335	2.8	10.7

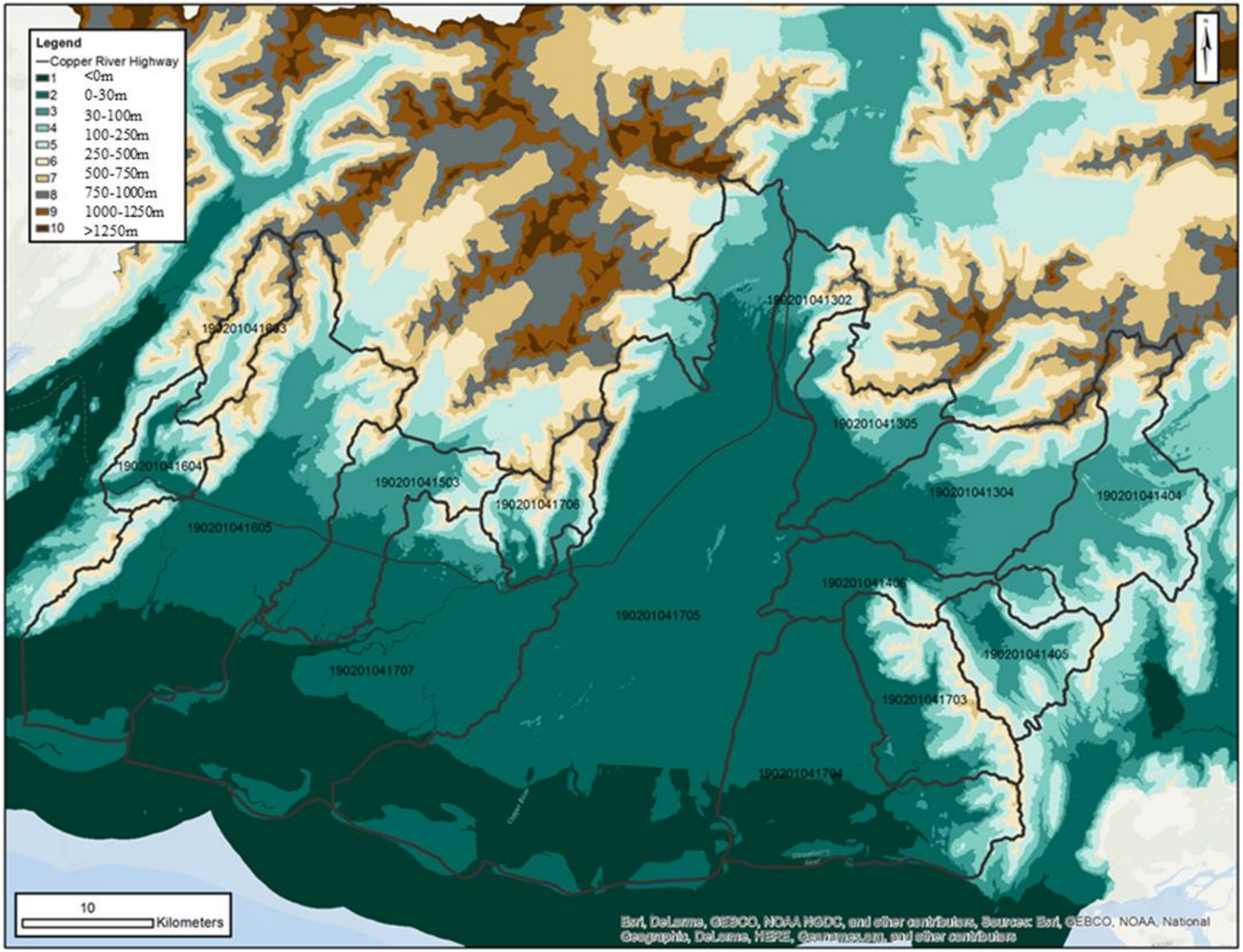

Figure 1.2 Map of HUC 12 units in the study area with elevation bands calculated from 5m IFSAR DEM.

Table 1.3 Percentage of selected land surface cover types calculated from National Land Cover data.

HUC12	NAME	(%) Percentage of HUC Area (%)									
		Developed intensity			Barren	Forested		Herbaceous		Wetland	
		Low	Medium	High		Deciduous	Evergreen	Shrub/ Scrub	Grassland/ Herbaceous	Woody Wetlands	Emergent Herbaceous
190201041707	Alaganik Slough-Frontal Gulf of Alaska	0.2	0.0	0.0	13.9	0.1	6.1	2.9	0.1	34.8	7.4
190201041704	Mirror Slough-Frontal Gulf of Alaska	0.0	0.0	0.0	8.5	0.1	8.5	3.8	0.0	44.3	8.4
190201041703	Martin River Slough	0.0	0.0	0.0	6.1	0.1	25.2	27.7	0.3	26.1	9.0
190201041603	Power Creek	0.2	0.0	0.0	33.1	0.0	23.1	25.7	0.4	0.3	0.0
190201041304	190201041304	0.0	0.0	0.0	3.8	0.1	23.5	19.8	0.7	32.7	12.9
190201041302	Goat Mountain	0.5	0.0	0.0	14.0	19.1	23.7	29.2	0.5	5.7	0.1
190201041503	Glacier River-Sheridan River	0.4	0.0	0.0	5.2	0.8	18.3	15.7	0.3	34.2	9.1
190201041305	Sheep Creek	0.0	0.0	0.0	7.1	0.8	19.2	31.5	1.1	31.6	2.4
190201041705	Outlet Copper River-Frontal Gulf of Alaska	0.1	0.0	0.0	18.0	0.8	2.5	8.0	0.2	13.0	3.6
190201041406	Outlet Martin River	0.0	0.0	0.0	1.2	0.0	18.7	12.1	1.1	59.1	2.6
190201041405	Martin Lake	0.0	0.0	0.0	3.7	0.3	28.2	42.1	0.9	13.2	1.1
190201041604	Eyak Lake	1.6	0.1	0.1	4.3	0.0	46.4	24.3	0.2	4.1	0.0
190201041605	Eyak River-Frontal Gulf of Alaska	0.2	0.1	0.0	19.7	0.1	12.9	15.1	0.4	21.0	7.8
190201041404	Headwaters Martin River	0.0	0.0	0.0	9.0	0.3	37.9	25.7	0.4	10.6	0.0
190201041706	Salmon Creek	0.0	0.0	0.0	14.0	0.2	33.2	23.7	0.3	4.3	0.0

Table 1.4 Percentages of land surface composed of selected surficial geology types as calculated from USGS data.

(%) Percentage of Land Surface (%)						
HUC12	NAME	Selected Geology Types				
		Surficial deposits (Quaternary)		Bedrock (Tertiary)		
		Till, marine, & eolian sediments	Drift & colluvium	Intrusive	Sedimentary	Volcanic
190201041707	Alaganik Slough-Frontal Gulf of Alaska	20.5	54.9	3.3	4.1	0.0
190201041704	Mirror Slough-Frontal Gulf of Alaska	26.2	53.6	0.0	9.8	3.5
190201041703	Martin River Slough	22.0	18.1	0.1	27.0	30.7
190201041603	Power Creek	2.9	11.3	7.5	18.1	38.0
190201041304	190201041304	22.6	47.6	7.0	0.1	19.2
190201041302	Goat Mountain	5.7	54.9	0.0	37.1	0.5
190201041503	Glacier River-Sheridan River	6.0	60.1	11.6	8.1	0.0
190201041305	Sheep Creek	2.7	55.2	1.3	27.5	9.4
190201041705	Outlet Copper River-Frontal Gulf of Alaska	10.5	38.7	0.0	4.5	0.3
190201041406	Outlet Martin River	0.1	67.9	0.0	18.1	9.4
190201041405	Martin Lake	9.2	14.8	0.0	53.0	11.3
190201041604	Eyak Lake	0.0	8.3	0.0	57.3	15.9
190201041605	Eyak River-Frontal Gulf of Alaska	0.0	60.9	0.0	30.7	0.0
190201041404	Headwaters Martin River	22.0	27.2	4.7	32.0	1.5
190201041706	Salmon Creek	4.4	14.4	1.5	56.4	0.0

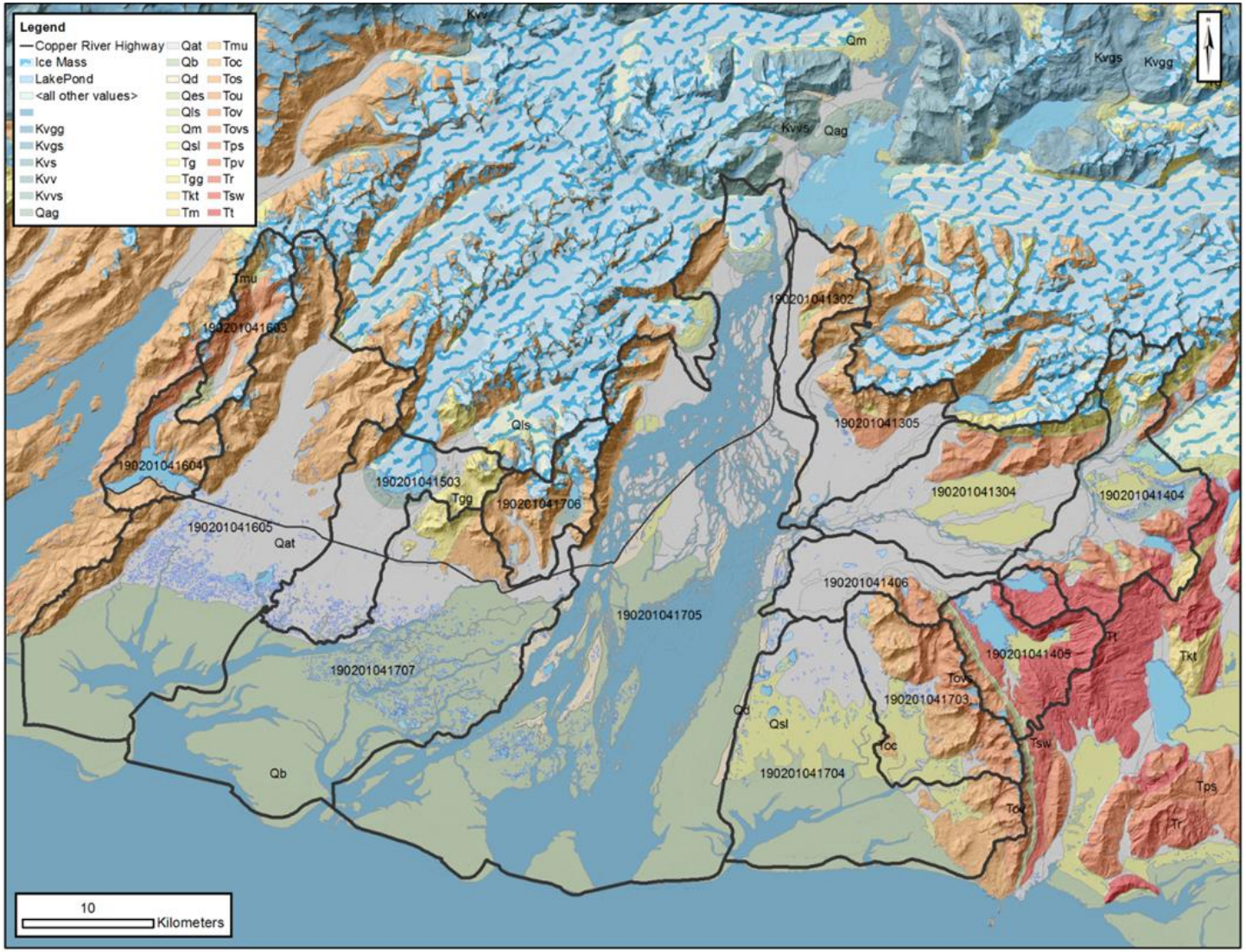

Figure 1.3 Surficial Geology of the study area. Glaciofluvial drift (Qat) is gray, marine sediment (Qb) are green. A complete key is available online: http://pubs.usgs.gov/sim/3110/sim3110_pamphlet.pdf.

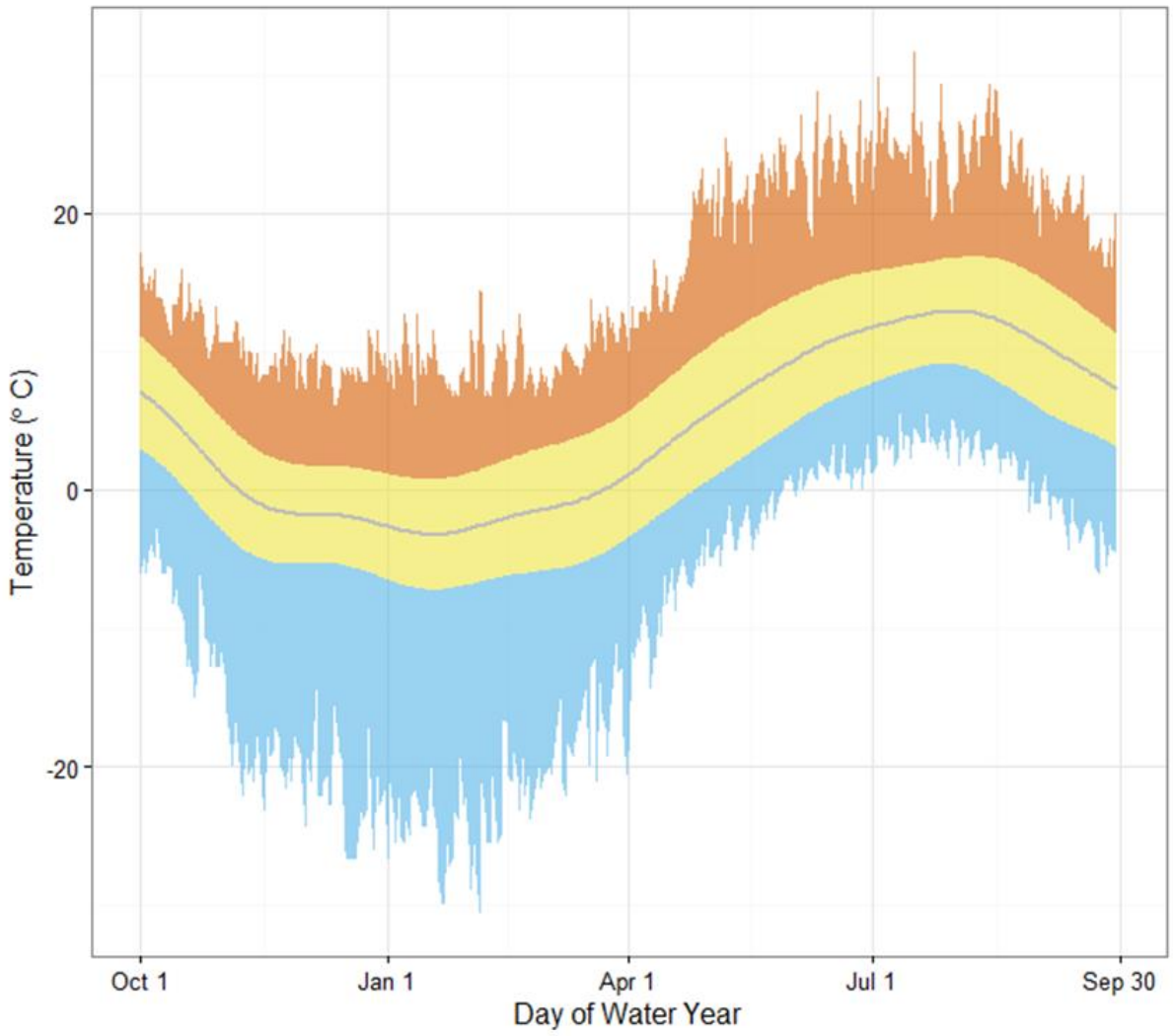

Figure 1.4 Mean (gray line), Normal (yellow band), and extreme (orange and blue bands) surface air temperatures based on 31 years of record (1980-2010) at the M.H. Smith Airport within the study area.

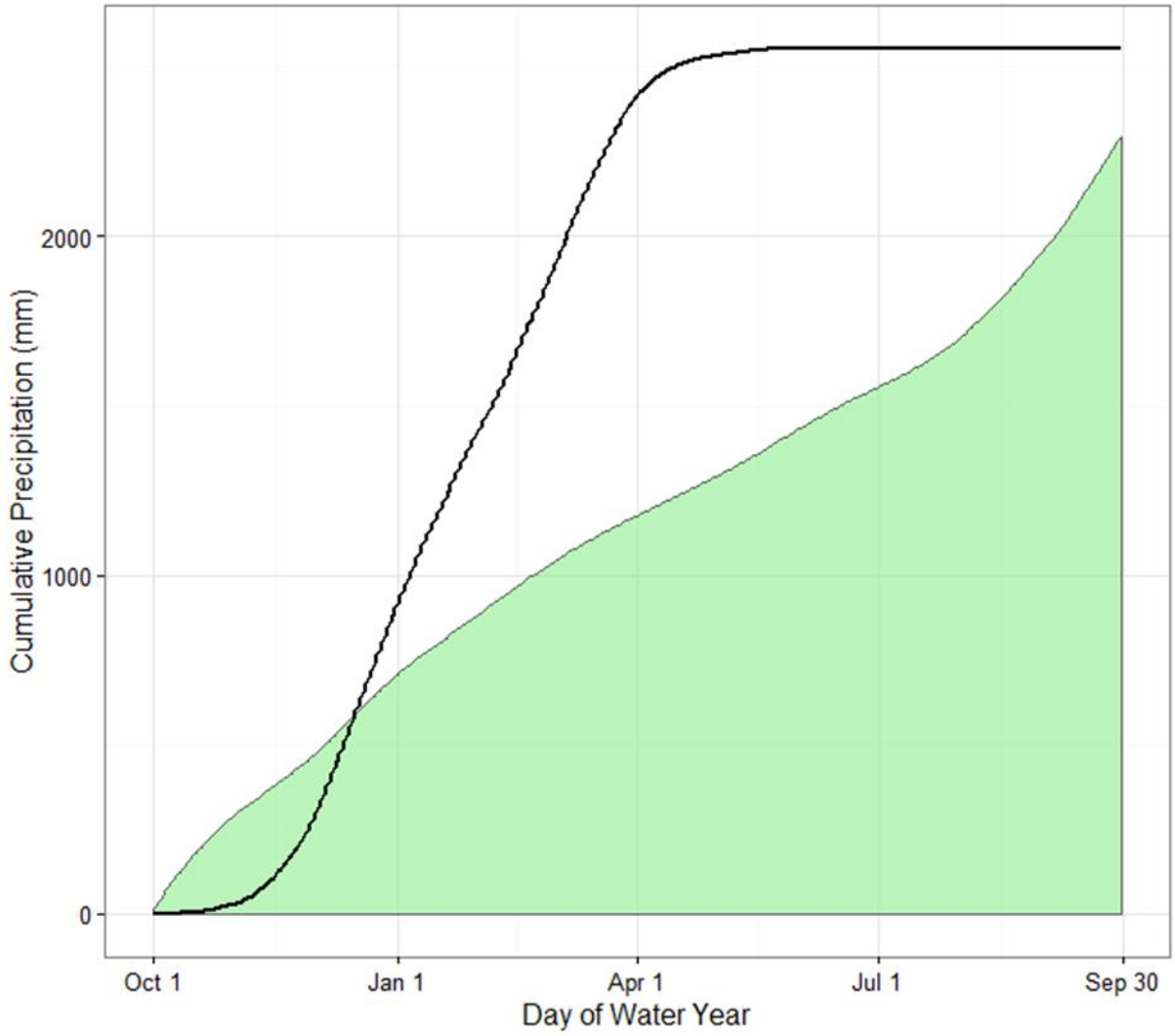

Figure 1.5 Cumulative mean daily precipitation (green ribbon) and cumulative mean daily snowfall (black line) based on 31 years of record (1980-2010) at the M.H. Smith Airport within the study area.

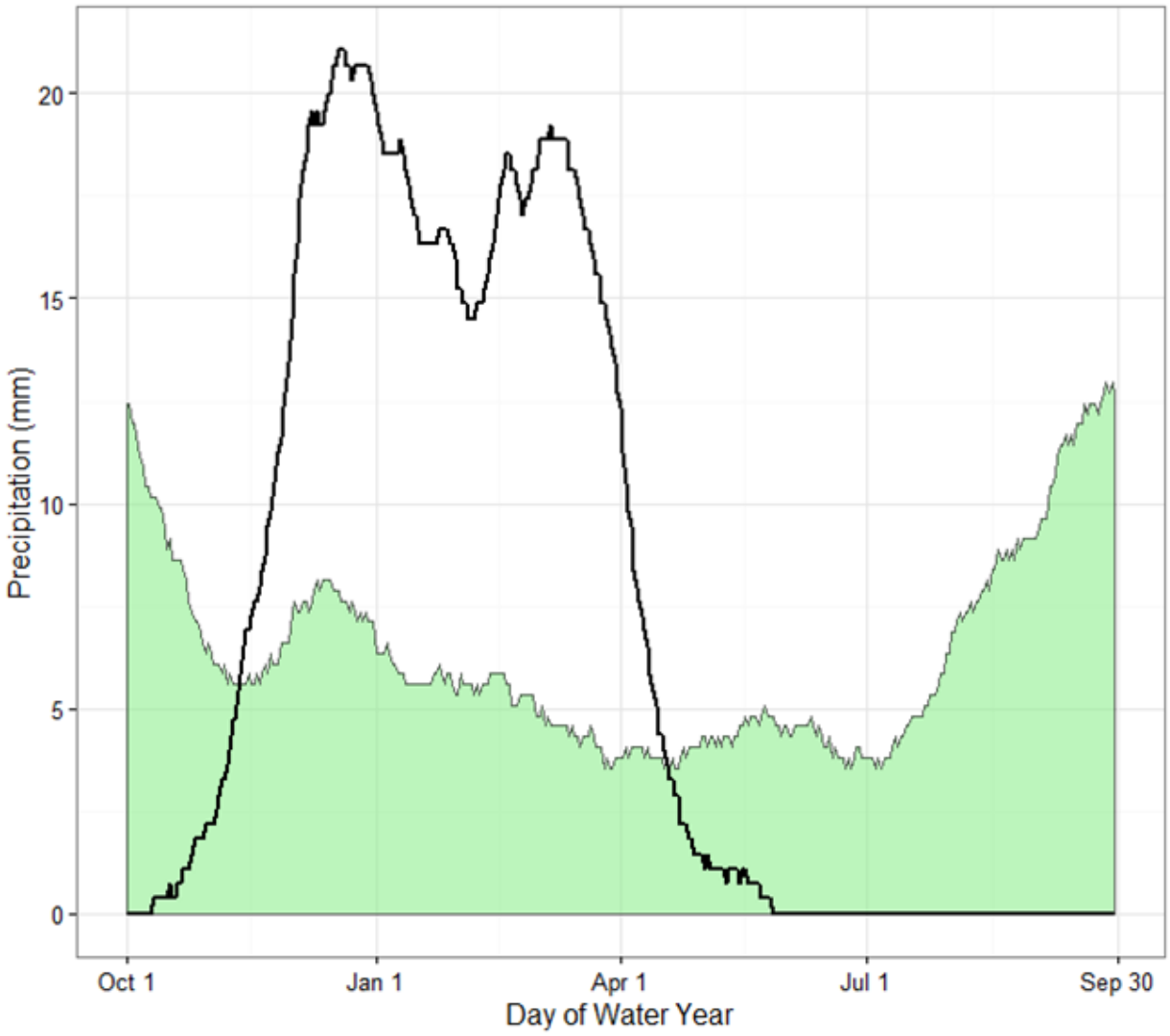

Figure 1.6 Climatological mean daily precipitation (green ribbon) and snowfall (black line) accumulation in millimeters based on 31 years of record (1980-2010) at the M.H. Smith Airport within the study area.

Table 1.5 Locations and statistics for U.S. Geological Survey streamgages located within the study area.

Station		NAD 27		Active	Years of	Catchment	Specific Discharge (mm hr^{-1})	
Name	ID	Latitude	Longitude	(?)	record	Area (km^2)	Mean	Peak
Glacier River Tributary	15215900	60° 32'00"	145° 22'43"	Yes	4	5.7	0.31	4
Middle Arm Eyak Lake	15216003	60° 33'29"	145° 37'44"	No	2	7.5	0.56	13.44
Power Creek	15216000	60° 35'14"	145° 37'05"	No	48	53	0.49	11.55

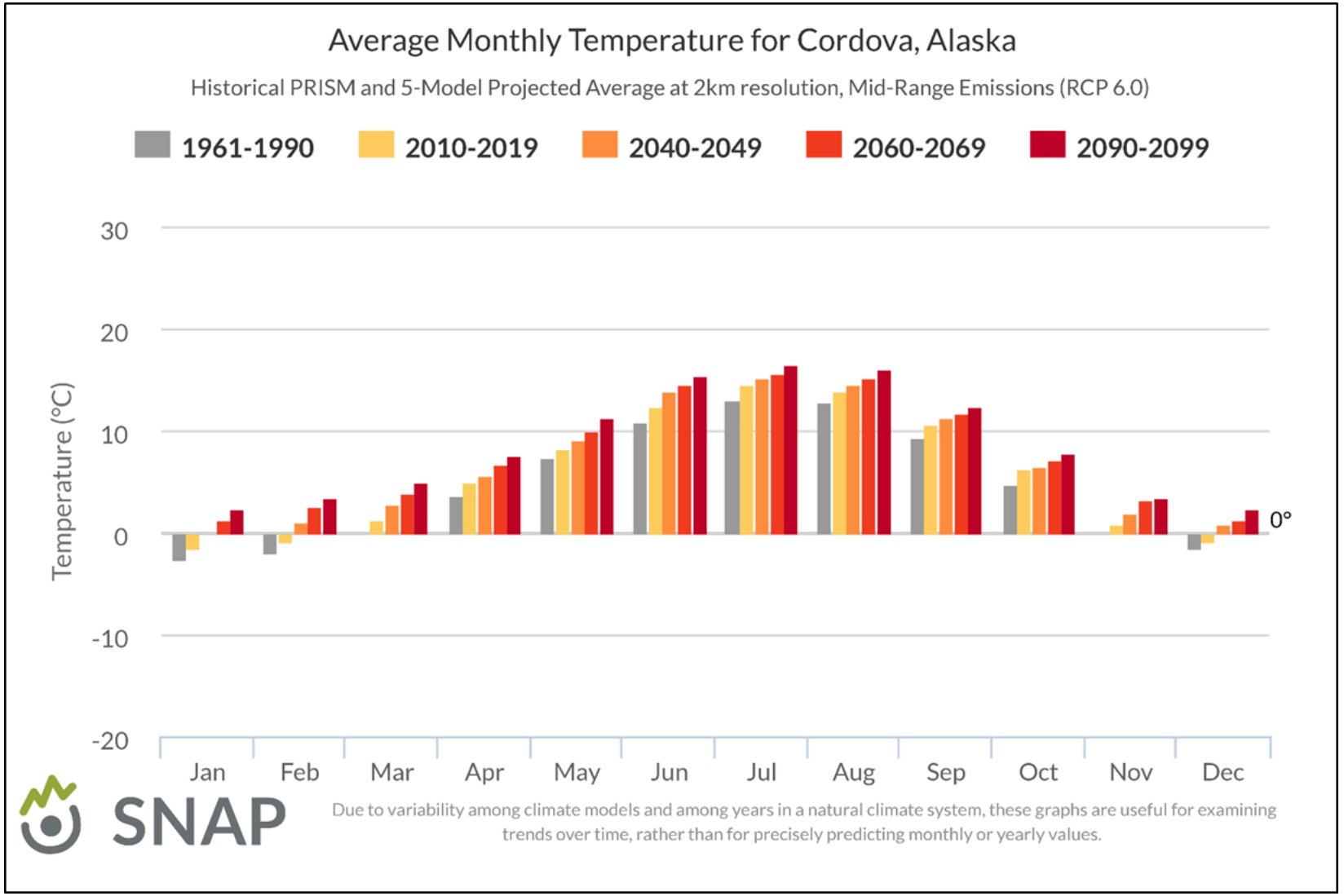

Figure 1.7 Historical PRISM and 5-model blended average monthly air temperature projections for Cordova, AK area grid cell at 2 km resolution (from snap.uaf.edu).

2 Geomorphic and Climatic Controls on Surface Water Temperature at Salmon Spawning and Rearing Sites, Copper River Delta, Alaska

2.1 Abstract

Projected increases in surface air temperature along the southern coast of Alaska are expected to elevate the rain-snow line, with potentially major consequences for catchment hydrology and year-round water temperatures in salmon spawning and rearing habitats. Water temperature is controlled by climatic and geomorphic factors including water source, residence time, and flowpath. This study tests the abilities of regression techniques to model year-round water temperature at 18 salmon spawning and rearing sites on the Copper River Delta, a complex landform with multiple water sources (groundwater, snow and ice melt, and precipitation). Considerable variability in water temperature was observed on spatial and temporal scales. Both weekly temperature maxima and the frequency of freezing conditions (<0.5°C) were positively correlated with lakes and negatively correlated with catchment elevation and slope. Upwelling groundwater was poorly correlated with landscape predictors, but was correlated with warm (>2°C) conditions during the incubation period (Oct.–May). Linear and logistic regression models were fitted to air and water temperature data collected between WY 2010 and WY 2014. Sites with upwelling groundwater and sites with high-relief, high elevation catchments exhibited lower thermal sensitivity and are anticipated to be less impacted by projected climatic changes. Projected reductions in melt water sources may limit the utility of these regression models as predictive tools. We tested the ability of these models to hindcast water temperature during WY 2015, an anomalously warm year (+1.3°C) when melt water was greatly reduced. The models underestimated water temperature, particularly during the spring, suggesting 1) reductions in melt water sources contributed to the observed increases in water temperature (mean +1°C) and 2) predictions generated with regression models may provide conservative estimates of future water temperatures.

2.2 Introduction

Water temperature regulates a wide range of biological processes that are important to Pacific Salmon (*Oncorhynchus* spp.) and other salmonids. Dissolved oxygen concentrations, salmonid metabolic and growth rates [*Beacham and Murray*, 1990; *McCullough*, 1999], and the phenology of important food resources [*Schindler et al.*, 2013] are all temperature dependent. Climatic changes are projected to alter the magnitude and seasonality of water temperature and may substantially impact many salmonid populations [*McCullough et al.*, 2009; *Mantua et al.*, 2010]. Maximum water temperatures in many salmonid-bearing streams at mid-latitudes in North America are already reaching thermal tolerance limits [*Mohseni et al.*, 2003], leading to concern that these habitats may become too warm for coldwater species in the future. These concerns have focused considerable research effort on summer (JJAS) maximum temperatures [*Mantua et al.*, 2010; *Mayer*, 2012; *Luce et al.*, 2014]; however, water temperature changes during the other eight months of the year may also significantly impact salmonids.

Autumn (ON), winter (DJF), and spring (MAM) water temperatures play a critical role in salmonid embryo and juvenile development rates [*Murray and McPhail*, 1988]. Increases in water temperature have been linked to accelerated development rates in embryos and juveniles and these changes have been demonstrated to have life-long impacts on viability [*Holtby*, 1988; *Jonsson et al.*, 2005]. The relationship between development rate and temperature is non-linear [*Beer and Anderson*, 2011] and highly species- and life phase-specific [*McCullough*, 1999], thus, the impacts of climate change on salmonids are anticipated to be highly variable over time and space [*Crozier and Zabel*, 2006]. Both positive and negative impacts are anticipated and the magnitude of the impacts are likely to depend on the net changes to the duration of optimal thermal conditions [*Beer and Anderson*, 2011] and the plasticity of salmonid life history strategies and physiology [*Crozier et al.*, 2008]. Assessment of the relationship between water temperature, catchment geomorphology, and atmospheric conditions is a critical step towards quantifying anticipated changes to salmonid populations.

Water temperature is influenced by heat fluxes that occur at the water's surface as well as at the streambed interface [*Caissie*, 2006]. Solar radiation is the major positive

energy flux [*Webb and Zhang*, 1997], but varies seasonally at mid and high latitudes, temporally with cloud cover, and locally due to shading (from both topography and canopy cover) [*Leach and Moore*, 2010]. Streambed friction is a smaller positive heat flux that contributes significant warming in steep streams, particularly during winter [*Webb and Zhang*, 1997] and in cold ablation-fed streams [*Magnusson et al.*, 2012].

Longwave radiative and sensible and latent heat fluxes contribute to, and subtract from, the heat energy in a stream, depending on the ambient water temperature, the air temperature and humidity, wind speed, cloud cover, and shade [*Sinokrot and Stefan*, 1993]. Similarly, conduction and advection of heat through the streambed interface can warm or cool surface water [*Webb and Zhang*, 1997; *Caissie et al.*, 2014]. Heat flux at the water's surface tends to be net negative in the late autumn (ON) and winter (DJF) at mid and high latitudes due largely to reduced solar radiation and reduced air temperature [*Leach and Moore*, 2010]; however, advection of heat can contribute to positive net energy flux in some stream reaches. For example, the advection of groundwater can prevent winter freezing near groundwater upwellings [*O'Driscoll and DeWalle*, 2006] and in stream reaches with sufficient hyporheic exchange [*Hannah et al.*, 2009], even when atmospheric fluxes are strongly negative. Similarly, advection of heat from lateral storm flows can warm streams during autumn and winter rain storms in maritime climates [*Leach and Moore*, 2014]

Spatial and temporal heterogeneity in water temperature is a result of not only variable atmospheric conditions, but also landscape-scale differences in water sources, mean residence time, and flowpaths [*Poole and Berman*, 2001]. These differences, which are largely controlled by catchment geomorphology, help determine the sensitivity of water temperature to atmospheric energy fluxes on both daily and seasonal timescales. For example, shading by canopy cover reduces solar radiation and increases longwave radiation, attenuating diel temperature fluctuations [*Moore et al.*, 2005; *Caissie*, 2006]. Advection associated with upwelling groundwater generally cools stream water during JJAS and warms stream water during ONDJF [*O'Driscoll and DeWalle*, 2006; *Kelleher et al.*, 2012].

The physical relationships between atmospheric conditions, catchment geomorphology, and water temperature can be represented reasonably well by regression

models at weekly to monthly time scales [*Mohseni and Stefan*, 1999; *Caissie*, 2006]. Regression models commonly utilize air temperature as a proxy for atmospheric energy fluxes [*Mohseni et al.*, 1998; *Kelleher et al.*, 2012], but have also been applied to correlate catchment characteristics to relative differences in temperature across the landscape [*Lisi et al.*, 2013].

The appeal of regression models is simplicity; compared to more physically-based models, little input data are needed. Catchment characteristics are readily available through remote sensing products and previous work has demonstrated that regional or interpolated air temperature are sufficient [*Mohseni et al.*, 1998; *Caldwell et al.*, 2015]. Furthermore, the slope of an air-water regression is an index of sensitivity to atmospheric conditions that has been broadly applied to assess the impacts of projected climatic changes [*Mantua et al.*, 2010; *Kelleher et al.*, 2012; *Mayer*, 2012].

Regression models assume stationarity. That is, the models are parameterized using historical data so that projections of future conditions using these models must assume that the relationships will not change significantly in the future. This assumption might be poorly supported when projecting the influence of climate change. As the climate warms, the relative importance of energy flux components may shift and the assumed correlations between water temperature, catchment characteristics, and air temperature may be altered. This may be particularly problematic where human activities directly disturb hydrologic function or when climatic changes affect available water sources [*Arismendi et al.*, 2014]. Despite these inherent constraints, regression models remain useful tools, particularly in remote areas where meteorological measurements are limited.

Coastal Alaska is remote, and meteorological and hydrological data are sparse [*Neal et al.*, 2002]. Regression-based modelling has been successfully utilized to better understand water temperatures in some basins. Air-water temperature correlation was applied to assess the relative sensitivity of water temperatures to projected temperature scenarios at U.S. Geological Survey (USGS) gaging stations in the Cook Inlet Region [*Kyle and Brabets*, 2001]. Multiple linear regression (MLR) has been utilized to correlate catchment characteristics with summer (JJA) water temperature near Bristol Bay [*Lisi et al.*, 2013, 2015] and ablation season (May- October) water temperatures in Southeast Alaska

[*Fellman et al.*, 2014]. These studies have also begun to elucidate the relative importance of snow and ice melt to water temperatures in streams used by salmon.

Climate projections suggest the magnitude of DJF air temperature changes will generally increase with latitude. Rising DJF temperatures along the southern coast of Alaska are projected to induce a transition from snow-dominated to rain-dominated streamflow patterns in low elevation catchments utilized by Pacific Salmon [*McAfee et al.*, 2014; *Shanley et al.*, 2015]. Snow and ice melt are important water sources [*Fellman et al.*, 2014; *Lisi et al.*, 2015] and the projected hydrologic changes may impact year-round water temperatures in salmon spawning and rearing habitats.

In this region, most Pacific salmon spawn in summer and embryos incubate in streambed gravels throughout the autumn, winter, and early spring months. Coho salmon (*O. kisutch*), typically spawn the latest and require the longest incubation [*Beacham and Murray*, 1990]. The time of spawning is highly variable across the landscape and the duration of incubation is highly temperature dependent, but for this purposes of this study, the late autumn (ON), winter (DJF), and spring (MAM) months will be referred to as "the incubation period."

Hydrologic changes during the incubation period are anticipated to impact the development and survival of salmon embryos as well as fry overwintering in freshwater streams [*Leppi et al.*, 2014; *Shanley and Albert*, 2014; *Wobus et al.*, 2015]. Although the potential for major hydrologic changes during the incubation period in coastal Alaska is well-recognized, the relationships between incubation period water temperatures, catchment geomorphology, and atmospheric conditions has not yet been adequately investigated.

Here, I utilize year-round (incubation period and summer) water temperature data to characterize geomorphic and climatic controls on water temperature at salmon spawning and rearing sites on the Copper River Delta (CRD). The CRD has complex geomorphology and exhibits considerable spatial and temporal variability in water temperature. Climatological mean DJF temperatures presently hover near the freezing isotherm and, similar to other locations along the southern coast of Alaska, projected increases in air temperatures are anticipated to raise the rain-snow line with major consequences for

catchment hydrology and water temperature [*McAfee et al.*, 2014; *Romero-Lankao et al.*, 2014; *University of Alaska*, 2015].

To help elucidate the importance of geomorphic and climatic controls on water temperatures at salmon spawning sites, I address two questions: 1) Can a multiple linear regression (MLR) model correlate weekly water temperature metrics with catchment characteristics across salmon spawning locations with heterogeneous water sources (groundwater, snow and ice melt, and precipitation)? 2) Can air-water regression models developed under historically normal climate conditions accurately hindcast mean monthly water temperatures during an anomalously warm year when seasonal snowpack was absent?

2.3 Methods

2.3.1 The Copper River Delta Study Area

The Copper River Delta (60.5 °N, 145.2 °W) extends along 80 km of Gulf of Alaska coastline, adjacent to the southern piedmont of the Chugach Mountains. The CRD is a Holocene landform, formed during the last 9,000 years. The 450 km^3 deltaic pile includes both marine and subaerial habitats. Its structure and morphology are due to the abundant supply of glacigenic sediment distributed by the Copper River, the reworking of sediment by marine processes, tectonic activity, and the dynamics of proximal valley glaciers that discharge directly onto the CRD [*Reimnitz*, 1966; *Jaeger et al.*, 1998].

Deposition from the proximal valley glaciers covers much of the 1,000 km^2 subaerial deltaic plain and this portion of the CRD effectively functions as a low-relief glacial foreland [*Reimnitz*, 1966; *Barclay et al.*, 2013]. The substrates are a heterogeneous mix of glacigenic sands and gravels and fine organic materials, which accumulate in peatlands and marshes [*Reimnitz*, 1966; *Galloway*, 1976].

Large meltwater distributaries, lakes, and streams are present on the CRD. Small unglaciated piedmont catchments discharge onto the margins of the outwash deposits, forming streams and shallow lakes where the outwashes meet bedrock hillslopes. The thick layers of sand and gravel enable phreatic storage and upwelling groundwater has been

observed in streams and rivers across the landscape. Streams and ponds are also present in the driftless portions of the CRD that have not aggraded outwash deposits. These streams aggrade thin and localized deposits of spawning gravel on the low-relief deltaic pile. Surficial geology in the piedmont catchments is primarily composed of shallow till and peat over sedimentary bedrock (Orca Group), localized granitic intrusions, and basalt [*Reimnitz*, 1966; *Winkler et al.*, 1992]. Catchment storage is presumed to have shorter residence times in the piedmont than in the outwash gravels. Despite the range of geomorphic conditions exhibited by freshwater habitats on the CRD, Pacific Salmon, particularly Coho Salmon, are widely distributed.

2.3.2 Temperature Study Sites

I utilized surface (stream) water temperature data collected by the U.S. Forest Service (USFS) at 18 salmon spawning and rearing sites, each in a unique catchment on the Copper River Delta (Figure 1). Water temperatures were recorded hourly using HOBO Pro v2 data loggers (Onset Comp. Corp.; manufacturer reported ± 0.2 °C accuracy) sheltered in open-ended, 6" long sections of 1 ½" galvanized steel pipe. The study period was water year (Oct 1 to Sept 30) (WY) 2010 through WY 2015, although the date of initial site installation varied considerably and data gaps exist due to buried, lost, or malfunctioning data loggers (Table 2.1). Particularly notable are 2 week to 5 month long data gaps at the end of WY 2015 at 6 of the sites. These data gaps are a consequence of the data download cycle. Due to logistical constraints, some sites are only downloaded once per year and at these sites, the rest of the WY 2015 data will not be available until summer, 2016.

All the study sites (n=18) were known spawning and rearing habitats for Coho Salmon (*O. kisutch*). Nine of the sites were also utilized for spawning and rearing by Sockeye Salmon (*O. nerka*). The study sites were located between 5 and 48 m above sea level, and were generally located near the slope break between the high-relief piedmont and the low-relief deltaic plain, where substrate particle sizes were most suitable for spawning (Table 2.1). Three of the sites were located at lake inlets, within the range of influence of the lake at high water.

Five of the sites are known to have upwelling groundwater (Table 2.1). I have categorized these sites, based on observed positive vertical head gradients in the shallow streambed and low diel and annual variance in temperature (presented in section *2.4 Results*). These characteristics are consistent with upwelling long-residence time groundwater in other locations [*O'Driscoll and DeWalle*, 2006; *Tague et al.*, 2008; *Kelleher et al.*, 2012]. Although I have categorized these sites based on the presence of upwelling groundwater, mixed water sources are likely during storm flow events and during the ablation season.

Catchment boundaries were interpolated based on surficial topography from the U.S. Geological Survey (USGS) interferometric synthetic aperture radar (IFSAR) 5m digital elevation model (DEM) using spatial analyst tools in ArcGIS 10.3 (Environmental Systems Research Institute, Redlands, CA, USA). The study catchments varied in total area (61 to 5426 ha), mean elevation (21 to 622 m), and mean slope (1 to 28 deg.) but these catchment characteristics were generally positively correlated (Table 2.1).

Catchment lake and ice coverage were calculated with data from USGS National Hydrography Dataset (NHD) (Table 2.2) [*U.S. Geological Survey*, 2013]. Half of the study catchments contained shallow lakes and three of the catchments had perennial ice. Maximum lake and ice cover was 15.4% and 12.7% of total catchment area respectively (Table 2.2).

Land cover statistics were calculated using USGS National Land Cover Database 2011 (NLCD) data (Table 2.2) [*Homer et al.*, 2015]. Most of the CRD is presently managed as "critical habitat" for fisheries and wildlife and the study catchments were generally uninfluenced by human development, although double-lane gravel roads were present in nine catchments. The most impacted site (Power Creek) was downstream from a run-of-the-river micro-hydropower facility. The impacts of this facility on stream temperature were assumed to be negligible. Study catchments were generally heavily vegetated with trees, shrubs, and woody wetlands. Hemlock (*Tsuga* spp.), Sitka spruce (*Picea sitchensis*), and Sitka alder (*Alnus crispa*) were dominate species. High elevation (> ~900 m) land surfaces were barren or perennially covered with snow and ice.

Surficial geology statistics were calculated using geologic mapping data from USGS [*Wilson et al.*, 2008]. Surficial geology was variable. Glaciofluvial drift was abundant in catchments located on glacial outwashes while shallow till over bedrock was prevalent in the piedmont catchments (Table 2.2). Drift and colluvium were present in the valley bottoms of the largest piedmont catchments.

2.3.3 Historical Climate Conditions

I calculated historical climate statistics from 1980-2010 weather records from Global Historical Climatology Network site #26410, which is operated by the National Oceanic and Atmospheric Administration (NOAA) within the study area. The climate was maritime, with cool and wet conditions throughout the year. The mean annual daily temperature was 4.3°C. The highest normal daily maxima occurred in early August (16.9°C) while the lowest normal daily minima occurred in mid-January (-7.2°C). Midwinter (DJF) temperatures normally hovered near the freezing point, but thaw events were common and daily minima exceeded 0°C on 24% of days. Conversely, cold and dry continental air masses periodically influenced the study area during the late fall, winter, and early spring months and daily low temperatures below -20°C have been recorded from early November through March (Figure 2.2). These influences are known to be particularly pronounced down valley from the Copper River Canyon, where a local gap wind transports cold interior air onto the eastern third of the CRD [*Reimnitz*, 1966].

Rainfall was common every month of the year and snowfall was common from early October until May. Mean annual precipitation was 230 cm and mean cumulative daily snowfall was 255 cm per year based on 1980-2010 records from the weather station (Figure 2.2).

Considerably more precipitation accumulates at higher elevations and in localized areas that are favorable to orographic lifting [*Kargel et al.*, 2014]. Historical accounts suggest that a shallow snowpack is typically present from November until late April at sea level and deep snowpacks (>3 m) accumulate in the piedmont mountains and persist throughout the summer months [*Reimnitz*, 1966].

2.3.4 Study Period Weather Conditions

Monthly temperature anomalies during the study period (WY 2010 to WY 2015) ranged from +5°C to -5°C and precipitation anomalies ranged from +300 mm to -200 mm (Figure 3.3). The largest anomalies were observed during the autumn and winter months. While monthly temperatures were variable in WY 2010 to WY 2014, the mean monthly temperatures were similar to the historic record. Water Year 2015, on the other hand, was anomalously warm every month of the year except October and September. The incubation period (October through May) surface air temperature anomaly was +1.7°C. Mid-winter air temperatures were particularly warm (+2.5°C DJF anomaly) and the monthly mean air temperature was above the freezing point every month of the year except for January (-0.9°C) and February (-0.2°C) (Figure 2.4). In contrast to the first 5 years of the study period, snowfall was nearly absent during WY 2015 and a snowpack never developed at low elevations (Figure 2.5).

Climate models project increasing mean air temperatures in future decades. The WY 2015 observed air temperatures are comparable to projected mean temperatures for the 2020 to 2040 time period under a mid-range greenhouse gas emissions scenario (Table 2.3) [*University of Alaska*, 2015]. Here, I test if a regression model developed with water temperature observations during climatological mean conditions (WY 2010 to WY 2014) can predict monthly mean water temperatures during anomalously warm WY 2015.

2.3.5 Data Analyses

Hourly surface water temperature data were summarized into daily mean values by site for all days during the study period. Variance was calculated for each site on three time steps, 1) year-round, 2) incubation period (October through May), and 3) summer (JJAS). Maximum and minimum daily temperatures were calculated for each site during the incubation period and summer. Mean monthly water temperatures were calculated for each site for every month with at least 28 days of complete daily data.

Regression models were used to elucidate the importance of 1) landscape and 2) climate controls on water temperature variability across space and time in salmon spawning and rearing areas on the CRD.

2.3.6 Landscape Model

Principal components analysis (PCA) was used to summarize model correlations between eleven water temperature metrics and four landscape predictors that have been successfully applied to predict magnitude of May-October [*Fellman et al.*, 2014] and June-August [*Lisi et al.*, 2013] water temperatures in other regions of coastal Alaska. The four landscape predictors were: 1) mean catchment elevation (m), 2) catchment area (log-transformed hectares), 3) mean catchment slope (degrees), and 4) percent of catchment area covered by lakes.

Multiple linear regression was applied to develop slope and intercept coefficients that best predict water temperature metrics of magnitude, variability and frequency for year-round, incubation period, and summer temperatures based on PC 1 and PC 2 scores. The temperature metrics were: 1) the 7 day average of the daily mean values ("avg. mean"), 2) the 7 day maximum of the daily maximum values ("max."), 3) Variance calculated from weekly (7 day) mean values, 4) the percentage of cold and warm days represents the percentage of the 243 day incubation season with water temperatures below 0.5 or above 2 °C. The model was applied to the entire dataset ("Model A," n=18) and to a subset of the data with upwelling groundwater sites removed ("Model B," n=13) and goodness-of-fit metrics were compared (Table 2.4).

2.3.7 Climate Sensitivity Model

Four regression models were fit to the observed monthly mean air and water temperatures during WY 2010 - WY 2014 (model equations are presented in Table 2.4). Model 1 is a commonly used linear regression model fitted to all air temperatures > 0 °C [*Kelleher et al.*, 2012; *Caldwell et al.*, 2015]. The ability of linear regression models to project winter water temperatures is typically reduced by the asymptotic nature of the freezing point [*Mohseni and Stefan*, 1999]. Nonetheless, we applied Model 2, a linear regression fitted to all water temperatures > 0.5 °C as a demonstrative (rather than a predictive) tool. Model 3 was a four parameter logistic regression fitted to all data [*Mohseni et al.*, 1998; *Mantua et al.*, 2010]. Model 4 was a two-part, four parameter logistic

regression fitted to rising (February to July) and falling (August to January) limbs to account for seasonal hysteresis [*Mohseni et al.*, 1998; *Kyle and Brabets*, 2001].

Model fit was compared using adjusted R^2 and root mean square error (RMSE) metrics. Water Year 2015 observed monthly air temperatures were applied to each model and the model results were compared to preliminary WY 2015 water temperature observations. All data analyses were performed in R v 3.2.3 [*R Core Team*, 2015].

2.4 Results

Water temperature exhibited spatial heterogeneity across the Copper River Delta. Summer (JJAS) daily mean water temperature maxima ranged among sites from 4.1°C to 20.2°C and minima ranged from 1.2°C to 6.4°C (Table 2.5). Incubation period (October to May) daily mean water temperature maxima ranged from 3.1°C to 19.0°C while minima hovered near freezing (< 1°C) (Table 2.5). Variance during the full period of record ranged from around 1 at known upwelling groundwater sites to 36.8. Incubation period variance was generally higher than JJAS variance (Table 2.5). Monthly mean water temperatures varied between 16 °C and the freezing point over the full period of record (Figure 2.6). Freezing (<0.5°C) monthly mean water temperatures were observed in winter at most sites (n=12) between WY 2010 and 2014, but at only one site in WY 2015 (Figure 2.6).

Water Year 2015 monthly mean temperatures were generally warmer (mean +1°C) than the WY 2010-2014 averages (Figure 2.7). The mean temperature difference between the WY 2015 monthly mean temperatures and the WY 2010-2014 averages was lower at the 5 groundwater upwelling sites (+0.65°C) than at the remaining sites (n=13) (+1.16°C), suggesting groundwater upwelling was correlated with less atmospheric sensitivity.

Temperature differences were typically greater during the incubation period and the largest differences were observed in May (Figure 2.7). The mean May 2015 water temperature difference (+2.4°C) was greater than the monthly air temperature anomaly (+1.6°C). The May water temperature differences were particularly large (≥ +6°C) at the two sites with the highest percentage of lake area upstream (LMart and Ot.Ca) (Figure 2.7).

2.4.1 Landscape Predictor Model Results

Principal components (PC) 1 and 2 explained 65% and 26% of the variance between sites based on four landscape predictors (Figure 2.8). Catchment mean elevation (m) and mean slope (deg.) were positively correlated and had high loadings on PC 1. Lake area (%), had a high loading on PC 2. Log-transformed catchment area (ha) was associated with high loadings on both axes. The sites that had positive PC 1 scores were located in the high-relief piedmont catchments while the sites with negative PC 1 scores were low-relief, low elevation catchments (Figure 2.8). Sites with positive PC 2 scores were the largest catchments that had the highest percentage of lake area (Figure 2.8).

Multiple linear regression (MLR) models performed best for weekly maximum JJAS water temperatures (adj. R^2 0.39-0.71, p value ≤0.01) (Table 2.6). Model B (n=13, known groundwater upwelling sites removed) fit better than Model A (n=18, all sites) for all metrics tested (Figure 2.9). The fit of both models was significant ($p \leq 0.05$) for weekly maximum temperatures (regardless of season), weekly mean temperatures during JJAS, year-round variance, and the frequency of incubation period cold (<0.5°C) days (Table 2.6). The fit of model A was also significant for JJAS variance ($p = 0.05$) while the fit of Model B was significant for year-round mean temperatures ($p = 0.02$) (Table 2.6).

The frequency of warm (>2°C) days during the incubation period was strongly correlated with groundwater upwelling and was not significantly captured by either model (Figure 2.9). Model fit was notably poor for incubation period mean temperatures (adj. $R^2 \leq 0$, p value ≥ 0.48).

Metrics of temperature magnitude were negatively correlated with PC 1 and were positively correlated with PC 2 (Table 2.6). In other words, high-relief mountain catchments had cooler maximum water temperatures than low-relief catchments at low elevations, particularly those low-relief catchments that contain lakes. Metrics of variance were strongly correlated with magnitude and exhibited similar relationships with PC 1 and PC 2 (Table 2.6).

Interestingly, the frequency of near-freezing temperatures (“cold days”) during the incubation period exhibited the same pattern: positive correlation with PC 1 and negative correlation with PC 2 (Table 2.6). This indicates that the high-relief mountain catchments

had a lower propensity to freeze than the low-relief catchments at low elevation. Thus, the salmon spawning sites that had the lowest maximum water temperatures also had the fewest days of freezing conditions and exhibited low variance and low thermal sensitivity.

2.4.2 Climate Sensitivity Model Results

Air-water temperature regression modelling also captured the substantial variation in thermal sensitivity across the study sites. Model 1 slope coefficients ranged from 0.1 to 1.2, (Figure 2.10), indicating that, on average, a 1°C rise in monthly mean air temperature was correlated with a 0.1°C rise in monthly mean water temperature at the most stable site (groundwater upwelling site TF.Mi) and with a 1.2°C rise in monthly mean water temperature at the most sensitive sites (LMart and Ot.Ca).

Linear and logistic regression models had generally good fit (mean RMSE ≤ 1.2°C) for WY 2010 to 2014 monthly mean air-water temperature data (Figure 2.10). Logistic Model 4, which accounts for seasonal hysteresis, had equal or superior fit to the other models at all study sites (Table 2.7). Linear Models 1 and 2 had similar R^2 values (Table 2.7). Linear slope values were similar between the models, but when the slopes differed, the Model 1 slopes were slightly steeper (Table 2.8). Model 2 *Y* intercept values were higher than Model 1 *Y* intercept values at all sites (Table 2. 8).

2.4.3 Hindcasting for WY 2015

The four models tended to underestimate WY 2015 water temperatures, particularly at sites with high thermal sensitivity (Figures 2.11 & 2.12). Mean RMSE ranged from 1.0°C (Model 2) to 1.3°C (Model 1). Model 2 fit the WY 2015 data slightly better than the WY 2010 -2014 data, but the other three models fit the WY 2015 slightly worse than the WY 2010-2014 data.

All four models performed most poorly in the late spring (AM) and the late autumn (ON) months at sites with high thermal sensitivity (Figure 2.12). Large residuals (2-4°C) were observed downstream from lakes (LMart and Ot.Ca) during AM and at lake inlets (EyakL and McKin) during ON (Figure 2.12).

2.5 Discussion

The observed spatial heterogeneity in water temperature suggests salmon spawning locations on the CRD have variable sensitivity to atmospheric energy fluxes. This variability is likely due to differences in water sources, residence times, and flowpaths that attenuate (or accentuate) atmospheric heat fluxes to varying degrees [*Poole and Berman*, 2001]. For example, groundwater upwelling sites exhibited low variance (≤ 5.5) (Table 2.5) and shallow air-water regression slopes (Figure 2.10), suggesting upstream flowpaths are generally sheltered from atmospheric influences. Conversely, sites downstream from shallow lakes (LMart and Ot.Ca), exhibited high variance (≥ 32.9) (Table 2.5) and steep air-water regression slopes (Figure 2.10), indicating high sensitivity to the atmosphere.

Water sources, residence times, and flowpaths are controlled by both geomorphic and climatic factors [*Poole and Berman*, 2001]. Landscape predictor and climate sensitivity modelling were useful tools to elucidate the relative importance of these factors as water temperature controls across the CRD.

2.5.1 Landscape Predictor Model Performance

The multiple linear regression (MLR) models correlated landscape predictors with some of the observed variability in water temperature. Similar MLR models have produced similar results in Southeast Alaska [*Fellman et al.*, 2014] and Bristol Bay [*Lisi et al.*, 2013, 2015]. The sum of the evidence suggests that maximum water temperatures in coastal Alaska are negatively correlated with catchment elevation and are positively correlated with lake area. In both cases, isotopic analysis linked reduced water temperatures to meltwater sources [*Fellman et al.*, 2014; *Lisi et al.*, 2015], suggesting maximum water temperature is controlled by both climatic and geomorphic factors.

Maximum temperature is just one of many useful temperature metrics [*Arismendi et al.*, 2013]. This study also investigated variance and the frequency of freezing (<0.5°C) and warm (>2°C) days during the incubation period. Variance was highly correlated with maximum temperatures and provided little additional information, however, models fit to the metrics of frequency proved useful.

Landscape predictors had similar correlation with both cooler summer maxima and a reduced frequency of freezing water temperatures during the incubation period. This finding suggests that the correlation between elevation and water temperature cannot be attributed to melt water sources alone. Melt water sources are greatly reduced during periods of freezing conditions, suggesting that physical geomorphic characteristics play a role in elevating incubation period temperatures above freezing in high-relief, high-mean elevation catchments.

Mean catchment elevation, slope, and area were highly correlated and all three characteristics may contribute to reductions in freezing conditions. Valley bottoms within large catchments in the study area contain deposits of coarse glaciofluvial and colluvial materials that are favorable to both upwelling groundwater and hyporheic exchanges. Advection of water across the streambed interface moderates water temperatures year-round by increasing advective and conductive heat fluxes [*O'Driscoll and DeWalle*, 2006; *Gariglio et al.*, 2013; *Caissie et al.*, 2014]. Larger catchment area is correlated with higher mean streamflow. Streamflow is negatively correlated with year-round thermal sensitivity [*Poole and Berman*, 2001]. Steeper mean slope is correlated with greater streambed friction, which contributes modest, but significant heat energy and also may help prevent freezing when atmospheric energy fluxes are strongly negative [*Webb and Zhang*, 1997; *Magnusson et al.*, 2012].

Model B (known upwelling groundwater sites removed) had considerably better fit than Model A (all sites), suggesting that these four landscape predictors were poorly correlated with upwelling groundwater. The upwelling groundwater sites on the CRD are likely a product of well-sorted glaciofluvial drift and a slope break near the transition from the high-relief piedmont to the low-relief deltaic plain. Changes in lateral or vertical confinement imparted by bedrock constriction, or changes in permeable layer thickness may also contribute to groundwater upwelling [*Baxter and Hauer*, 2000]. Layers of silts and organics that were originally deposited in marine, lacustrine, and wetland environments likely add complexity to the level of confinement of the aquifer and the location and strength of upwelling. These complexities were poorly represented by the landscape predictors applied in the MLR model.

For example, the MLR models found no significant trends in the percentage of warm (>2°C) days during the incubation period; however, upwelling groundwater was positively correlated with this metric (Figure 2.9). The exception to this observation was site Ibeck, which exhibited an anomalously low percentage of warm days. This site is located proximal to a glacial terminus and remained cold year-round (4.1°C JJAS daily maxima). We suspect glacial melt is an important recharge source at this aquifer. The extent of spatial variability amongst groundwater recharge sources across the CRD is presently unknown. Better assessment of recharge sources, particularly for shallow and unconfined aquifers, will be critical to assessing long-term climate sensitivity [*Kurylyk et al.*, 2014].

2.5.2 Climate sensitivity

Models 1-4 did a reasonable job fitting observed temperature data, suggesting atmospheric conditions generally determined monthly water temperatures at the study sites and that monthly air temperatures were consistently correlated with both atmospheric conditions and monthly water temperatures (RMSE <1.2°C). Landscape characteristics influence both the exposure of water to the atmosphere [*Leach and Moore*, 2010; *Kelleher et al.*, 2012] and the availability of melt [*Lisi et al.*, 2015] and groundwater sources [*Tague et al.*, 2008]. This differential atmospheric sensitivity was captured by the regression slope coefficients, which varied from 0.1 to 1.2 across the study sites.

Although the performance of the four models was similar, an analysis of the differences highlights the importance of water sources to temperature. Model 1 uses air temperature as a proxy for atmospheric energy fluxes [*Caissie*, 2006]. One assumption behind this model is that atmospheric conditions drive water temperature. If air temperatures are below 0°C, this model assumes that the water is near freezing and the relationship between water temperature and air temperature is no longer linear [*Webb and Nobilis*, 1997; *Morrill et al.*, 2005; *Kelleher et al.*, 2012].

This assumption is valid as long as the atmosphere is driving the energy balance, however, above freezing mean water temperatures were observed during months with below freezing mean air temperatures at all of our study sites, as denoted by the red points in Figure 2.10. The prevalence of above freezing monthly water temperatures when mean

monthly air temperatures are below freezing demonstrates the importance of heat exchanges at the streambed interface, particularly advection and conduction associated with upwelling groundwater [*O'Driscoll and DeWalle*, 2006] and lateral flows during rain events [*Leach and Moore*, 2014].

In contrast to Model 1, Model 2 incorporates all above freezing (≥ 0.5 °C) water temperatures, regardless of air temperature. Model 2 slope coefficients were similar to model 1, but the *Y* intercept values were higher, demonstrating the role that advection plays in elevating incubation period water temperatures. One shortcoming of Model 2 is its propensity to model below 0°C water temperatures, although this problem is easily corrected by setting a minimum y value equal to the freezing point. Model 2 also fails to incorporate the months that are characterized by winter and early spring thaw events, when monthly mean air temperatures exceed freezing, but monthly mean water temperatures are near freezing (<0.5 °C). These months, represented by blue points in Figure 2.10, are the periods of strongest temperature hysteresis, and signify periods when melt water sources strongly overwhelm atmospheric drivers.

Logistic regression captures the non-linearity of the air-water relationship at low (near freezing) and high (≥ 20°C) temperatures [*Mohseni and Stefan*, 1999]. The two-limb logistic model (model 4) most directly incorporated seasonal hysteresis and performed the best with WY 2010 to WY 2014 data. This finding is consistent with other modelling efforts in regions with seasonal melt hysteresis [*Mohseni et al.*, 1998; *Kyle and Brabets*, 2001] and suggests that the addition of meltwater as a water source during the spring and early summer has historically had a significant impact on water temperature at many of the study sites.

2.5.3 Hindcasting for WY 2015

We observed that both linear and logistic models underestimated year-round water temperatures during WY 2015, an anomalously warm year when snow and ice was nearly absent. Model performance may have been impacted by reduced melt hysteresis. The greatest differences between observed and modeled data occurred during the spring (MAM), the season of greatest seasonal snow and ice melt under climatologically normal

conditions [*Zhang et al.*, 1997]. Model 2, the model that excludes months with a strong meltwater signature (as described in the last section), provided the most accurate hindcast of the WY 2015 data.

2.5.4 Implications for Pacific Salmon

Winter (DJF) monthly mean water temperatures were near freezing (< 0.5°C) at many study sites (n=12) during climatological mean conditions (WY 2010 – 2014) and were likely sub-optimal for Pacific Salmon embryo and juvenile development [*McCullough*, 1999]. The low-elevation, low-relief catchments with shallow flowpaths and lakes exhibited the highest thermal sensitivity, the highest maximum mean daily temperatures (~20°C), and the highest frequency of near-freezing (<0.5°C) conditions. In contrast, upwelling groundwater was correlated with warm (>2°C) DJF water temperatures and these sites generally provided a warm and temporally stable incubation environment for salmon.

Considerable increases in mean monthly water temperature (+1.0°C mean, +7°C max) were observed in WY 2015, an anomalously warm year. The greatest increases in incubation period temperature were observed at high sensitivity catchments with shallow flowpaths and lakes. Since these sites had the greatest frequency of near-freezing conditions at climatological mean temperatures, even small changes in temperature will be proportionally large.

Monthly mean temperatures are highly correlated with accumulated thermal units, or "degree days," a biologically relevant metric used to model Pacific salmon incubation [*Neuheimer and Taggart*, 2007]. Small increases in incubation period monthly mean water temperatures will greatly increase accumulated thermal units and may accelerate embryo development [*Holtby*, 1988; *Murray and McPhail*, 1988; *McCullough*, 1999]. Thus, the warming observed during WY 2015 may have accelerated embryo development rates.

Studies conducted at mid-latitudes have hypothesized that accelerated development has negative implications for salmon viability. For example, rapid development has been correlated with reduced juvenile length at emergence due to reductions in the rate and efficiency of yolk use [*Beacham and Murray*, 1990]. Egg size is correlated with yolk reserve

and Pacific Salmon tend to have larger eggs at lower latitudes due to the reduced efficiency of yolk conversion at warmer temperatures [*Fleming and Gross*, 1990]. The viability of juveniles hatching from smaller eggs could be reduced by elevated temperatures under projected warming scenarios.

Changes during incubation may have lifelong impacts on viability. Holtby [1988] reported increased year-round stream temperatures after timber harvest accelerated Coho Salmon emergence by up to 6 weeks. Earlier emergence effectively lengthened the growing season and a large proportion of juveniles completed their freshwater life phase after one year rather than two. The age 1+ Coho Salmon smolts were smaller than the age 2+ smolts and the author hypothesized that marine survival would decrease.

In coastal Alaska, however, researchers have generally hypothesized that projected increases in water temperature could improve Pacific Salmon growth and survival, particularly for juvenile salmon rearing in catchments with permanent snow and ice cover [*Milner et al.*, 2008; *Bryant*, 2009; *Schindler et al.*, 2013; *Fellman et al.*, 2014; *Leppi et al.*, 2014].

Incubation period water temperatures observed at my study sites on the CRD were generally relatively cool under climatological mean conditions (mean = 2.6°C). Thus, the warmer temperatures observed in WY 2015 may have prolonged the duration of optimal growth conditions for juvenile Pacific Salmon [*Beer and Anderson*, 2011].

2.6 Conclusions

- Considerable spatial heterogeneity was observed in year-round water temperatures at 18 salmon spawning and rearing sites on the Copper River Delta.
- Weekly temperature maxima were positively correlated with lakes and negatively correlated with catchment elevation and slope. Interestingly, similar correlations were observed for the frequency of freezing conditions during the incubation period, suggesting that catchments with high mean

elevation and slope are both the coolest in the summer and the warmest in the winter.

- Upwelling groundwater was poorly correlated with landscape predictors, but was highly correlated with the frequency of warm (>2°C) conditions during the incubation period.
- Sites with upwelling groundwater or high-relief, high elevation catchments exhibited lower thermal sensitivity and are anticipated to be less impacted by projected climatic changes.
- Increases in monthly mean water temperature (mean = +1°C) were observed during an anomalously warm year when snowfall and melt was greatly reduced.
- Linear and logistic air-water regression models underestimated the temperature increases, particularly during MAM. This observation suggests that reduced melt hysteresis contributed to the observed water temperature changes and that future water temperature projections produced by air-water regression models may be conservative estimates in catchments were reductions in snowpack are anticipated.

2.7 Acknowledgements

The author thanks Emily Campbell for sharing surface water data for 5 study sites.

2.8 References

Arcement Jr., G. J., and V. R. Schneider (1989), Guide for selecting Manning's roughness coefficients for natural channels and flood plains, *U.S. Geol. Surv. Water-Supply Pap. 2339*.

Arismendi, I., S. L. Johnson, J. B. Dunham, and R. Haggerty (2013), Descriptors of natural thermal regimes in streams and their responsiveness to change in the Pacific Northwest of North America, *Freshw. Biol.*, *58*(5), 880–894, doi:10.1111/fwb.12094.

Arismendi, I., M. Safeeq, J. B. Dunham, and S. L. Johnson (2014), Can air temperature be used to project influences of climate change on stream temperature?, *Environ. Res. Lett.*, *9*(8), 084015, doi:10.1088/1748-9326/9/8/084015.

Barclay, D. J., E. M. Yager, J. Graves, M. Kloczko, and P. E. Calkin (2013), Late Holocene Glacial History of the Copper River Delta, Coastal South-central Alaska, and Controls on Valley Glacier Fluctuations, *Quat. Sci. Rev.*, *81*, 74–89, doi:10.1016/j.quascirev.2013.10.001.

Battin, J., M. W. Wiley, M. H. Ruckelshaus, R. N. Palmer, E. Korb, K. K. Bartz, and H. Imaki (2007), Projected impacts of climate change on salmon habitat restoration., *Proc. Natl. Acad. Sci. U. S. A.*, *104*(16), 6720–5, doi:10.1073/pnas.0701685104.

Baxter, C. V., and F. R. Hauer (2000), Geomorphology, hyporheic exchange, and selection of spawning habitat by bull trout (*Salvelinus confluentus*), *Can. J. Fish. Aquat. Sci.*, *57*(7), 1470–1481, doi:10.1139/cjfas-57-7-1470.

Beacham, T. D., and C. B. Murray (1990), Temperature, Egg Size, and Development of Embryos and Alevins of Five Species of Pacific Salmon: A Comparative Analysis, *Trans. Am. Fish. Soc.*, *119*(6), 927–945.

Beer, W. N., and J. J. Anderson (2011), Sensitivity of juvenile salmonid growth to future climate trends, *River Res. Appl.*, *27*(5), 663–669, doi:10.1002/rra.1390.

Benda, L., T. J. Beechie, R. C. Wissmar, and A. Johnson (1992), Morphology and Evolution of Salmonid Habitats in a Recently Deglaciated River Basin, Washington State, USA, *Can. J. Fish. Aquat. Sci.*, *49*(6), 1246–1256, doi:10.1139/f92-140.

van den Berghe, E. P., and M. R. Gross (1984), Female Size and nest depth in coho salmon (Oncorhynchus kisutch), *Can. J. Fish. Aquat. Sci.*, *41*, 204–206.

Bisson, P. a., J. B. Dunham, and G. H. Reeves (2009), Freshwater ecosystems and resilience of Pacific salmon: habitat management based on natural variability, *Ecol. Soc.*, *14*(1), 45, doi:45.

Boggs, K. (2000), Classification of Community Types, Successional Sequences, and Landscapes of the Copper River Delta, Alaska, *Gen. Tech. Rep. - Pacific Northwest Res. Station. USDA For. Serv.*, (PNW-GTR-469), 244 pp.

Brabets, T. P. (1997), Geomorphology of the lower Copper River, Alaska, *U.S. Geol. Surv. Prof. Pap. #1581*, 89.

Braun, D. C., D. A. Patterson, and J. D. Reynolds (2013), Maternal and environmental influences on egg size and juvenile life-history traits in Pacific salmon, *Ecol. Evol.*, *3*(6), 1727–1740, doi:10.1002/ece3.555.

Bryant, M. D. (1992), The Copper River Delta pulse study: an interdisciplinary survey of the aquatic habitats, *Gen. Tech. Rep. - Pacific Northwest Res. Station. USDA For. Serv.*, *PNW-GTR-28*, 43.

Bryant, M. D. (2009), Global climate change and potential effects on Pacific salmonids in freshwater ecosystems of southeast Alaska, *Clim. Change*, *95*(1-2), 169–193, doi:10.1007/s10584-008-9530-x.

Bunte, K., and S. R. Abt (2001), Sampling Surface and Subsurface Particle-Size Distributions in Wadable Gravel- and Cobble-Bed Streams for Analyses in Sediment Transport ,

Hydraulics , and Streambed Monitoring, *0*, 450.

Caissie, D. (2006), The thermal regime of rivers: a review, *Freshw. Biol.*, *51*(8), 1389–1406, doi:10.1111/j.1365-2427.2006.01597.x.

Caissie, D., B. L. Kurylyk, A. St-Hilaire, N. El-Jabi, and K. T. B. MacQuarrie (2014), Streambed temperature dynamics and corresponding heat fluxes in small streams experiencing seasonal ice cover, *J. Hydrol.*, *519*, 1441–1452, doi:10.1016/j.jhydrol.2014.09.034.

Caldwell, P., C. Segura, S. Gull Laird, G. Sun, S. G. McNulty, M. Sandercock, J. Boggs, and J. M. Vose (2015), Short-term stream water temperature observations permit rapid assessment of potential climate change impacts, *Hydrol. Process.*, *29*(9), 2196–2211, doi:10.1002/hyp.10358.

Case, J. E., D. F. Barnes, G. Plafker, and S. L. Robbins (1966), Gravity Survey and Regional Geology of the Prince William Sound Epicentral Region, Alaska, in *The Alaska Earthquake, March 27, 1964: Regional Effects*, United States Government Printing Office.

Christensen, H. H. (2000), *Alaska's Copper River: Humankind in a Changing World*, U.S. Dept. of Agriculture, Forest Service, Pacific Northwest Research Station GTR 480.

Cooper, E. E. (2007), Beaver Ecology on the West Copper River Delta, Alaska., Oregon State University.

Crozier, L. G., and R. W. Zabel (2006), Climate impacts at multiple scales: Evidence for differential population responses in juvenile Chinook salmon, *J. Anim. Ecol.*, *75*(5), 1100–1109, doi:10.1111/j.1365-2656.2006.01130.x.

Crozier, L. G., A. P. Hendry, P. W. Lawson, T. P. Quinn, N. J. Mantua, J. Battin, R. G. Shaw, and R. B. Huey (2008), PERSPECTIVE: Potential responses to climate change in organisms with complex life histories: evolution and plasticity in Pacific salmon, *Evol. Appl.*, *1*(2), 252–270, doi:10.1111/j.1752-4571.2008.00033.x.

DeVries, P. (1997), Riverine salmonid egg burial depths: review of published data and implications for scour studies, *Can. J. Fish. Aquat. Sci.*, *54*(8), 1685–1698, doi:10.1139/cjfas-54-8-1685.

Dingman, S. L. (2002), *Physical Hydrology*, 2nd ed., Waveland Press, Inc, Long Grove, IL.

Dorava, J. M., and J. M. Sokup (1994), Overview of Environmental and Hydrogeologic Conditions at the Merle K. "Mudhole" Smith Airport, Near Cordova Alaska, *U.S. Geol. Surv. Open-File Rep. 94-328*, 1–15.

Everest, F. H., C. E. McLemore, and W. J.F. (1980), An improved tritube cryogenic gravel sampler., *Res. Note PNW-350. USDA For. Serv. Northwest For. Range Exp. Station. Portland, Or .*

Fellman, J. B., S. Nagorski, S. Pyare, A. W. Vermilyea, D. Scott, and E. Hood (2014), Stream temperature response to variable glacier coverage in coastal watersheds of Southeast Alaska, *Hydrol. Process.*, *28*(4), 2062–2073, doi:10.1002/hyp.9742.

Fleming, I. A., and M. R. Gross (1990), Latitudinal Clines : A Trade-Off between Egg Number and Size in Pacific Salmon, *Ecology*, *71*(1), 1–11.

Galloway, W. E. (1976), Copper River Fan-Delta, *J. Sediment. Petrol.*, *46*(3), 726–737.

Gariglio, F. P., D. Tonina, and C. H. Luce (2013), Spatiotemporal variability of hyporheic exchange through a pool-riffle-pool sequence, *Water Resour. Res.*, *49*(11), 7185–7204, doi:10.1002/wrcr.20419.

Goode, J. R., J. M. Buffington, D. Tonina, D. J. Isaak, R. F. Thurow, S. Wenger, D. Nagel, C. Luce, D. Tetzlaff, and C. Soulsby (2013), Potential effects of climate change on streambed scour and risks to salmonid survival in snow-dominated mountain basins, *Hydrol. Process.*, *27*(5), 750–765, doi:10.1002/hyp.9728.

Grantz, A., G. Plafker, and R. Kachadoorian (1964), Alaska's Good Friday earthquake, March 27, 1964: A Preliminary Geologic Evaluation, *U.S. Geol. Surv. Prof. Pap.*, 1–35.

Hall, D. K. (1988), Assessment of Polar Climate Change using Satellite Technology, *Rev. Geophys.*, *26*(1), 26–39, doi:10.1029/RG026i001p00026.

Hannah, D. M., I. A. Malcolm, and C. Bradley (2009), Seasonal hyporheic temperature dynamics over riffle bedforms, *Hydrol. Process.*, *23*, 2178–2194, doi:10.1002/hyp.7256.

Haschenburger, J. K. (1999), A probability model of scour and fill depths in gravel-bed channels, *Water Resour. Res.*, *35*(9), 2857–2869.

Hinch, S., M. C. Healey, R. Em, K. A. Thornson, R. Hourston, M. A. Henderson, and F. Juanes (1995), Potential effects of climate change on marine growth and survival of Fraser River sockeye salmon, *Can. J. Fish. Aquat. Sci.*, *52*, 2651–2659.

Holtby, L. B. (1988), Effects of Logging on Stream Temperatures in Carnation Creek, British, *Can. J. Fish. Aquat. Sci.*, *45*, 502–515, doi:10.1139/f88-060.

Holtby, L. B., and M. C. Healey (1986), Selection for Adult Size in Female Coho Salmon (Oncorhynchus kisutch), *Can. J. Fish. Aquat. Sci.*, *43*, 1946–1959.

Homer, C. G., J. A. Dewitz, L. Yang, S. Jin, P. Danielson, G. Xian, J. Coulston, N. D. Herold, J. D. Wickham, and K. Megown (2015), Completion of the 2011 National Land Cover Database for the conterminous United States-Representing a decade of land cover change information, *Photogramm. Eng. Remote Sensing*, *81*(5), 345–354.

Jaeger, J. M., C. A. Nittrouer, N. D. Scott, and J. D. Milliman (1998), Sediment accumulation along a glacially impacted mountainous coastline: north-east Gulf of Alaska, *Basin Res.*, *10*(1), 155–173, doi:10.1046/j.1365-2117.1998.00059.x.

Jonsson, N., B. Jonsson, and L. P. Hansen (2005), Does climate during embryonic development influence parr growth and age of seaward migration in Atlantic salmon (Salmo salar)?, *Can. J. Fish. Aquat. Sci.*, *62*(11), 2502–2508, doi:10.1139/F05-154.

Kargel, J. S. et al. (2014), Multispectral image analysis of glaciers and glacier lakes in the Chugach Mountains, Alaska, in *Global Land Ice Measurements from Space*, edited by J. S. Kargel, pp. 297–332, Springer Praxis Books, Berlin Heidelberg.

Kelleher, C., T. Wagener, M. Gooseff, B. McGlynn, K. McGuire, and L. Marshall (2012), Investigating controls on the thermal sensitivity of Pennsylvania streams, *Hydrol. Process.*, *26*(5), 771–785, doi:10.1002/hyp.8186.

Kurylyk, B. L., K. T. B. MacQuarrie, and C. I. Voss (2014), Climate change impacts on the temperature and magnitude of groundwater discharge from shallow, unconfined aquifers, *Water Resour. Res.*, *50*(4), 3253–3274, doi:10.1002/2013WR014588.

Kyle, R. E., and T. P. Brabets (2001), Water Temperature of Streams in the Cook Inlet Basin, Alaska, and Implications of Climate Change, *Wri 01-4109*, 32, doi:Water-Resources Investigations Report 01-4109.

Lamb, M. P., W. E. Dietrich, and J. G. Venditti (2008), Is the critical shields stress for incipient sediment motion dependent on channel-bed slope?, *J. Geophys. Res. Earth Surf.*, *113*(2), 1–20, doi:10.1029/2007JF000831.

Leach, J. A., and R. D. Moore (2010), Above-stream microclimate and stream surface energy exchanges in a wildfire-disturbed riparian zone, *Hydrol. Process.*, *24*(17), 2369–2381, doi:10.1002/hyp.7639.

Leach, J. A., and R. D. Moore (2014), Winter stream temperature in the rain-on-snow zone of the Pacific Northwest: Influences of hillslope runoff and transient snow cover, *Hydrol. Earth Syst. Sci.*, *18*(2), 819–838, doi:10.5194/hess-18-819-2014.

Leppi, J. C., D. J. Rinella, R. R. Wilson, and W. M. Loya (2014), Linking climate change projections for an Alaskan watershed to future coho salmon production, *Glob. Chang. Biol.*, *20*(6), 1808–1820, doi:10.1111/gcb.12492.

Lisi, P. J., D. E. Schindler, K. T. Bentley, and G. R. Pess (2013), Association between geomorphic attributes of watersheds, water temperature, and salmon spawn timing in Alaskan streams, *Geomorphology*, *185*, 78–86, doi:10.1016/j.geomorph.2012.12.013.

Lisi, P. J., D. E. Schindler, T. J. Cline, M. D. Scheuerell, and P. B. Walsh (2015), Watershed geomorphology and snowmelt control stream thermal sensitivity to air temperature, *Geophys. Res. Lett.*, *42*(9), 3380–3388, doi:10.1002/2015GL064083.Received.

Lotspeich, F. B., and B. H. Reid (1980), Tri-tube Freeze-core Procedure for Sampling Stream Gravels, *Progress. Fish-Culturist*, *42*(2), 96–99, doi:10.1577/1548-8659(1980)42.

Luce, C., B. Staab, M. Kramer, S. Wenger, D. Isaak, and C. McConnell (2014), Sensitivity of summer streamtemperatures to climate variability in the Pacific Northwest, *Water Resour. Res.*, *50*, 3428–3443, doi:10.1002/2013WR014329.Received.

Magnusson, J., T. Jonas, and J. W. Kirchner (2012), Temperature dynamics of a proglacial stream: Identifying dominant energy balance components and inferring spatially integrated hydraulic geometry, *Water Resour. Res.*, *48*(6), W06510, doi:10.1029/2011WR011378.

Mann, D. H., A. L. Crowell, T. D. Hamilton, and B. P. . Finney (1998), Holocene Geologic and Climatic History Around The Gulf of Alaska, *Artic Anthropol.*, *35*(1), 112–131.

Mantua, N., I. Tohver, and A. Hamlet (2010), Climate change impacts on streamflow

extremes and summertime stream temperature and their possible consequences for freshwater salmon habitat in Washington State, *Clim. Change*, *102*(1-2), 187–223, doi:10.1007/s10584-010-9845-2.

Mantua, N. J., S. R. Hare, Y. Zhang, J. M. Wallace, and R. C. Francis (1997), A Pacific Interdecadal Climate Oscillation with Impacts on Salmon Production, *Bull. Am. Meteorol. Soc.*, *78*(6), 1069–1079, doi:10.1175/1520-0477(1997)078<1069:APICOW>2.0.CO;2.

May, C. L., B. Pryor, T. E. Lisle, and M. Lang (2009), Coupling hydrodynamic modeling and empirical measures of bed mobility to predict the risk of scour and fill of salmon redds in a large regulated river, *Water Resour. Res.*, *45*(5), doi:10.1029/2007WR006498.

Mayer, T. D. (2012), Controls of summer stream temperature in the Pacific Northwest, *J. Hydrol.*, *475*, 323–335, doi:10.1016/j.jhydrol.2012.10.012.

McAfee, S. A., J. Walsh, and T. S. Rupp (2014), Statistically downscaled projections of snow/rain partitioning for Alaska, *Hydrol. Process.*, *28*(12), 3930–3946, doi:10.1002/hyp.9934.

McCullough, D. A. (1999), *A Review and Synthesis of Effects of Alterations to the Water Temperature Regime on Freshwater Life Stages of Salmonids, with Special Reference to Chinook Salmon, Region 10 Water Resources Assessment Report No. 910-R-99-010,* U.S. Environmental Protection Agency.

McCullough, D. A. et al. (2009), Research in Thermal Biology: Burning Questions for Coldwater Stream Fishes, *Rev. Fish. Sci.*, *17*(1), 90–115, doi:10.1080/10641260802590152.

McKean, J., and D. Tonina (2013), Bed stability in unconfined gravel bed mountain streams: With implications for salmon spawning viability in future climates, *J. Geophys. Res. Earth Surf.*, *118*(3), 1227–1240, doi:10.1002/jgrf.20092.

Milliman, J. D., and R. H. Meade (1983), World-Wide Delivery of River Sediment to the Oceans, *J. Geol.*, *91*(1), 1–21.

Milner, A. M., A. L. Robertson, K. a. Monaghan, A. J. Veal, and E. a. Flory (2008), Colonization and development of an Alaskan stream community over 28 years, *Front. Ecol. Environ.*, *6*(8), 413–419, doi:10.1890/060149.

Mohseni, O., and H. G. Stefan (1999), Stream temperature/air temperature relationship: A physical interpretation, *J. Hydrol.*, *218*(3-4), 128–141, doi:10.1016/S0022-1694(99)00034-7.

Mohseni, O., H. G. Stefan, and T. R. Erickson (1998), A nonlinear regression model for weekly stream temperatures, *Water Resour. Res.*, *34*(10), 2685–2692.

Mohseni, O., H. G. Stefan, and J. G. Eaton (2003), Global Warming and Potential Changes in Fish Habitat, *Environ. Prot.*, *59*(1995), 389–409, doi:10.1023/A:1024847723344.

Montgomery, D. R., J. M. Buffington, N. P. Peterson, D. Schuett-Hames, and T. P. Quinn (1996), Stream-bed scour, egg burial depths, and the influence of salmonid spawning

on bed surface mobility and embryo survival, *Can. J. Fish. Aquat. Sci.*, *53*(5), 1061–1070, doi:10.1139/f96-028.

Montgomery, D. R., E. M. Beamer, G. R. Pess, and T. P. Quinn (1999), Channel type and salmonid spawning distribution and abundance, *Can. J. Fish. Aquat. Sci.*, *56*(3), 377–387, doi:10.1139/f98-181.

Moore, R. D., D. L. Spittlehouse, and A. Story (2005), Riparian microclimate and stream temperature response to forest harvesting: A review, *J. Am. Water Resour. Assoc.*, *7*(4), 813–834, doi:10.1111/j.1752-1688.2005.tb04465.x.

Morrill, J., R. Bales, and M. Conklin (2005), Estimating Stream Temperature from Air Temperature: Implications for Future Water Quality, *J. Environ. Eng.*, *131*(1), 139–146, doi:doi:10.1061/(ASCE)0733-9372(2005)131:1(139).

Mote, P. W. et al. (2003), Preparing for climatic change: The water, salmon, and forests of the Pacific Northwest, *Clim. Change*, *61*(1-2), 45–88, doi:10.1023/A:1026302914358.

Murray, C. B., and J. D. McPhail (1988), Effect of incubation temperature on the development of five species of Pacific salmon (Oncorhynchus) embryos and alevins, *Can. J. Zool.*, *66*(1), 266–273, doi:10.1139/z88-038.

Neal, E. G., M. Todd Walter, and C. Coffeen (2002), Linking the pacific decadal oscillation to seasonal stream discharge patterns in Southeast Alaska, *J. Hydrol.*, *263*(1-4), 188–197, doi:10.1016/S0022-1694(02)00058-6.

Neuheimer, A. B., and C. T. Taggart (2007), The growing degree-day and fish size-at-age: the overlooked metric, *Can. J. Fish. Aquat. Sci.*, *64*(2), 375–385, doi:10.1139/f07-003.

Nichols, J. E., D. M. Peteet, C. M. Moy, I. S. Castaneda, A. McGeachy, and M. Perez (2014), Impacts of climate and vegetation change on carbon accumulation in a south-central Alaskan peatland assessed with novel organic geochemical techniques, *The Holocene*, *24*(9), 1146–1155, doi:10.1177/0959683614540729.

O'Driscoll, M. a., and D. R. DeWalle (2006), Stream–air temperature relations to classify stream–ground water interactions in a karst setting, central Pennsylvania, USA, *J. Hydrol.*, *329*(1-2), 140–153, doi:10.1016/j.jhydrol.2006.02.010.

Pitlick, J., E. R. Mueller, C. Segura, R. Cress, and M. Torizzo (2008), Relation between flow, surface-layer armoring and sediment transport in gravel-bed rivers, *Earth Surf. Process. Landforms*, *33*, 1192–1209, doi:10.1002/esp.1607.

Plafker, G. (1990), Regional vertical tectonic displacement of shorelines in south-central Alaska during and between great earthquakes, *Northwest Sci.*, *64*(5), 250–258.

Poole, G. C., and C. H. Berman (2001), An Ecological Perspective on In-Stream Temperature: Natural Heat Dynamics and Mechanisms of Human-Caused Thermal Degradation, *Environ. Manage.*, *27*(6), 787–802, doi:10.1007/s002670010188.

R Core Team (2015), R: A language and environment for statistical computing, R Foundation for Statistical Computing, Vienna, Austria,

Reimnitz, E. (1966), Late Quaternary History and Sedimentation of the Copper River Delta and Vicinity, Alaska. PhD Dissertation, University of California, San Diego.

Romero-Lankao, P., J. B. Smith, D. J. Davidson, N. S. Diffenbaugh, P. L. Kinney, P. Kirshen, P. Kovacs, and L. V. Ruiz (2014), Chpt 26. North America. In: Climate Change 2014: Impacts, Adaptation, and Vulnerability. Part B: Regional Aspects. Contribution of Working Group II to the Fifth Assessment Report of the Intergovernmental Panel on Climate Change, in *Climate Change 2014: Impacts, Adaptation, and Vulnerability. Part B: Regional Aspects. Contribution of Working Group II to the Fifth Assessment Report of the Intergovernmental Panel on Climate Change*, edited by V. R. Barros et al., pp. 1439–1498, Cambridge University Press, Cambridge, United Kingdom and New York, NY, USA.

Schindler, D. E., D. E. Rogers, M. D. Scheuerell, and C. A. Abrey (2013), Effects of Changing Climate on Zooplankton and Juvenile Sockeye Salmon Growth in Southwestern Alaska, *Ecology*, *86*(1), 198–209.

Shanley, C. S., and D. M. Albert (2014), Climate Change Sensitivity Index for Pacific Salmon Habitat in Southeast Alaska, *PLoS One*, *9*(8), e104799, doi:10.1371/journal.pone.0104799.

Shanley, C. S. et al. (2015), Climate change implications in the northern coastal temperate rainforest of North America, *Clim. Change*, *130*(2), 155–170, doi:10.1007/s10584-015-1355-9.

Shepard, B. G., G. F. Hartman, and W. J. Wilson (1986), Relationships between stream and intra-gravel temperatures in coastal drainage, and some implications for fisheries workers, *Can. J. Fish. Aquat. Sci.*, *43*, 1818–1822.

Sinokrot, B. a., and H. G. Stefan (1993), Stream temperature dynamics: measurements and modeling, *Water Resour. Res.*, *29*(7), 2299–2312, doi:10.1029/93WR00540.

Smith, C. T., R. J. Nelson, C. C. Wood, and B. F. Koop (2001), Glacial biogeography of North American coho salmon (Oncorhynchus kisutch)., *Mol. Ecol.*, *10*, 2775–2785, doi:10.1046/j.1365-294X.2001.t01-1-01405.x.

Tague, C., G. Grant, M. Farrell, J. Choate, and A. Jefferson (2008), Deep groundwater mediates streamflow response to climate warming in the Oregon Cascades, *Clim. Change*, *86*(1-2), 189–210, doi:10.1007/s10584-007-9294-8.

Tarr, R. S., and L. Martin (1914), *Alaskan Glacier Studies*, The National Geographic Society, Washington.

Thilenius, J. F. (1990a), Plant Succession on Earthquake Uplifted Coastal Wetlands, Copper River Delta, Alaska, *Northwest Sci.*, *64*(5), 259–262.

Thilenius, J. F. (1990b), Woody plant succession on earthquake-uplifted coastal wetlands of the Copper River Delta, Alaska, *For. Ecol. Manage.*, *33/34*, 439–462.

Tuthill, S. J., and W. M. Laird (1966), Geomorphic Effects of the Earthquake of March 27, 1964 In the Martin-Bering Rivers Area, Alaska, *U.S. Geol. Surv. Prof. Pap.*, *543-B*, 1–28.

U.S. Geological Survey (2013), National Hydrography Geodatabase, *Natl. Map Viewer available World Wide Web (http//viewer.nationalmap.gov/viewer/nhd.html?p=nhd), accessed Oct. 2015.*

University of Alaska (2015), Scenarios Network for Alaska and Arctic Planning, *www.snap.uaf.edu*.

Waller, R. M. (1966), Effects on Hydrologic Regimen, in *The Alaska Earthquake March 27, 1964: Effects on Hydrologic Regimen*, vol. 544-A, pp. 1–27.

Waples, R. S., T. Beechie, and G. R. Pess (2009), Evolutionary History, Habitat Disturbance Regimes, and Anthropogenic Changes: What Do These Mean for Resilience of Pacific Salmon Populations ?, *Ecol. Soc.*, *14*(1), 18.

Wawrzyniak, V., H. Piégay, P. Allemand, L. Vaudor, and P. Grandjean (2013), Prediction of water temperature heterogeneity of braided rivers using very high resolution thermal infrared (TIR) images, *Int. J. Remote Sens.*, *34*(13), 4812–4831, doi:10.1080/01431161.2013.782113.

Webb, B. W., and F. Nobilis (1997), Long-term perspective on the nature of the air-water temperature relationship: A case study, *Hydrol. Process.*, *11*(2), 137–147, doi:10.1002/(SICI)1099-1085(199702)11:2<137::AID-HYP405>3.0.CO;2-2.

Webb, B. W., and Y. Zhang (1997), Spatial and seasonal variability in the components of the river heat budget, *Hydrol. Process.*, *11*, 79–101, doi:10.1002/(SICI)1099-1085(199701)11:1<79::AID-HYP404>3.3.CO;2-E.

Wiedmer, M., D. R. Montgomery, A. R. Gillespie, and H. Greenberg (2010), Late Quaternary megafloods from Glacial Lake Atna, Southcentral Alaska, U.S.A., *Quat. Res.*, *73*(3), 413–424, doi:10.1016/j.yqres.2010.02.005.

Wilson, F. H., C. P. Hults, K. A. Labay, and N. Shew (2008), Digital data for the reconnaissance geologic map for Prince William Sound and the Kenai Peninsula, Alaska, *U.S. Geol. Surv. Open-File Rep. 2008-1002*.

Winkler, B. G. R., G. Plafker, R. J. Goldfarb, J. E. Case, and D. L. Peck (1992), *The Alaska Mineral Resource Assessment Program : Background Information to Accompany Geologic and Mineral-Resource Maps of the Cordova and Middleton Island Quadrangles , Southern Alaska*.

Wobus, C., R. Prucha, D. Albert, C. Woll, M. Loinaz, and R. Jones (2015), Hydrologic Alterations from Climate Change Inform Assessment of Ecological Risk to Pacific Salmon in Bristol Bay, Alaska, *PLoS One*, *10*(12), e0143905, doi:10.1371/journal.pone.0143905.

Zhang, T., S. A. Bowling, and K. Stamnes (1997), Impact of the atmosphere on surface radiative fluxes and snowmelt in the Artic and Subartic, *J. Geophys. Res.*, *102*(D4), 4287–4303, doi:10.1175/1520-0442(1996)009<2110:IOCOSR>2.0.CO;2.

Zimmerman, C. E., and J. E. Finn (2012), A Simple Method for In Situ Monitoring of Water Temperature in Substrates Used by Spawning Salmonids, *J. Fish Wildl. Manag.*, *3*(2),

288–295, doi:10.3996/032012-JFWM-025.

2.9 Figures

Table 2.1 Location and description of temperature monitoring sites used in this study (n=18). Catchment characteristics were calculated from 5m resolution DEM data

ID	Site Information								Catchment Characteristics					
	Latitude decimal degrees	Longitude degrees	Installation Date	Last Reading	Days of data (%	Salmon Sp. Present	Lake Inlet?	Upwelling Groundwater?	Area (ha)	Elevation (m)			Slope (deg)	
										Min	Max	Mean	Mean	SD
Black	60.45	-145.24	21-Sep-2013	30-Sep-2015	739 (100)	Coho			424	8	715	118	14	13
Clear	60.57	-144.78	19-Oct-2010	16-Sep-2015	1793 (100)	Sockeye, coho		Y	3504	19	1329	337	23	20
ET.MF	60.46	-145.31	19-Sep-2012	30-Sep-2015	1106 (100)	Coho			955	9	908	212	19	16
ET.Mi	60.46	-145.29	13-Nov-2009	30-Sep-2015	2147 (100)	Coho			188	8	83	33	7	5
ET.WF	60.46	-145.32	17-Apr-2013	30-Sep-2015	1054 (95)	Coho			201	9	115	23	5	8
EyakL	60.56	-145.64	19-Oct-2010	4-May-2015	1389 (100)	Sockeye, coho	Y		792	5	962	433	28	13
Hatch	60.59	-145.64	19-Sep-2011	30-Sep-2015	1472 (100)	Sockeye, coho		Y	454	8	886	308	24	13
Ibeck	60.59	-145.47	18-Jun-2011	8-Sep-2015	1543 (100)	Coho		Y	336	48	109	74	3	2
LMart	60.40	-144.61	20-Oct-2010	7-Jun-2015	1691 (100)	Sockeye, coho			2156	29	547	158	11	11
LoIbe	60.55	-145.50	1-Oct-2012	18-Jun-2015	990 (100)	Coho			202	21	61	40	1	1
Marti	60.34	-144.52	20-Oct-2010	6-Jun-2015	1690 (100)	Sockeye, coho	Y		2274	27	986	271	20	14
McKin	60.47	-145.19	13-Nov-2009	28-Jul-2015	1274 (73)	Sockeye, coho	Y		155	9	715	224	24	12
Ot.Ca	60.53	-145.46	26-Jul-2011	30-Sep-2015	1493 (98)	Coho			166	20	214	83	11	7
Power	60.59	-145.62	13-Nov-2009	30-Sep-2015	1939 (90)	Sockeye, coho			5426	16	1468	622	27	14
S.Bag	60.44	-145.14	4-Oct-2012	30-Sep-2015	1091 (100)	Coho			418	12	676	160	13	13
Salmo	60.45	-145.17	13-Nov-2009	30-Sep-2015	1985 (92)	Sockeye, coho		Y	2267	11	1257	388	26	15
Sheri	60.48	-145.40	4-Oct-2012	30-Sep-2015	1091 (100)	Coho			110	16	34	21	2	2
TF.Mi	60.44	-145.12	19-Oct-2010	30-Sep-2015	1807 (100)	Sockeye, coho		Y	61	11	42	25	3	2

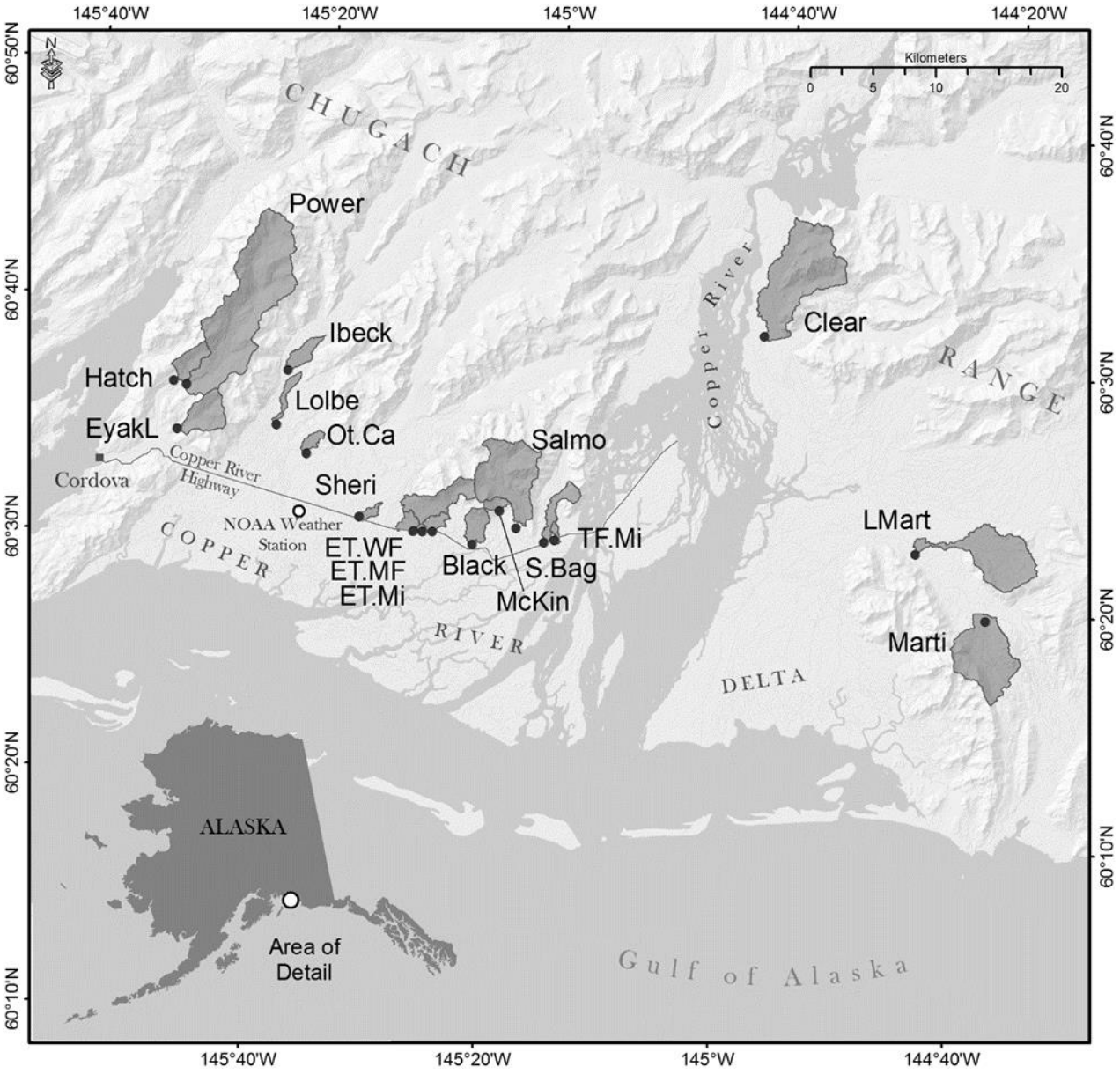

Figure 2.1 Map of study site locations on the Copper River Delta, Alaska. Study catchments were interpolated from surficial topography using a 5m resolution DTM. Map produced by K. Christiansen, USFS

Table 2.2 Land cover statistics for the study catchments. Statistics calculated from National Hydrography Dataset (NHD), National Land Cover (NLC), and U.S. Geological Survey (USGS) surficial geology data

ID	Percent of Catchment Area												
	NHD Waterbody		NLC Land Cover							USGS Surficial Geology			
										Deposits	Bedrock		
	Lake	Ice	Developed-light	Barren	Forested	Shrub/ Grassland	Herb-acious	Woody Wetland	Emergent Wetland	Drift & Colluvium	Granitic	Sedimentary	Basaltic
Black	0.6	0.0	0.0	0.0	47.1	34.7	0.1	18.0	0.0	0.0	0.0	98.0	0.0
Clear	0.3	1.8	0.4	20.2	35.6	35.2	0.7	0.8	0.0	35.0	0.0	53.3	0.6
ET.MF	0.5	0.0	0.1	0.4	46.4	35.9	0.3	15.4	0.0	25.2	62.6	12.1	0.0
ET.Mi	0.0	0.0	0.5	0.0	56.8	10.1	0.0	30.4	0.4	13.0	70.6	16.0	0.0
ET.WF	1.2	0.0	2.2	0.0	30.9	15.4	0.0	50.7	0.0	87.2	14.9	0.0	0.0
EyakL	0.0	0.0	0.0	18.2	42.5	34.2	0.1	0.0	0.0	0.0	0.0	95.4	0.0
Hatch	0.0	0.0	0.8	0.7	51.2	45.5	1.2	0.0	0.0	23.0	0.0	0.0	77.2
Ibeck	0.0	0.0	0.0	12.7	3.6	60.1	7.0	16.4	0.0	100.0	0.0	0.0	0.0
LMart	15.4	0.0	0.0	0.6	46.8	20.4	1.1	16.1	0.0	24.6	0.0	60.1	0.0
LoIbe	0.0	0.0	0.0	86.1	0.0	0.2	0.0	12.0	0.2	100.0	0.0	0.0	0.0
Marti	1.3	0.0	0.0	8.8	28.3	49.7	0.9	8.4	0.7	21.0	0.0	46.2	21.4
McKin	0.0	0.0	0.0	1.3	74.6	23.2	0.3	0.6	0.0	0.0	0.0	100.0	0.0
Ot.Ca	6.7	0.0	0.0	0.0	49.0	37.6	0.0	11.5	0.0	0.0	0.0	99.7	0.0
Power	0.0	12.7	0.2	33.2	23.1	25.7	0.4	0.3	0.0	12.0	7.3	16.8	38.0
S.Bag	0.0	0.0	1.5	1.3	69.7	22.2	1.6	3.8	0.0	54.5	0.0	41.3	0.0
Salmo	0.1	7.2	0.0	15.2	45.6	31.2	0.2	0.3	0.0	9.8	7.2	71.6	0.0
Sheri	0.0	0.0	1.2	0.0	2.0	0.1	0.0	96.1	0.2	100.0	0.0	0.0	0.0
TF.Mi	0.0	0.0	0.9	0.0	43.5	16.7	0.3	38.5	0.0	100.0	0.0	0.0	0.0

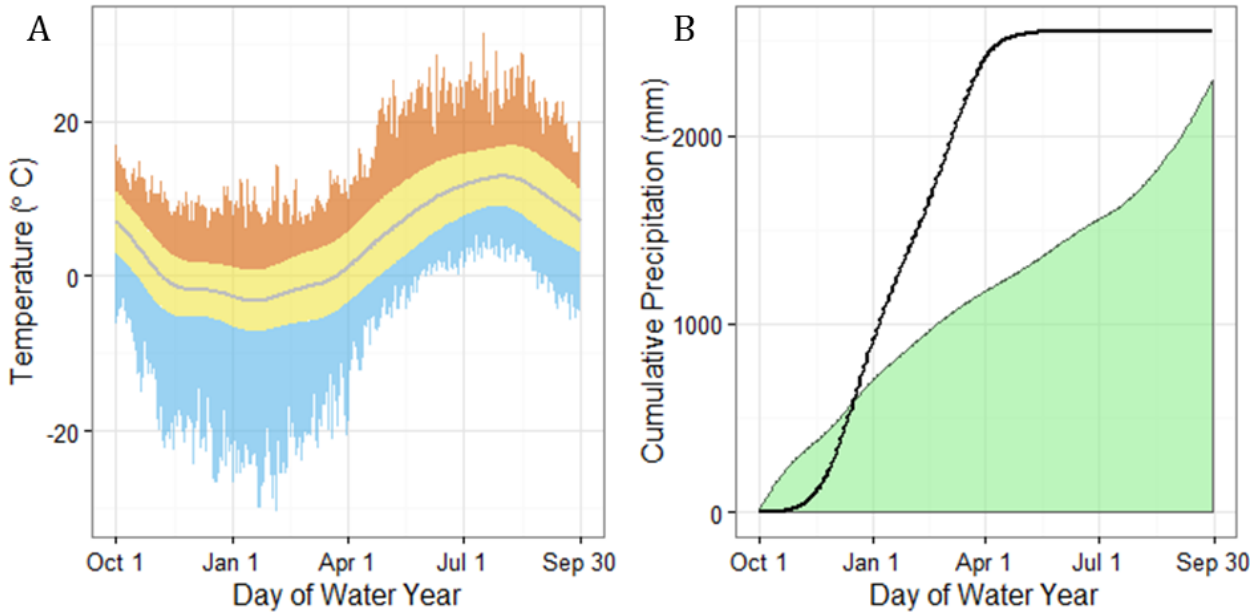

Figure 2.2 A) Climatological daily mean (gray line), normal daily range (yellow ribbon), and daily record low (blue) and high (orange) air temperatures and B) cumulative normal daily precipitation accumulation in mm (green) and cumulative normal daily snowfall accumulation in mm (black line) based on 31 years of record (1980-2010) at 13 m elevation within the study area.

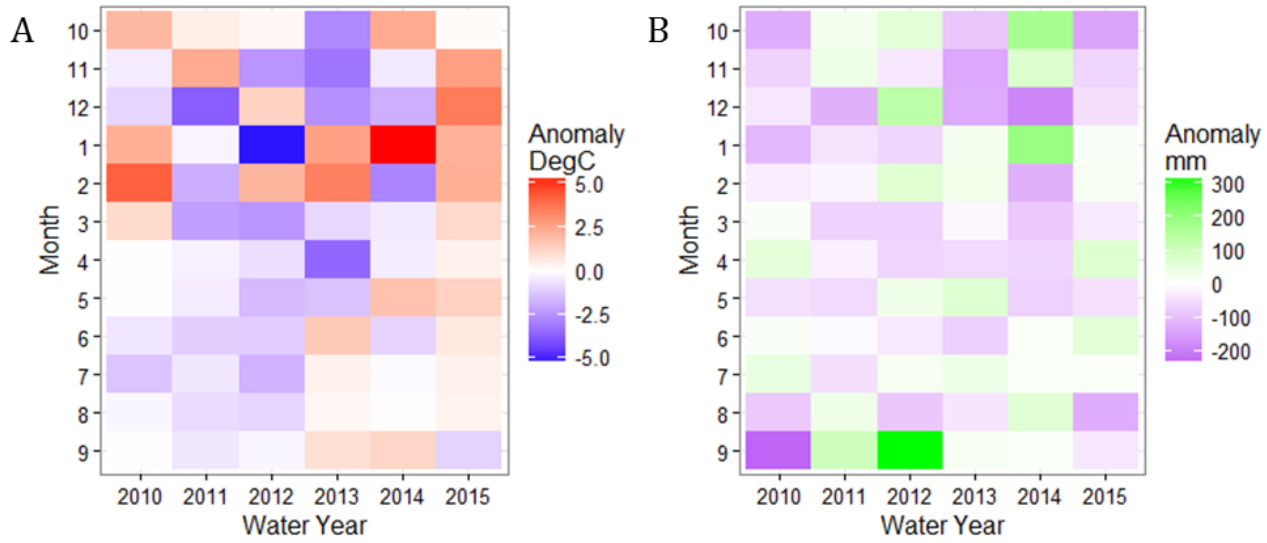

Figure 2.3 A) Monthly air temperature anomalies (°C) and B) monthly precipitation anomalies (mm) during the study period.

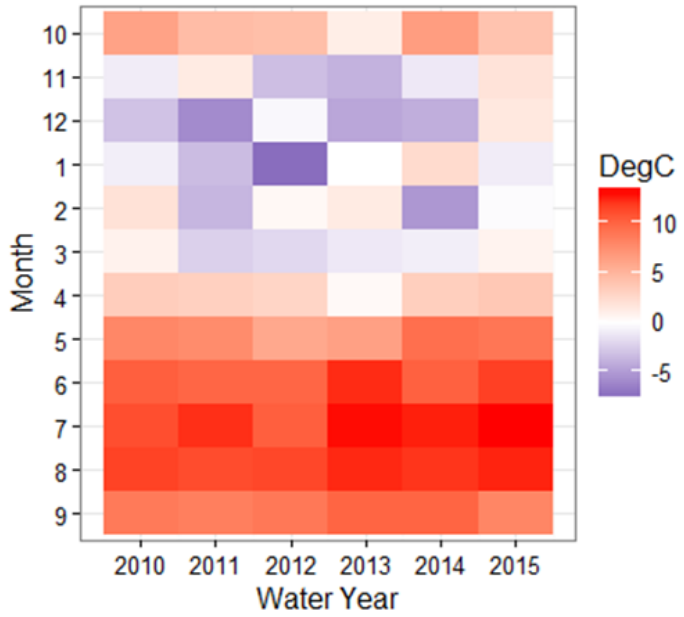

Figure 2.4 Monthly mean air temperature (°C) recorded during the study period at l3 m elevation within the study area.

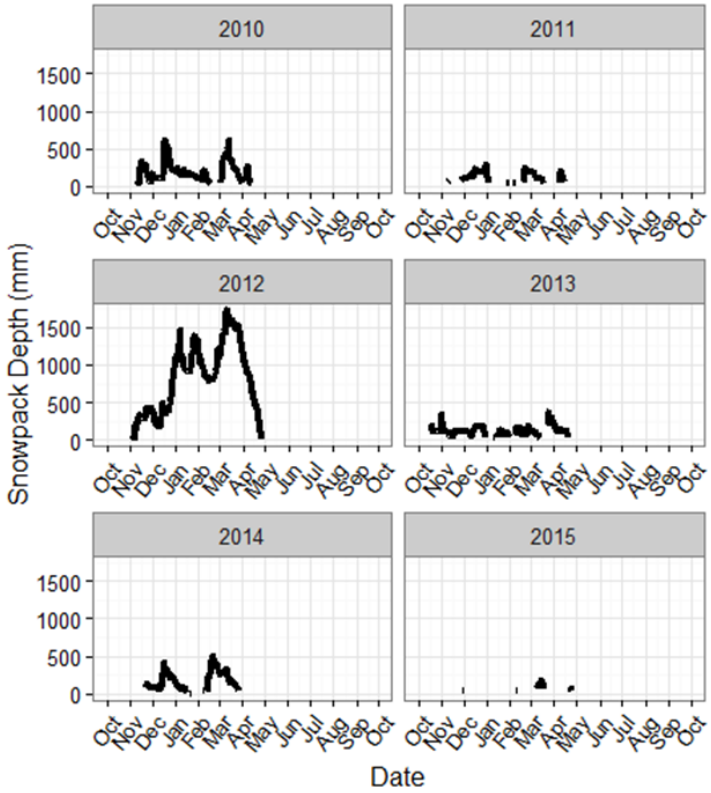

Figure 2.5 Snowpack depth (mm) measured during the study period at 13 m elevation within the study area.

Table 2.3 Observed and projected air temperatures for the study area. GHCN observed data were from NOAA weather station #26410. PRISM-interpolated historical data and projected air temperatures were from Scenarios Network for Arctic Planning (snap.uaf.edu). Projected air temperatures were based on a five-model average at 2 km resolution under a mid-range (RCP 6.0) emissions scenario. Anomalies were calculated based on 1980-2010 GHCN averages.

Month	Observed Air Temperature °C				Projected Air Temperature °C by Decade			
	Interpolated from PRISM (1961-1990)	GHCN						
		1980-2010	WY 2010-WY 2014	WY 2015	2010-2019	2040-2049	2060-2069	2090-2099
Oct	4.7	4.3	4.7	4.1	6.3	6.6	7.1	7.9
Nov	0.1	-0.9	-1.8	1.9	0.9	2.0	3.2	3.4
Dec	-1.6	-2.0	-3.6	1.6	-0.9	0.8	1.3	2.4
Jan	-2.7	-3.0	-2.1	-0.9	-1.5	0.0	1.4	2.3
Feb	-1.9	-2.0	-1.1	-0.2	-0.9	1.1	2.7	3.5
Mar	-0.1	-0.4	-1.5	0.8	1.4	2.8	3.9	4.9
Apr	3.8	3.3	2.3	3.8	5.0	5.6	6.8	7.7
May	7.4	7.4	7.1	9.0	8.3	9.1	10.1	11.3
Jun	10.9	10.7	10.2	11.7	12.4	14.0	14.5	15.4
Jul	13.1	12.4	11.8	13.1	14.5	15.3	15.7	16.6
Aug	12.8	12.1	11.8	12.6	14.0	14.6	15.2	16.0
Sep	9.4	9.0	9.2	8.1	10.6	11.2	11.8	12.5
Winter (DJF) Anomaly			+0.1	+2.5	+1.2	+3.0	+4.1	+5.1
Incubation Season (Oct-May) Anomaly			-0.3	+1.7	+1.5	+2.7	+3.7	+4.6

Table 2.4 Model equations applied to landscape and climate sensitivity data. Landscape models A & B use site-specific scores of principal component axes 1 & 2 (PC1 & PC2) to predict T*, which represents eleven different weekly temperature metrics (listed in the text and Table 6). Linear climate sensitivity models 1 &2 correlate T_w (mean monthly water temperature) with variable T_a (monthly mean air temperature) and coefficients for slope (*m*) and intercept (*B*). Logistic climate sensitivity models 3 & 4 correlate T_w with T_a utilizing four parameters of fit: mu (μ), alpha (α), beta (β), and gamma (γ) [*Mohseni et al.*, 1998]. Model 4 incorporates rising and falling limbs to account for seasonal hysteresis.

Type	Form	Model ID	Data Constraints	Equation
Landscape	MLR	A	n=18, all sites	$T^* = B + m_1 PC1 + m_2 PC2$
		B	n=13, GW sites removed	
Climate Sensitivity	Linear	1	$T_a > 0$ °C	$T_w = B + mT_a$
		2	$T_w > 0.5$ °C	
	4-Parameter Logistic	3	None	$T_w = \mu + \frac{\alpha - \mu}{1 + e^{\gamma(\beta - T_a)}}$
		4: falling limb	T_a from months: Aug, Sep, Oct, Nov, Dec, Jan	
		4: rising limb	T_a from months: Feb, Mar, Apr, May, Jun, Jul	

Table 2.5 Temperature statistics for all recorded daily mean temperatures by site.

Site ID	Full Record	Incubation Period (Oct-May)			Summer (Jun-Sep)		
	Variance	Maxima ° C	Minima ° C	Variance	Maxima ° C	Minima ° C	Variance
Black	14.2	9.3	0.0	6.1	12.5	5.1	1.9
Clear	5.5	8.6	0.0	2.5	9.3	3.6	1.5
ET.MF	29.0	17.2	0.0	13.6	18.9	6.3	6.0
ET.Mi	17.7	14.8	0.0	6.3	16.0	4.1	5.0
ET.WF	18.7	12.1	0.1	8.4	14.5	5.2	3.0
EyakL	5.5	7.6	0.0	2.8	9.9	2.1	3.4
Hatch	1.4	5.5	0.8	0.6	8.6	2.4	1.2
Ibeck	1.0	3.1	0.1	0.3	4.1	1.2	0.3
LMart	32.9	19.0	0.0	11.4	20.2	2.8	9.5
LoIbe	15.4	11.4	0.0	7.2	13.5	5.4	2.7
Marti	7.9	10.4	0.0	3.2	10.8	1.4	4.0
McKin	7.7	8.2	0.0	4.0	10.3	3.5	1.5
Ot.Ca	36.8	17.4	0.0	10.6	19.6	3.6	9.7
Power	3.7	6.6	0.0	1.8	8.0	3.1	0.9
S.Bag	13.5	14.2	0.0	6.6	12.7	5.1	2.6
Salmo	1.5	6.8	0.9	0.7	8.5	3.4	0.8
Sheri	31.7	17.6	0.0	17.5	18.4	0.7	14.2
TF.Mi	1.1	7.5	0.0	0.8	8.1	4.0	0.2

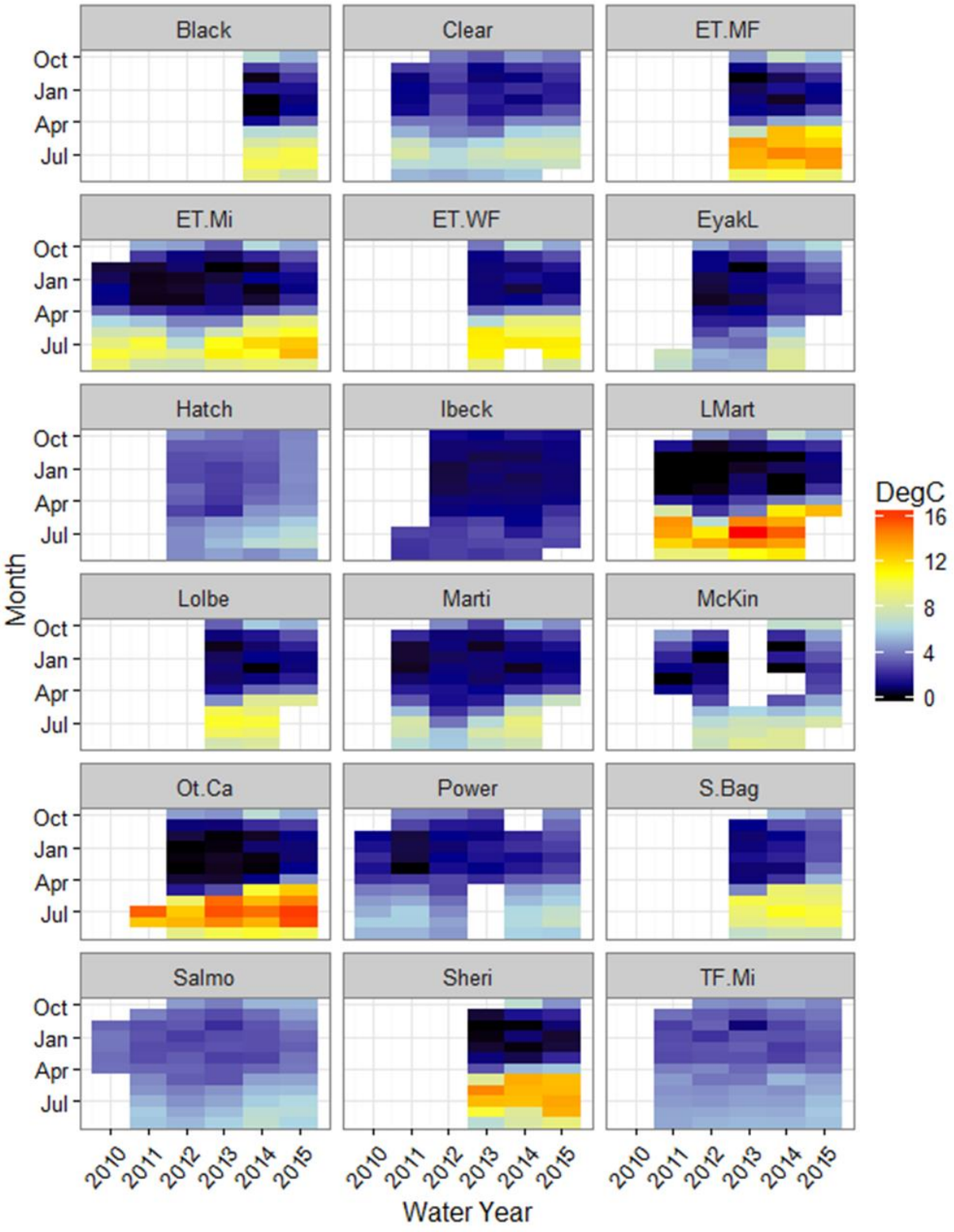

Figure 2.6 Monthly mean water temperature (°C) by site. Freezing (< 0.5 °C) temperatures are denoted by black squares.

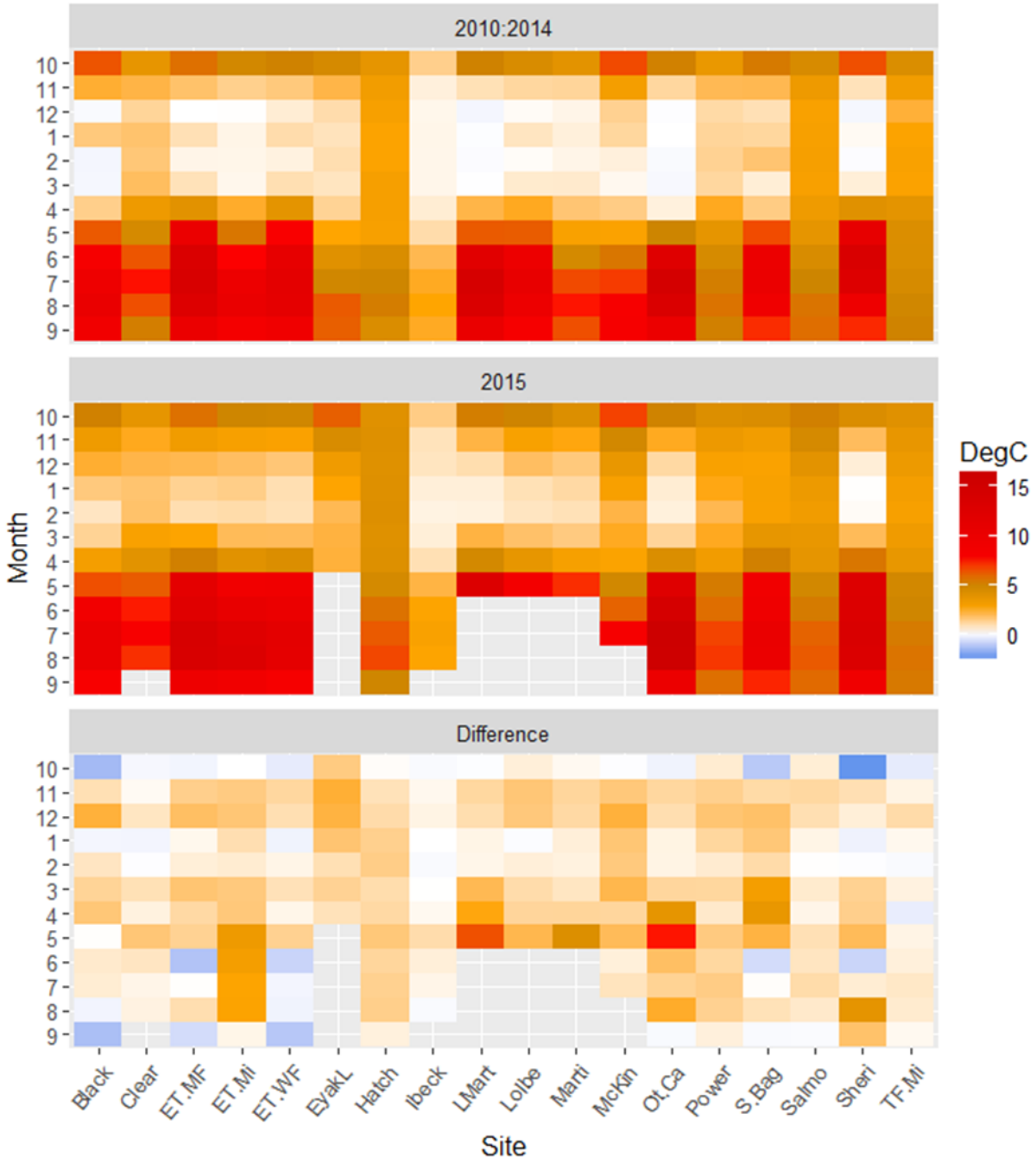

Figure 2.7 The difference (bottom panel) between monthly mean water temperature in WY 2015 (middle panel) and the average of all WY 2010-2014 monthly mean water temperatures (top panel).

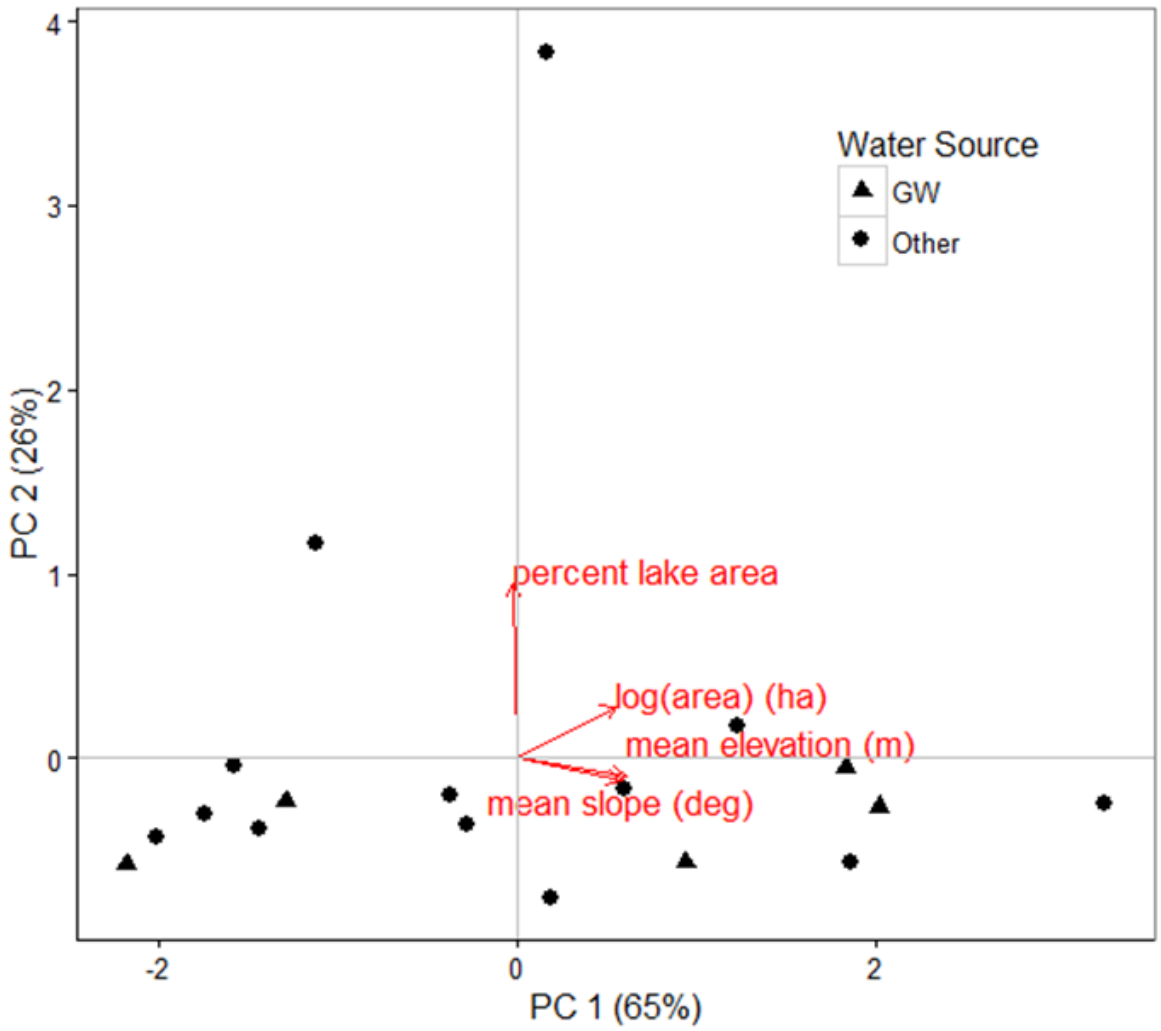

Figure 2.8 Ordination plot based on the four landscape predictors. The landscape predictors are: 1) mean catchment elevation (m), 2) catchment area (log-transformed hectares), 3) mean catchment slope (degrees), and 4) percent of catchment area covered by lakes. Points denote scores for the 18 study catchments. Triangles denote the sites with known upwelling groundwater (n=5).

Table 2.6 . Multiple linear regression models fitting PC 1 and PC 2 to eleven temperature metrics. The significance of slope and intercept values is denoted with stars.

Type	Time Period	Metric	*All Sites (n=18)*					*Groundwater Sites Removed (n=13)*				
			Intercept	**Slope 1**	**Slope 2**	**adj. R^2**	**P Value**	**Intercept**	**Slope 1**	**Slope 2**	**adj. R^2**	**P Value**
Magnitude	Incubation	Avg. mean temperature	2.43***	0.00	-0.12	-0.10	0.78	2.33***	-0.08	-0.08	-0.03	0.48
	Incubation	Max. temperature	11.82***	-1.05	2.32*	0.29	0.03	13.11***	-1.31	1.83*	0.35	0.05
	Summer	Avg. mean temperature	8.13***	-0.77	1.51*	0.31	0.03	9.11***	-1.21**	1.13*	0.65	0.005
	Summer	Max. temperature	12.78***	-1.31*	2.74*	0.39	0.01	14.28***	-2.01**	2.12**	0.71	0.001
	Year-round	Avg. mean temperature	3.99***	-0.23	0.35	0.12	0.16	4.17***	-0.44**	0.28	0.46	0.02
	Year-round	Max. temperature	13.21***	-1.16	2.59*	0.38	0.02	14.70***	-1.55**	2.03**	0.62	0.004
Variability	Incubation	Variance	4.89***	-1.12	1.51	0.19	0.09	6.19***	-1.52	1.01	0.25	0.1
	Summer	Variance	2.82***	-0.51	1.51*	0.25	0.05	3.48**	-0.71	1.26	0.23	0.12
	Year-round	Variance	12.54***	-2.81*	6.23**	0.44	0.01	15.63***	-3.78*	5.03*	0.59	0.005
Frequency	Incubation	% cold (<0.5 ^{o}C) days	23.11***	-4.65*	8.53*	0.39	0.01	27.22***	-4.42	6.73*	0.44	0.03
	Incubation	% warm (>2 ^{o}C) days	50.11***	3.62	-6.35	0.01	0.37	42.12***	0.69	-2.72	-0.01	0.42
							significance stars	* p<0.05	**p<0.01	***p<0.001		

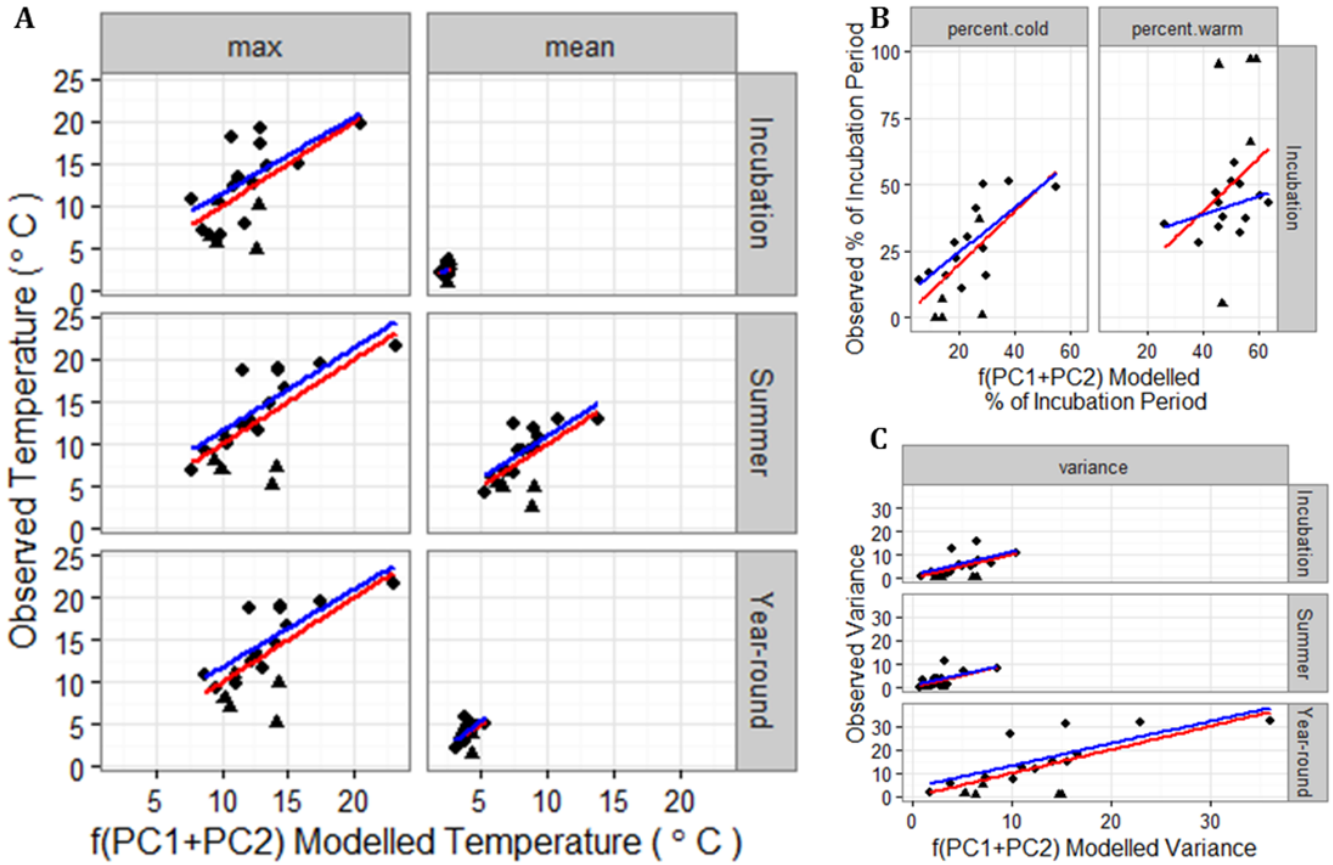

Figure 2.9 Linear regressions of MLR modelled data vs. observed data. A) MLR modelled temperature vs. observed temperature (°C) for average mean and maximum recorded temperature, B) MLR modelled percentage of incubation period in days vs. observed percentage of incubation period in days for percent cold (<0.5 °C) and percent warm (>2°C), and C) MLR modelled variance vs. observed variance in daily mean temperature. Groundwater sites are denoted by triangles. Modelled vs. observed regression lines indicate goodness of fit. The red line fits Model A (all sites) and the blue line fits Model B (groundwater-dominated sites removed)

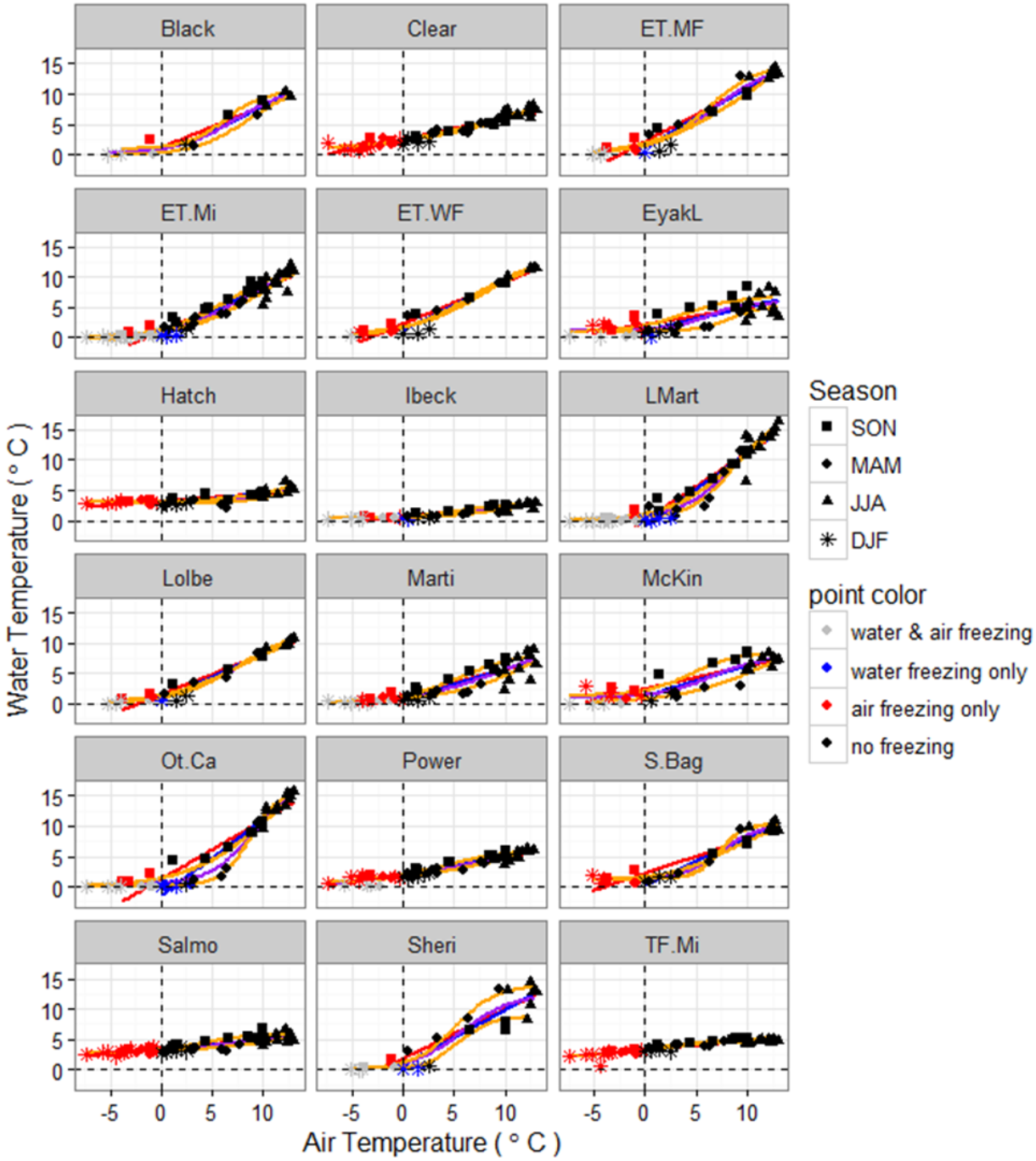

Figure 2.10 Linear and logistic regressions of monthly air vs. water temperature (°C) for all sites, for all months WY 2010-2014. The blue lines were fitted using linear Model 1 (air temperature >0 °C), the red lines were fitted using linear Model 2 (water temperature >0.5 °C), the purple lines were fitted using logistic Model 3 (all data), and the orange lines were fitted using logistic Model 4 (all data, split by seasonal hysteresis). The red points were used by Model 2 only, blue points by Model 1 only, black points by all

models, and gray points by logistic models only. Point shape denotes the season of the observation.

Table 2.7 Metrics of goodness-of-fit for 4 models of the monthly mean air-water temperature relationship using WY 2010 - 2014 data.

Site ID	Adjusted R^2		Root Mean Squared Error (°C)				
	Model 1	Model 2	Model 1	Model 2	Model 3	Model 4 falling limb	Model 4 rising limb
Black	0.92	0.85	0.8	1.2	0.9	0.7	0.2
Clear	0.89	0.90	0.6	0.7	0.6	0.5	0.6
ET.MF	0.93	0.92	1.3	1.4	1.1	1.0	0.8
ET.Mi	0.90	0.86	1.1	1.2	1.0	0.7	1.0
ET.WF	0.94	0.93	0.9	1.1	0.8	0.8	0.7
EyakL	0.50	0.48	1.6	1.6	1.5	1.2	1.1
Hatch	0.62	0.55	0.7	0.7	0.5	0.5	0.6
Ibeck	0.78	0.76	0.4	0.4	0.3	0.2	0.3
LMart	0.90	0.86	1.7	1.9	1.2	0.8	1.5
LoIbe	0.96	0.93	0.7	0.9	0.6	0.7	0.5
Marti	0.69	0.73	1.4	1.4	1.2	0.6	1.2
McKin	0.63	0.67	1.5	1.5	1.3	1.0	0.7
Ot.Ca	0.92	0.83	1.7	2.2	1.1	0.9	0.5
Power	0.86	0.87	0.6	0.6	0.6	0.5	0.5
S.Bag	0.94	0.86	0.9	1.4	0.8	0.6	0.5
Salmo	0.60	0.70	0.7	0.6	0.6	0.5	0.4
Sheri	0.77	0.76	2.2	2.2	1.8	0.9	0.9
TF.Mi	0.64	0.80	0.4	0.4	0.4	0.5	0.3
mean	0.80	0.79	1.1	1.2	0.9	0.7	0.7

Table 2.8 Coefficients of fit for models 1-4 generated with monthly mean data from WY 2010 - 2014.

Site ID	Linear				4 Parameter Logistic											
	Model 1		Model 2		Model 3				Model 4							
									falling limb				rising limb			
	Slope	Intercept	Slope	Intercept	Mu	Alpha	Gamma	Beta	Mu	Alpha	Gamma	Beta	Mu	Alpha	Gamma	Beta
Black	0.9	-0.5	0.7	1.2	0.1	11.2	0.4	7.0	0.9	10.5	0.5	6.1	0.0	11.5	0.4	8.5
Clear	0.4	2.0	0.3	2.6	0.4	12.2	0.2	10.6	0.7	11.4	0.2	10.7	0.0	12.1	0.2	9.5
ET.MF	1.0	1.1	0.9	2.2	0.1	15.7	0.3	6.9	0.0	18.6	0.2	9.1	0.3	14.8	0.4	6.0
ET.Mi	0.8	0.3	0.7	1.1	0.0	12.9	0.3	7.9	0.0	12.0	0.3	6.3	0.0	14.3	0.3	9.4
ET.WF	0.8	1.3	0.7	2.3	0.3	13.5	0.3	7.0	0.5	13.5	0.3	7.5	0.0	13.3	0.3	6.5
EyakL	0.4	1.1	0.3	2.2	1.2	5.8	0.6	6.0	0.9	6.7	0.4	3.6	1.0	5.1	0.7	8.3
Hatch	0.2	2.5	0.1	3.2	3.0	5.5	0.9	9.7	3.0	6.5	0.3	10.2	2.9	4.8	7.5	9.2
Ibeck	0.2	0.4	0.2	0.6	0.4	2.9	0.4	7.4	0.4	2.9	0.4	5.7	0.3	3.8	0.3	10.8
LMart	1.2	-0.8	1.1	0.2	0.0	19.0	0.4	9.0	0.0	17.9	0.3	8.3	0.2	17.6	0.5	8.7
LoIbe	0.8	0.6	0.7	1.5	0.0	12.7	0.3	7.8	0.0	12.4	0.3	7.7	0.0	12.4	0.3	7.5
Marti	0.5	0.6	0.4	1.3	0.0	10.8	0.2	9.6	0.1	8.4	0.3	5.4	0.2	19.0	0.2	15.4
McKin	0.5	1.2	0.4	2.4	1.0	7.8	0.4	6.4	1.4	8.3	0.5	4.4	0.2	11.1	0.3	10.8
Ot.Ca	1.2	-1.4	1.0	1.3	0.3	17.8	0.5	9.0	0.0	21.6	0.3	10.1	0.1	16.4	0.7	8.8
Power	0.3	1.7	0.3	2.1	0.0	8.9	0.2	8.5	0.5	6.3	0.3	3.7	0.0	14.7	0.1	15.7
S.Bag	0.8	0.3	0.6	2.2	1.2	10.2	0.6	7.2	1.1	10.7	0.3	8.0	1.2	10.3	0.9	7.2
Salmo	0.2	3.0	0.2	3.3	2.8	5.8	0.3	6.4	2.7	6.1	0.4	4.1	2.8	6.8	0.2	11.4
Sheri	0.9	0.7	0.8	1.9	0.0	12.2	0.4	5.6	0.2	8.7	0.7	5.5	0.1	13.9	0.5	5.0
TF.Mi	0.1	3.4	0.1	3.2	1.9	5.0	0.3	0.8	1.8	5.3	0.3	0.9	2.3	4.7	0.3	1.5

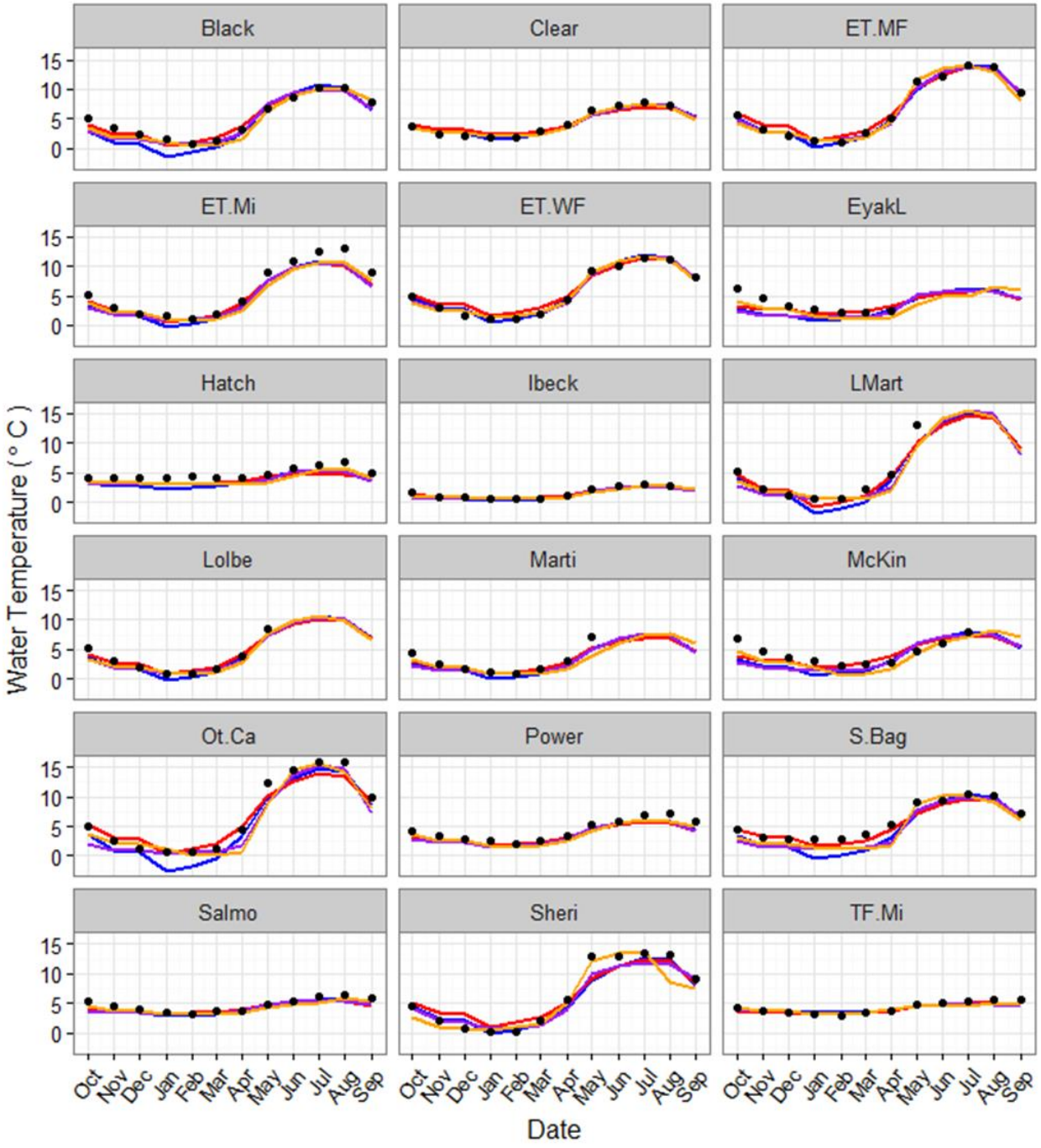

Figure 2.11 Observed (points) vs. hindcasted (lines) monthly water temperature data by site for water year 2015. Line colors follow Figure 2.10.

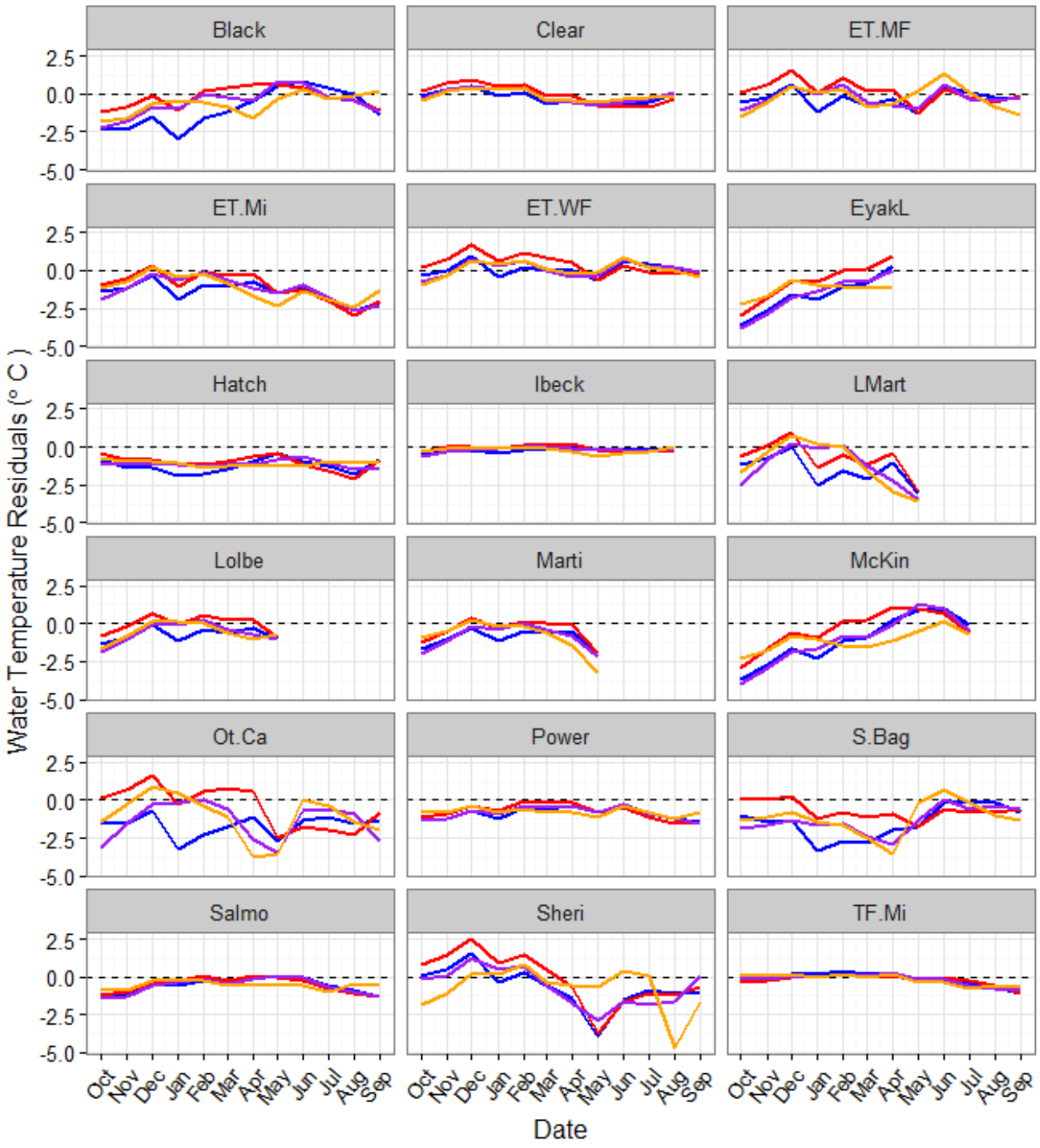

Figure 2.12 The differences between observed and hindcast monthly mean water temperatures for the four models. Line colors follow Figure 2.10. Data gaps in the spring and summer months indicate sites where the observed data have yet to be retrieved from the field.

3 Winter Severity and Catchment Geomorphology Influence Water Temperature and Scour Potential within Pacific Salmon Incubation Gravels, Copper River Delta, Alaska.

3.1 Abstract

Climatic changes are projected to impact Pacific Salmon egg incubation by increasing the magnitude and frequency of winter freshets and by raising water temperatures. More powerful and more frequent winter freshets could reduce the survival of salmon eggs by increasing streambed scour. Projected increases in water temperature may accelerate embryo development, impacting juvenile viability. I collected water temperature and stream stage data year-round and surveyed channel geometry at salmon spawning reaches on the Copper River Delta, a large coastal foreland in Southcentral Alaska. I calculated streambed scour and compared water temperatures during climatological mean and anomalously warm incubation periods to elucidate potential climate change impacts. Reach-scale mean scour depth ranged between 3 and 72 cm, suggesting the impacts of scour on egg mortality will be variable across the landscape. The magnitude and seasonality of accumulated thermal units (^{o}C/day) (ATU) within spawning gravels varied significantly between severe and mild winters at shallow flowpath sites, but not at groundwater upwelling sites. When seasonal snow and ice was absent, increases in spring (MAM) ATU at shallow flowpath sites were particularly significant. Our observations suggest both water temperature and streambed scour responses to climatic changes are likely to vary across the landscape, even at small spatial scales, because of heterogeneity in catchment and channel characteristics and upwelling of groundwater.

3.2 Introduction

Pacific salmon (*Oncorhynchus* spp.) and other salmonids face numerous challenges associated with climate change. Most research in this area has focused on the potential effects of elevated summer (JJAS) temperatures on adults and juveniles; however, climatic changes are also projected to significantly alter the streambed incubation environment of embryos during the late autumn (ON), winter (DJF), and spring (MAM) seasons. These

impacts may have a greater effect than summer temperatures on the production of fall-spawning salmon at high latitudes, including coastal Alaska.

Climate models project mean monthly air temperatures along the Gulf of Alaska coastline to increase 3-5°C by 2080, based on mid-range emissions scenarios [*Romero-Lankao et al.*, 2014; *Shanley and Albert*, 2014; *University of Alaska*, 2015]. These changes will be particularly significant during winter. Mean DJF monthly air temperatures are projected to surpass the freezing point, greatly reducing low elevation snowpack and seasonal ice cover on waterways [*McAfee et al.*, 2014]. Meltwater from seasonal snow and ice is an important water source that contributes to discharge and significantly cools water temperatures throughout JJAS [*Kyle and Brabets*, 2001; *Neal et al.*, 2002; *Lisi et al.*, 2015] and recent research [*Leppi et al.*, 2014; *Shanley and Albert*, 2014; *Wobus et al.*, 2015] has also begun to shed light on the potential significance of these projected hydrologic changes during the incubation period.

Warming autumn, winter, and spring air temperatures will likely impact the hydrology of the incubation environment in coastal Alaska by: 1) increasing water temperature and 2) increasing the magnitude and frequency of winter freshets [*Leppi et al.*, 2014; *Shanley and Albert*, 2014; *Wobus et al.*, 2015]. These hydrologic changes are anticipated to impact the development and survival of salmon embryos, which typically incubate in the shallow streambed environment over the winter months. Increases in water temperature may accelerate embryo development, potentially impacting viability [*Holtby*, 1988; *Murray and McPhail*, 1988; *Neuheimer and Taggart*, 2007; *Braun et al.*, 2013]. Peak discharge was correlated with Coho salmon (*O. kisutch*) egg mortality at Carnation Creek, BC, likely due to increased scour [*Holtby and Healey*, 1986]. More powerful and more frequent winter freshets could reduce the survival of embryos by increasing streambed scour [*Battin et al.*, 2007; *Goode et al.*, 2013]. Fall-spawning Coho Salmon are expected to be particularly sensitive to these changes [*Bryant*, 2009; *Shanley and Albert*, 2014] and egg-to-fry survival is projected to be the most heavily impacted life stage [*Leppi et al.*, 2014]. However, the magnitude of these impacts is likely to vary across the landscape, particularly in regions with complex geomorphology [*Montgomery et al.*, 1999; *Shanley and Albert*, 2014; *Wobus et al.*, 2015].

Both streambed scour and water temperature are controlled both by climate and catchment geomorphology. The depth of scour and fill activity during floods is a function of stream power and substrate stability. Both of these variables are highly influenced by discharge as well as channel and floodplain geometry and roughness (including substrate composition) [*Montgomery et al.*, 1996; *Haschenburger*, 1999; *Lamb et al.*, 2008].

Water temperature is heavily impacted by both energy exchanges at the water's surface, and by advection, conduction, and friction at the streambed interface, particularly during the winter months when net radiative and sensible heat fluxes can be strongly negative [*Caissie et al.*, 2014; *Leach and Moore*, 2014]. In stream reaches where hyporheic exchange, groundwater upwelling, and lateral stormflow inputs are present, advection of energy can exert primary control on water temperature [*O'Driscoll and DeWalle*, 2006; *Tague et al.*, 2008; *Gariglio et al.*, 2013; *Leach and Moore*, 2014]. The mechanics of these energy exchanges are understood, but less is known about the relative importance of groundwater upwelling, lateral stormflow inputs, and meltwater hysteresis on mean water temperatures in the incubation environment of salmon embryos, particularly in regions where seasonal snow and ice melt are projected to be greatly reduced by climate change.

In this study, we use observed temperature, discharge, and channel geometry data to elucidate how increases in air temperature and decreases in seasonal snowpack and ice cover differentially impact heterogeneous spawning habitats on the Copper River Delta (CRD), a large coastal foreland in Southcentral Alaska. Specifically, we quantified accumulated thermal units (ATU) (°C/day) during the Coho Salmon incubation period, which we defined as the 243 day period from October 1 to May 31 (excluding February 29). Accumulated thermal units, also known as "degree days," are a metric commonly utilized to model embryo development [*Neuheimer and Taggart*, 2007; *Zimmerman and Finn*, 2012]. We compare incubation period ATU at eight spawning sites during two incubation periods characterized by near or below climatological mean temperatures ("severe winters") and two anomalously warm incubation periods which serve as proxies for conservative future climate scenarios ("mild winters"). We utilize this comparison to investigate the relative importance of upwelling groundwater, midwinter thaw, and seasonal melt hysteresis on ATU within salmon spawning gravels on the CRD. Additionally, we calculate potential

streambed scour depth at a subset of three sites and present an initial assessment of heterogeneity in scour risk at these reaches.

3.3 Methods

3.3.1 Copper River Delta Study Region

The subaerial extent of the CRD is a low-relief 1000 km^2 glacial outwash plain located between the Gulf of Alaska and the high-relief piedmont of the Chugach Mountains (Figure 3.1) [*Reimnitz*, 1966; *Boggs*, 2000; *Barclay et al.*, 2013]. The CRD has a cool and wet maritime climate. Based on 1980 to 2010 records at NOAA GHCN site #26410 (centrally located on the CRD and 13 m above sea level), the mean annual temperature is 4°C and mean annual precipitation is 235 cm. Climatological mean daily temperature minima are minus 5°C during January (the coldest month of the year) and climatological mean daily temperature maxima exceed the freezing point on every day of the year. Average monthly precipitation ranges from a minimum of 13 cm (June) to a maximum of 34 cm (September), but ± 20 cm monthly precipitation anomalies occur frequently during autumn and winter.

Incubation period weather conditions are often highly variable intra- and inter-annually. Cold and dry continental air masses periodically influence the study area between November and April and record temperature minima are below -20°C throughout these months. These influences are particularly pronounced down valley from the Copper River Canyon, where a local gap wind transports cold interior air onto the eastern third of the CRD. However, warm Pacific air masses also affect the region and DJF thaw and rainfall events are common. Midwinter temperature minima are warmer than freezing on 24% of days on average and record daily temperature maxima exceed 10°C in January.

Climatological mean incubation period conditions presently include an average of 250 cm of snowfall between late October and early May at the weather station, seasonal ice cover on waterbodies, and a shallow snowpack at sea level. Considerably heavier precipitation occurs in the piedmont and perennial snow and ice cover is prevalent above 1000 m.

Most CRD streams originate in the piedmont and snow and ice melt are important water sources. Small groundwater-fed creeks are also present where coarse glacigenic gravel substrates or colluvium support phreatic storage and the surficial geometry exposes the water table. Annual discharge minima have historically occurred during the mid-winter and early spring (DJFMA) months, when temperature, rainfall, and glacial ablation rates are low and seasonal snowpack is deepest (see section *1.3.2 Streamflow*). Based on a mid-range greenhouse gas emissions scenario, climate models project mean monthly temperatures will exceed freezing throughout the entire year by 2050 [*Romero-Lankao et al.*, 2014; *University of Alaska*, 2015], greatly reducing the extent and duration of seasonal ice cover and snowpack below 500 m on the CRD and the adjacent piedmont.

3.3.2 Study Catchments

This study utilizes surface and streambed water temperature data collected at eight known Coho Salmon spawning locations on the CRD during the typical incubation period (October 1 to May 31) in water years 2012 to 2015 (Table 3.1 & Figure 3.1).

Boundaries of each study catchment were interpolated from surficial topography mapped with U.S. Geological Survey (USGS) 5 m resolution digital elevation model data. Catchment area ranged from 61 to 3504 hectares. The study sites were low-elevation (less than 50 m). Two of the catchments (Ibeck and TF.Mi) were entirely located on glacial outwash deposits. The other 6 catchments included piedmont terrain, but maximum catchment elevations varied considerably, from 83 to 1329 m. We divided the sites into two categories, “groundwater” and “shallow flowpath” based on primary water sources and residence times.

Groundwater sites (Clear, Ibeck, Salmo, TF.Mi) are defined by positive vertical head gradients and low seasonal and diel temperature variability that signify local upwelling of relatively long residence time groundwater. Mixed water sources and flowpaths are likely to occur during runoff events at these catchments and the influences of additional water sources are particularly pronounced at the two larger catchments (Clear and Salmo), where groundwater upwelling is augmented by seasonal glacial and snowpack ablation and precipitation runoff, especially during JJAS. However, because upwelling groundwater

appears to be the dominant water source within the streambed incubation gravels at base flows and throughout the incubation period, we categorized these sites as “groundwater” for the purpose of this analysis.

Shallow flowpath sites (ET.Mi, LMart, Marti, Ot.Ca) are defined by neutral or negative vertical head gradients and high seasonal and diel temperature variability, suggesting shorter residence time, and, presumably, shallower flowpaths are present at these sites.

3.3.3 Winter Severity Categories

The four study years were divided into two categories based on severity of winter conditions. “Severe” winters were defined by climatological mean or anomalously cold seasonal temperatures and the presence of sea level snowpack. “Mild” winters were defined by anomalously warm seasonal temperatures and reduced sea level snowpack.

In the “severe” winter years (WY 2012 & WY 2013), seasonal sea level snowpack and persistent waterbody ice was observed. WY 2012 was anomalously cool and the autumn and winter seasons were anomalously wet (Figures 3.2 & 3.3). Snowfall occurred frequently (Figure 3.4). Sea level snowpack was atypically deep and persisted until May (Figure 3.5). At mid-elevations (~ 500 m) in the piedmont, snowpack persisted throughout the summer months. In WY 2013, air temperature oscillated around normal, although the autumn and spring months were anomalously cool (-2°C) (Figure 3.2). Snowfall occurred regularly throughout the winter, sustaining a shallow snowpack at sea level nearly continuously from late October until mid-April (Figures 3.3 & 3.4).

In the “mild” winter years (WY 2014 & 2015), seasonal snowpack and ice was noticeably less persistent (Figure 3.4). Air temperatures during WY 2014 were nearly normal, except during SON (+0.9°C anomaly) and the month of January (+5.0°C anomaly). Sea level snowpack was late to develop and subsequently melted during the record-breaking January thaw event. Late winter conditions were seasonable and a snowpack re-developed, but precipitation was below average and the sea level snowpack melted by late March, a month earlier than WY 2012 or WY 2013. Water Year 2015 was anomalously warm, particularly during the incubation period (+1.5°C anomaly). Mean monthly

temperatures exceeded freezing every month except January (-0.9°C) and February (-0.2°C). While mean temperatures stayed below freezing, the DJF temperature anomaly was +2.5°C, similar to projected normal temperatures for 2030-2040 based on a mid-range greenhouse gas emissions scenario [*University of Alaska*, 2015]. Autumn precipitation was anomalously low, but near normal precipitation was received during the rest of the year. Wintertime precipitation generally fell as rain and measureable snowfall accumulated on only ten days (Figure 3.4). Low-elevation snowpack was absent and waterbody ice cover was thin and transient.

3.3.4 Surface and Streambed Water Temperature Monitoring

Surface and streambed water temperatures were monitored hourly throughout the study period using data loggers with ± 0.2°C sensor accuracy (Onset Computer Corporation, Bourne, MA). Surface water temperature was recorded at each site with 1 HOBO Pro v2 data logger housed in a 15 cm long section of 4.1 cm internal diameter galvanized steel pipe to protect the sensor from physical damage and direct solar radiation. Surface water temperature loggers were placed as deeply into the stream as possible, typically in 50 to 80 cm of water. Some of the study sites had a high width-to-depth ratio and the water was shallow throughout the study reach. In these situations, the data logger was placed as deeply as possible, always more than 25 cm deep. The surface water at each study site was assumed to be well-mixed vertically and laterally by turbulent forces.

Streambed water temperature was measured 50 to 70 cm below the surface of the substrate. Coho Salmon egg burial depth ranges between 8 and 55 cm and is highly correlated with size of the maternal female [*van den Berghe and Gross*, 1984; *DeVries*, 1997]. By calculating ATU in the surface water and at 50 to 70 cm into the streambed, we assume we have captured the entire range of incubation temperature experienced by Coho Salmon eggs at each location. Streambed water temperature was measured using 2 interchangeable techniques: 1) a Pro v2 data logger was suspended near the bottom of a 101 cm long piezometer constructed from 4.1 cm internal diameter galvanized steel. The data logger sat in a 15 cm long ported section (a screen) above a tapered 10 cm driving point that also served as a sediment trap. A foam baffle minimized vertical water flux

within the piezometer. Each piezometer was capped with PVC to prevent rainwater intrusion. 2) a TidbiT v2 data logger was installed directly into the substrate using a custom-made two-piece steel driver that functioned similarly to a percussion drill [*Zimmerman and Finn*, 2012]. Both piezometers and TidbiT loggers were secured with stainless steel cables and earth anchors to prevent loss during potential scour events.

Two to four streambed loggers were deployed at each site using one or both deployment methods. All data loggers at each site were downloaded one or two times each year. If the data logger could be retrieved, it was redeployed in the same location throughout the study period. The data were reviewed for errors in Microsoft Excel using USFS Natural Resource Manager Aquatic Surveys QAQC add-in software (http://www.fs.fed.us/nrm/index.shtml) to flag unreasonable values and abnormally high hourly variance (which suggests the sensor was exposed to air). Erroneous values were removed before analysis. Daily mean temperature values were calculated for each data logger using the hourly data. The average of all the streambed logger daily mean values was utilized to calculate streambed ATU.

3.3.5 Stage and Discharge Monitoring

Water stage was measured hourly with a HOBO U20 pressure transducer housed vertically in a 4.1 cm internal diameter galvanized steel stilling well from May 1, 2013 through September 30, 2015 at 2 of the study sites (ET.Mi and TF.Mi) and from Apr 1, 2014 through May 1, 2015 at 1 study site (Salmo). Discharge measurements (n= 48) were taken opportunistically using a handheld Ott-Pro current meter.

3.3.6 Channel Survey and Sediment Particle Sampling

Channel geometry and sediment particle data were also collected at ET.Mi, Salmo, and TF.Mi. Surface topography was surveyed along the channel and streambanks over a 140 m reach at each gauging site using a TOPCON GTS 223 total station. Topography and water surface elevations were referenced to the NAD 83 datum using a Spectra Precision Ranger 3 Data Collector and a Trimble R8 GNSS Receiver.

Sediment samples (n=5 at each site) were collected from spawning gravels adjacent to the three gauging stations by tri-tube freeze coring with liquid CO_2 [*Everest et al.*, 1980;

Lotspeich and Reid, 1980]. Each core was ~20 cm in diameter and ~50 cm in depth. Samples were subdivided into 5 stacked strata, each ~10 cm thick. Organic materials were removed. Each strata was transported to the laboratory in a sealed plastic bag, dried overnight in an oven at 90 °C, and sieved using 10 square-mesh sieves (1 to 64 mm mesh sizes) and a Gilson Tapping Sieve Shaker. Mass of each retained size class was measured to the nearest 0.1 g with an electronic balance. The cumulative percent of passing material was calculated for each sieve size and the median diameter particle in mm (D_{50}) was interpolated using equation 2.15b from Bunte and Abt [2001]:

$$\boldsymbol{D_{50} = 10^{(\log(x_2)-\log(x_1)) \times \frac{50-y_1}{y_2-y_1}+\log(x_1)}} \quad \text{Eq. 3.1}$$

Where X_2 is the passing sieve size (mm) and Y_2 is the corresponding percentage of material above the cumulative 50% objective and X_1 is the passing sieve size and Y_1 is the corresponding percentage of material below the cumulative 50% objective.

3.3.7 Temperature Data Analysis

Incubation period ATU was calculated as the cumulative sum of the daily mean temperature (≥ 0 °C) during the 243 day period from October 1 until May 31 of each water year. February 29 was excluded from WY 2012. While spawning and emergence timing varies, this period was selected to encompass the typical range of observed spawning and emergence dates for Coho Salmon on the CRD. Welch's *T* tests were utilized to compare surface and streambed ATU under different winter intensities (severe vs. mild) and at sites with different primary flowpaths (shallow vs. groundwater).

Total ATU and the percent of ATU were also calculated for equal 81-day sub-periods at each site during each incubation period: The "early" sub-period was Oct 1- Dec 20, the "middle" sub-period was Dec 21-Mar 11, and the "late" sub-period was Mar 12- May 31. The sub-period totals and percentages were also compared under different winter intensities and flowpaths using Welch's *T* tests.

3.3.8 Discharge Analysis

Stage-discharge relationships were quantified utilizing observed and modelled data. No discharge measurements were taken at flood stages, so velocity and cross-sectional area

were used to model discharge at high water stages. The Manning equation was used to calculate velocity (U) (m/s):

$$\boldsymbol{U = \frac{R^{2/3} \times S^{1/2}}{n}} \qquad \text{Eq. 3.2}$$

Where: R is hydraulic radius (m), S is water surface slope (m/m), and *n* is Manning's n, a dimensionless coefficient that characterizes channel roughness [*Dingman*, 2002].

Manning's n was correlated with water surface elevation based on observed discharges and tabled values of streambank roughness [*Arcement Jr. and Schneider*, 1989] and *n* values ranged from 0.08 to 0.34 (Figure 3.6). Streambed cross-sectional shape was interpolated from channel survey measurements and was utilized to calculate cross-sectional area and hydraulic radius (Figure 3.6). Stream slope was calculated as the difference in water surface elevation at riffle crests on the upstream and downstream extents of the surveyed reach divided by the distance along the channel centerline. Rating curves were developed for each site using the modelled discharge data (Table 3.2 & Figure 3.7). The rating curves were applied to calculate daily mean and specific discharge from the hourly stage record.

3.3.9 Shear Stress Analysis

In unconfined channels, maximum shear stress at the streambed interface occurs at near bankfull discharges [*Goode et al.*, 2013; *McKean and Tonina*, 2013]. Maximum shear stress and reach-scale mean scour depth were calculated at bankfull discharge at sites ET.Mi, Salmo, and TF.Mi.

Average dimensionless shear stress (τ*) was calculated using the equation 3 from Haschenburger (1999):

$$\boldsymbol{\tau^* = \frac{\tau_0}{g(\rho_s - \rho)D_{50}}\ ;\ \tau_0 = g\rho Rs} \qquad \text{Eq. 3.3}$$

Where: D_{50} is the median particle diameter (m), g is the acceleration of gravity (9.81 m s^{-2}), ρ is the density of water (1000 kg m^{-3}), ρ_s is the density of sediment (2650 kg m^{-3} on the CRD), R is the mean depth (m), an approximation for hydraulic radius, and s is the bed slope (m/m) [*Case et al.*, 1966; *Haschenburger*, 1999; *Goode et al.*, 2013].

Bed scour depth (θ) in cm was calculated using equation 6 from Haschenburger (1999):

$$\boldsymbol{\theta = \left(3.33 e^{-1.52\tau^{*}/\tau_{c}}\right)^{-1}} \quad \text{Eq. 3.4}$$

Where τ_c is critical dimensionless shear stress. A range of critical dimensionless shear stresses was calculated for each site based on channel slope (S) using equation 10 from Pitlick et al. [2008] and equation 3 from Lamb et al. [2008]:

$$\boldsymbol{0.36 S^{0.46} \leq \tau_{c} \leq 0.15 S^{0.25}} \quad \text{Eq. 3.5}$$

All data analyses were performed in R v 3.2.3 except where noted otherwise [*R Core Team*, 2015].

3.4 Results

3.4.1 Incubation Period Accumulated Thermal Units

Incubation period ATU varied throughout the study period at both groundwater (74 to 1002 ATU) and shallow flowpath (246 to 938 ATU) sites (Figure 3.8). Streambed and surface thermal environments differed by more than 100 ATU in 37% of observations. And the streambed accumulated more ATU than the surface water in 70% of observations (Figure 3.8). Shallow flowpath sites (ET.Mi, LMart, Marti, Ot.Ca) generally accumulated more ATU in the streambed than in the surface water, particularly during DJF and MAM (Figure 3.9).

Significant differences ($p = 0.013$) in incubation period ATU were observed between shallow and groundwater flowpath sites during years with severe winters (2012 & 2013), but no significant differences ($p = 0.17$) were observed during years with mild winters (2014 & 2015) (Figure 3.10). Incubation period ATU at shallow flowpath sites differed significantly ($p<0.001$) between severe and mild winters. This contrasts to groundwater flowpath sites, where we observed no significant differences ($p > 0.67$) associated with winter intensity (Figure 3.10).

The seasonality of ATU accumulation varied with winter severity at shallow flowpath sites. Sub-period accumulation of ATU was significantly different ($p < 0.03$) between mild and severe winters in all sub-periods (early, middle, late) in the surface

water and in the early and late sub-periods in the streambed water at the shallow flowpath systems. No significant differences ($p > 0.30$) were observed during the middle sub-period in the streambed at shallow flowpath systems, nor during any sub-period at the groundwater flowpath systems (Figure 3.11).

The relative percentage of total ATU accumulated during each sub-period stayed consistent regardless of winter intensity at the groundwater sites. The percentage of total ATU accumulated in the late sub-period was greater during mild winters at the shallow flowpath sites (Figure 3.12).

3.4.2 Discharge and Potential Scour Depth

Mean, maximum, and minimum discharges and discharge standard deviation varied with catchment size (Table 3.3). Both Salmo and TF.Mi had strong upwelling groundwater and relatively stable thermal environments, but the hydrographs were different (Figure 3.13). Daily mean discharge varied by over 80 $m^3 s^{-1}$ at Salmo and by less than 0.5 $m^3 s^{-1}$ at TF.Mi. Four bankfull flow events were recorded at Salmo (the largest and highest relief catchment), while TF.Mi stayed within its channel throughout the year. Daily mean specific discharge varied from 0.26 mm hr^{-1} (Salmo) to 1.36 mm hr^{-1} (TF.Mi) (Figure 3.14).

Median particle diameter (D_{50}) at the surface ranged from 11.5 to 15.8 mm (Table 3.4). Calculated bankfull dimensionless shear stress was greater than the range of critical dimensionless shear stress at all three gauging stations; however, calculated scour depth varied from 3 cm – 8 cm (ET.Mi) to 11 cm - 72 cm (Salmo).

3.5 Discussion

We observed significant differences in ATU between shallow flowpath and groundwater sites suggesting inherent spatial variability amongst incubation environments on the CRD. The heterogeneous response of shallow flowpath and groundwater sites to reduced winter severity suggests that ATU accumulation at these sites will be differentially impacted by projected climatic changes.

3.5.1 ATU at Deep Groundwater Sites

The accumulation of thermal units (ATU) at deep groundwater sites showed little inter-annual and seasonal variability, regardless of winter severity. In other words, the

proportion of ATU accumulated during each incubation period and during each of the three 81-day sub-periods (early, middle, and late) was consistent regardless of atmospheric conditions (Figure 3.12). This stability suggests upwelling groundwater exhibited stronger control on incubation period ATU than atmospheric conditions. Although inter-annual variability was low, ATU accumulations at the individual sites was markedly different.

Both TF.Mi and Ibeck are upwelling groundwater sites located on low-relief glacial outwashes, yet incubation period ATU at these sites varied by up to 880 thermal units. The differences in ATU at groundwater sites suggest different water sources. Groundwater preserves the thermal signature of the recharge water sources. One of the streambed data loggers at Ibeck recorded <0.5°C all year-round while one of the streambed data loggers at TF.Mi hovered within half a degree of 4°C, the annual mean air temperature, throughout the entire study period. Based on the observed water temperatures and the outwash geometry, we suspect that glacial melt is the primary recharge water source for the Ibeck aquifer while precipitation or mixed water sources are likely recharge water sources for the TF.Mi aquifer. The different water sources at groundwater sites contributed to landscape-scale heterogeneity in water temperature and incubation period ATU.

Although ATU accumulation was not significantly different between severe and mild winters at the four groundwater sites, considerable inter-annual differences were observed in the surface water at Clear and at Salmo (Figure 3.11). These differences can be explained by the mixed water sources at these sites. Clear distributes discharge from the Copper River during the ablation season (MJJASO). The streambed temperature is controlled by strong groundwater upwelling, but these intrusions of glacial meltwater episodically reduce surface water temperature during the shoulders of the incubation season. These impacts may become more frequent in the future if the duration of the ablation season increases as is projected [*McAfee et al.*, 2014].

At Salmo, incubation period ATU exhibited inter-annual variability that correlated with the variability observed at shallow flowpath sites. This suggests that, despite the presence of strong groundwater upwelling at this site, the incubation environment was impacted by atmospheric conditions, although the magnitude of these impacts was smaller than at the four spawning reaches we classified as shallow flowpath sites.

3.5.2 ATU at Shallow Flowpath Sites

Shallow flowpath sites exhibited surprising homogeneity in incubation period ATU across the landscape, but experienced significant inter-annual and seasonal variability. This duality can be explained by the exposure of shallow flowpaths to surface-atmospheric energy exchanges, particularly radiative and sensible heat fluxes that have been demonstrated to heavily influence water temperatures [*Webb and Zhang*, 1997; *Caissie*, 2006]. Consequently, these sites are likely to be more responsive to projected climatic changes than upwelling groundwater sites and the impacts will be relatively homogenous across these sites.

Energy fluxes were not measured or calculated, but sensible and latent heat fluxes and longwave radiative fluxes are highly influenced by atmospheric conditions, particularly temperature, humidity, and cloud cover, and we expect the net effect of these fluxes did not cool streams as much during the mild winters.

Shortwave radiative fluxes may be particularly important. At 60.5°N, solar radiation is limited in the late autumn (ON) and DJF. Shallow flowpath sites gained relatively few ATU during the middle sub-period (Dec 21-Mar 11), regardless of winter intensity. In contrast, solar radiation is abundant during MAM at high latitudes and contributes to the positive energy balance that warms and melts the snowpack [*Zhang et al.*, 1997].

After severe winters, I suspect that both seasonal snowpack and waterbody ice melt attenuated the influence of net-positive atmospheric energy fluxes during the late incubation period, minimizing MAM ATU. Late sub-period ATU was similar during deep snowpack (2012) and shallow snowpack (2013) years, suggesting the depth may be less important than the duration of low-elevation snowpack within the catchment. However, unaccounted for differences in atmospheric energy flux could also explain similarities between the two severe winter years.

Increased MAM ATU during mild winters (2014 & 2015) may represent a shift in the seasonality of energy accumulation. Significantly more ATU were gained during the late sub-period (Mar 12 – May 31) of mild winters (Figure 3.11), accounting for a much greater percentage of total ATU (Figure 3.12). I suspect the impact of atmospheric energy sources, particularly abundant MAM solar radiation, increased water temperatures when the

buffering effect of low-elevation snow and ice melt was reduced. Particularly large ATU accumulations were observed in MAM at Ot.Ca and LMart, the two sites that were downstream from shallow lakes, suggesting a positive correlation between atmospheric exposure and MAM ATU at shallow flowpath sites.

During severe winters, the shallow flowpath sites accumulated the highest percentage of ATU during the early sub-period (Oct 1-Dec 20). Residual JJAS heat energy is present in water and soil at this time of year and surface water temperatures often exceed surface air temperatures (*Chapter 2,* Figure 2.10). Large fall storms frequently impact the study region and additional heat is likely transferred into waterways by advection of lateral storm flows [*Leach and Moore*, 2014]. Significantly more ATU were accumulated in the early sub-period during mild winters, suggesting atmospheric conditions exhibit at least some control over ATU accumulation in autumn and early winter.

Climate change impacts may be realized by either more frequent warm winter storms or through chronic increases in mean temperature. In WY 2014 a record warm January storm was observed. Despite anomalously high temperatures and precipitation, this event had substantially less influence on total ATU than the early and late sub-period conditions. Although the frequency of warm mid-winter storms may increase in the future, our observations suggest these events contribute proportionally less to ATU than temperature increases early and late in the incubation period.

However, mid-winter rain storms (particularly latent heat inputs) increase snowpack and ice cover ablation. Increased ablation during DJF may shorten the duration of snow cover and reduce the buffering effects of meltwater during MAM, when atmospheric energy fluxes are generally positive. Furthermore, increased frequency or magnitude of midwinter freshets may increase the likelihood of egg scour.

3.5.3 Scour Frequency and Depth

Recent modelling efforts have suggested streambed scour is the greatest climate-change related threat to the freshwater life stages of Coho Salmon in coastal Alaska [*Leppi et al.*, 2014; *Shanley and Albert*, 2014]. Empirical research has determined that streambed mobility at salmon spawning locations varies considerably on both reach and landscape

scales, but is largely a function of slope, streambed composition and the upstream sediment supply, channel geometry and roughness, and channel confinement [*Montgomery et al.*, 1996; *Haschenburger*, 1999; *Goode et al.*, 2013; *McKean and Tonina*, 2013]. In this study, scour was only calculated for a single reach at three gauged sites, yet we observed considerable heterogeneity the estimated depth of scour.

ET.Mi is located at the margin of a glacial outwash. The low-elevation, shallow flowpath piedmont catchment characterized by thin till soils, forested slopes, and abundant peatlands. While we did not observe any bankfull discharges during the incubation period of WY 2015, the catchment characteristics (low elevation, shallow flowpaths) suggests that winter freshets may become more frequent at this site under future climate conditions. Although the catchment may be prone to winter freshets in the future, the channel geometry at the ET.Mi salmon spawing reach is not conductive to bed mobility, and our calculations to not suggest that bed scour will have reach-scale impacts on salmon eggs. Here, the two- to three-fold increase in ATU that is anticipated based on climate projections is likely to have more of an impact on the incubation environment than increased scour. Conversely, relatively small changes in ATU and variable streambed scour risk are anticipated at Salmo and TF.Mi, two groundwater-upwelling sites. The differences in mean streambed scour depths at these two sites reflects the geomorphic differences of the catchments.

The TF.Mi site is located on a broad proglacial outwash. The present-day water source is upwelling groundwater, but I suspect the channel, which is defined by a high surface area to depth ratio and a sinuous thalweg, was originally carved by glacial meltwater. Thus, the streambanks are considerably higher than the present day water levels and bankfull flows are unlikely to occur. Although I calculated a bankfull scour depth (7 cm – 19 cm) that might impact developing salmon eggs, observed discharge was considerably lower than bankfull (Figure 13). Within the range of observed discharges, including during a large storm in September 2014, reach-scale mean scour depth was minimal (<3 cm) at TF.Mi. Our observations suggest that TF.Mi is not likely to be affected by increased ATU and may only be impacted by streambed scour during extreme precipitation events.

The Salmo site, by comparison, is located in a large (2267 ha) and high-relief piedmont catchment. Incubation period base flows are dominated by groundwater upwelling, but meltwater (MJJAS) and rainfall (year-round) drive peak flows. The channel has the lowest surface area to depth ratio and the greatest risk of increased streambed scour.

The differences observed between groundwater and shallow flowpath systems suggest that climatic changes will impact salmon embryos differentially across the landscape. Landscape-scale impacts to ATU on the CRD will likely be buffered by phreatic water sources, however, where upwelling groundwater is associated with mountain valleys, the stable character of the thermal environment does not correlate with protection from bed scour during freshets. Winter freshets are projected to increase in frequency and magnitude, but our observations suggest the impacts of these changes on Coho Salmon production will be variable across the landscape, depending on channel morphology and other catchment characteristics.

3.5.4 Implications for Pacific Salmon

The observed correlation between winter intensity and ATU accumulation suggests the incubation environment is highly variable at shallow flowpath streams and is likely to become much warmer under projected climate scenarios. Holtby [1988] reported increased year-round stream temperatures after timber harvest appeared to accelerate Coho Salmon emergence by up to 6 weeks at Carnation Creek, BC. Earlier emergence effectively lengthened the growing season and a large proportion of juveniles completed their freshwater life phase after one year rather than two. Warmer temperatures during egg incubation also resulted in accelerated first year growth rates and increased percentages of age 1+ smolts in Atlantic Salmon *(Salmo salar)* [*Jonsson et al.*, 2005]. Both studies concluded that changes in temperature would have life-long impacts on salmon growth and viability. At Carnation Creek, the age 1+ Coho Salmon smolts were smaller than the age 2+ smolts and the author hypothesized that marine survival would decrease.

Increasing water temperatures and accelerated Pacific Salmon embryo development has also been correlated with reduced juvenile length at emergence due to reductions in

the rate and efficiency of yolk use [*Beacham and Murray*, 1990]. Egg size is correlated with yolk reserve and Pacific Salmon tend to have larger eggs at lower latitudes due to the reduced efficiency of yolk conversion at warmer temperatures [*Fleming and Gross*, 1990]. The viability of juveniles hatching from smaller eggs could be reduced by elevated temperatures under projected warming scenarios. In the absence of rapid physiological adaptation, these changes could be particularly pronounced in shallow flowpath streams on the CRD, where mean incubation period ATU under climatological mean conditions is low (~500) and projected increases will be proportionally large (more than two-fold).

While these findings may raise concern, it is important to remember studies conducted at mid-latitudes [*Holtby*, 1988; *Beacham and Murray*, 1990], where water temperatures are already within (or exceeding) the range that is considered optimal for Pacific Salmon [*McCullough*, 1999], may not accurately capture the impacts of rising temperatures at high latitudes. Water temperatures on the CRD are typically below the optimal range for Pacific Salmon (see Chapter 2, section *2.5.4 Implications for Pacific Salmon*). Researchers have hypothesized that projected increases in water temperature could improve Pacific Salmon growth and survival in coastal Alaska, particularly in catchments with permanent snow and ice cover [*Milner et al.*, 2008; *Bryant*, 2009; *Schindler et al.*, 2013; *Fellman et al.*, 2014]. Projected increases in temperatures are expected to be correlated with increases in incubation period stream discharge [*McAfee et al.*, 2014] and the full breadth of hydrologic changes should be considered.

Increased stream discharge has been correlated with egg mortality [*Holtby and Healey*, 1986]; however, other studies have observed that Pacific Salmon have likely adapted to mitigate scour risk by spawning in stable locations such as on channel margins and in coarser substrates [*May et al.*, 2009] and in low-gradient, unconfined reaches were high flows are dissipated onto the floodplain [*McKean and Tonina*, 2013]. On the CRD, Coho Salmon likely benefit from the low-relief topography and the abundance of unconfined stream channels with high width to depth ratios. Unlike many coastal Pacific streams, large wood is naturally sparse in CRD stream channels due to post-glacial morphology [*Reimnitz*, 1966]; however, stumps and logs are locally abundant at Salmo and likely contribute to gravel retention and sub-reach scale heterogeneity in scour depth.

Pacific Salmon may also adapt egg burial depth to ensure that embryos persist below the typical scour depth [*Montgomery et al.*, 1999]. The size of the maternal female is correlated with egg burial depth in Coho Salmon [*van den Berghe and Gross*, 1984]. Thus, projected decreases in adult salmon body size resulting from changing environmental conditions during the juvenile freshwater life phase [*Jonsson et al.*, 2005] or the marine life phase [*Hinch et al.*, 1995] could initiate a negative feedback cycle, where eggs laid by smaller female salmon are more scour-prone, reducing embryo survival in scour-prone reaches. Climatic shifts that increase scour depth directly (through increased magnitude of winter freshets) or indirectly (through changes in channel geomorphology or streambed particle size) could also increase egg mortality [*Goode et al.*, 2013].

Pacific Salmon have weathered dramatic climatic shifts throughout the Holocene, such as the Medieval Warm Period, when air temperatures along the Gulf of Alaska were presumed to be warmer than present-day climatological means [*Mann et al.*, 1998; *Nichols et al.*, 2014], and markedly cold periods, including four glacial advances in the last 2,000 years [*Barclay et al.*, 2013]. Although Pacific Salmon have demonstrated the ability to adapt complex life history strategies and avoid extirpation throughout these major climate shifts, the extent of their ability to rapidly adapt to abrupt changes in climate remains poorly understood [*Crozier et al.*, 2008; *Waples et al.*, 2009].

Furthermore, extirpation is not the only concern. The net magnitude of Pacific Salmon production is ecologically and economically important in coastal Alaska and has been linked to natural variability in climate, notably the Pacific Decadal Oscillation, which impacts both marine [*Mantua et al.*, 1997] and freshwater habitats [*Neal et al.*, 2002; *Schindler et al.*, 2013]. Climatic changes that influence habitat productivity could have a substantial impact on net salmon production.

Our observations shed light on some possible impacts of climate change, but we have not analyzed the inherent capacity of Coho Salmon populations on the CRD to withstand bed scour and variable ATU, nor to adapt to rapidly changing climatic conditions in the future. Understanding both the hydrology and the biology will be critical to accurately assess the impacts of projected climatic changes to Pacific Salmon production.

3.6 Conclusions

- Climate change impacts to Coho Salmon habitat on the CRD are anticipated to be highly variable due to inherent spatial heterogeneity in geomorphology and water flowpaths.
- Winter severity had little impact on incubation period accumulated thermal units (ATU) at groundwater upwelling sites, but we documented more than two-fold increases in incubation period ATU during mild winters at shallow flowpath sites.
- Mid-winter freshets contributed relatively little to incubation period ATU, but thaw events that reduce the duration of snow and ice cover may indirectly contribute to significant increases in ATU later in the incubation period, when seasonal snow and ice melt has historically buffered water temperatures under climatological mean conditions.
- We calculated reach-scale potential scour depth ranged between 3 and 72 cm, suggesting the impacts of scour on egg mortality will be variable across the CRD.

3.7 Acknowledgements

The author thanks John Buffington for providing valuable feedback on the scour depth analysis.

3.8 References

Arcement Jr., G. J., and V. R. Schneider (1989), Guide for selecting Manning's roughness coefficients for natural channels and flood plains, *U.S. Geol. Surv. Water-Supply Pap. 2339*.

Arismendi, I., S. L. Johnson, J. B. Dunham, and R. Haggerty (2013), Descriptors of natural thermal regimes in streams and their responsiveness to change in the Pacific Northwest of North America, *Freshw. Biol.*, *58*(5), 880–894, doi:10.1111/fwb.12094.

Arismendi, I., M. Safeeq, J. B. Dunham, and S. L. Johnson (2014), Can air temperature be used to project influences of climate change on stream temperature?, *Environ. Res. Lett.*, *9*(8), 084015, doi:10.1088/1748-9326/9/8/084015.

Barclay, D. J., E. M. Yager, J. Graves, M. Kloczko, and P. E. Calkin (2013), Late Holocene Glacial History of the Copper River Delta, Coastal South-central Alaska, and Controls on Valley Glacier Fluctuations, *Quat. Sci. Rev.*, *81*, 74–89,

doi:10.1016/j.quascirev.2013.10.001.

Battin, J., M. W. Wiley, M. H. Ruckelshaus, R. N. Palmer, E. Korb, K. K. Bartz, and H. Imaki (2007), Projected impacts of climate change on salmon habitat restoration., *Proc. Natl. Acad. Sci. U. S. A.*, *104*(16), 6720–5, doi:10.1073/pnas.0701685104.

Baxter, C. V., and F. R. Hauer (2000), Geomorphology, hyporheic exchange, and selection of spawning habitat by bull trout (*Salvelinus confluentus*), *Can. J. Fish. Aquat. Sci.*, *57*(7), 1470–1481, doi:10.1139/cjfas-57-7-1470.

Beacham, T. D., and C. B. Murray (1990), Temperature, Egg Size, and Development of Embryos and Alevins of Five Species of Pacific Salmon: A Comparative Analysis, *Trans. Am. Fish. Soc.*, *119*(6), 927–945.

Beer, W. N., and J. J. Anderson (2011), Sensitivity of juvenile salmonid growth to future climate trends, *River Res. Appl.*, *27*(5), 663–669, doi:10.1002/rra.1390.

Benda, L., T. J. Beechie, R. C. Wissmar, and A. Johnson (1992), Morphology and Evolution of Salmonid Habitats in a Recently Deglaciated River Basin, Washington State, USA, *Can. J. Fish. Aquat. Sci.*, *49*(6), 1246–1256, doi:10.1139/f92-140.

van den Berghe, E. P., and M. R. Gross (1984), Female Size and nest depth in coho salmon (Oncorhynchus kisutch), *Can. J. Fish. Aquat. Sci.*, *41*, 204–206.

Bisson, P. a., J. B. Dunham, and G. H. Reeves (2009), Freshwater ecosystems and resilience of Pacific salmon: habitat management based on natural variability, *Ecol. Soc.*, *14*(1), 45, doi:45.

Boggs, K. (2000), Classification of Community Types, Successional Sequences, and Landscapes of the Copper River Delta, Alaska, *Gen. Tech. Rep. - Pacific Northwest Res. Station. USDA For. Serv.*, (PNW-GTR-469), 244 pp.

Brabets, T. P. (1997), Geomorphology of the lower Copper River, Alaska, *U.S. Geol. Surv. Prof. Pap. #1581*, 89.

Braun, D. C., D. A. Patterson, and J. D. Reynolds (2013), Maternal and environmental influences on egg size and juvenile life-history traits in Pacific salmon, *Ecol. Evol.*, *3*(6), 1727–1740, doi:10.1002/ece3.555.

Bryant, M. D. (1992), The Copper River Delta pulse study: an interdisciplinary survey of the aquatic habitats, *Gen. Tech. Rep. - Pacific Northwest Res. Station. USDA For. Serv.*, *PNW-GTR-28*, 43.

Bryant, M. D. (2009), Global climate change and potential effects on Pacific salmonids in freshwater ecosystems of southeast Alaska, *Clim. Change*, *95*(1-2), 169–193, doi:10.1007/s10584-008-9530-x.

Bunte, K., and S. R. Abt (2001), Sampling Surface and Subsurface Particle-Size Distributions in Wadable Gravel- and Cobble-Bed Streams for Analyses in Sediment Transport , Hydraulics , and Streambed Monitoring, *0*, 450.

Caissie, D. (2006), The thermal regime of rivers: a review, *Freshw. Biol.*, *51*(8), 1389–1406,

doi:10.1111/j.1365-2427.2006.01597.x.

Caissie, D., B. L. Kurylyk, A. St-Hilaire, N. El-Jabi, and K. T. B. MacQuarrie (2014), Streambed temperature dynamics and corresponding heat fluxes in small streams experiencing seasonal ice cover, *J. Hydrol.*, *519*, 1441–1452, doi:10.1016/j.jhydrol.2014.09.034.

Caldwell, P., C. Segura, S. Gull Laird, G. Sun, S. G. McNulty, M. Sandercock, J. Boggs, and J. M. Vose (2015), Short-term stream water temperature observations permit rapid assessment of potential climate change impacts, *Hydrol. Process.*, *29*(9), 2196–2211, doi:10.1002/hyp.10358.

Case, J. E., D. F. Barnes, G. Plafker, and S. L. Robbins (1966), Gravity Survey and Regional Geology of the Prince William Sound Epicentral Region, Alaska, in *The Alaska Earthquake, March 27, 1964: Regional Effects*, United States Government Printing Office.

Christensen, H. H. (2000), *Alaska's Copper River: Humankind in a Changing World*, U.S. Dept. of Agriculture, Forest Service, Pacific Northwest Research Station GTR 480.

Cooper, E. E. (2007), Beaver Ecology on the West Copper River Delta, Alaska., Oregon State University.

Crozier, L. G., and R. W. Zabel (2006), Climate impacts at multiple scales: Evidence for differential population responses in juvenile Chinook salmon, *J. Anim. Ecol.*, *75*(5), 1100–1109, doi:10.1111/j.1365-2656.2006.01130.x.

Crozier, L. G., A. P. Hendry, P. W. Lawson, T. P. Quinn, N. J. Mantua, J. Battin, R. G. Shaw, and R. B. Huey (2008), PERSPECTIVE: Potential responses to climate change in organisms with complex life histories: evolution and plasticity in Pacific salmon, *Evol. Appl.*, *1*(2), 252–270, doi:10.1111/j.1752-4571.2008.00033.x.

DeVries, P. (1997), Riverine salmonid egg burial depths: review of published data and implications for scour studies, *Can. J. Fish. Aquat. Sci.*, *54*(8), 1685–1698, doi:10.1139/cjfas-54-8-1685.

Dingman, S. L. (2002), *Physical Hydrology*, 2nd ed., Waveland Press, Inc, Long Grove, IL.

Dorava, J. M., and J. M. Sokup (1994), Overview of Environmental and Hydrogeologic Conditions at the Merle K. "Mudhole" Smith Airport, Near Cordova Alaska, *U.S. Geol. Surv. Open-File Rep. 94-328*, 1–15.

Everest, F. H., C. E. McLemore, and W. J.F. (1980), An improved tritube cryogenic gravel sampler., *Res. Note PNW-350. USDA For. Serv. Northwest For. Range Exp. Station. Portland, Or .*

Fellman, J. B., S. Nagorski, S. Pyare, A. W. Vermilyea, D. Scott, and E. Hood (2014), Stream temperature response to variable glacier coverage in coastal watersheds of Southeast Alaska, *Hydrol. Process.*, *28*(4), 2062–2073, doi:10.1002/hyp.9742.

Fleming, I. A., and M. R. Gross (1990), Latitudinal Clines : A Trade-Off between Egg Number and Size in Pacific Salmon, *Ecology*, *71*(1), 1–11.

Galloway, W. E. (1976), Copper River Fan-Delta, *J. Sediment. Petrol.*, *46*(3), 726–737.

Gariglio, F. P., D. Tonina, and C. H. Luce (2013), Spatiotemporal variability of hyporheic exchange through a pool-riffle-pool sequence, *Water Resour. Res.*, *49*(11), 7185–7204, doi:10.1002/wrcr.20419.

Goode, J. R., J. M. Buffington, D. Tonina, D. J. Isaak, R. F. Thurow, S. Wenger, D. Nagel, C. Luce, D. Tetzlaff, and C. Soulsby (2013), Potential effects of climate change on streambed scour and risks to salmonid survival in snow-dominated mountain basins, *Hydrol. Process.*, *27*(5), 750–765, doi:10.1002/hyp.9728.

Grantz, A., G. Plafker, and R. Kachadoorian (1964), Alaska's Good Friday earthquake, March 27, 1964: A Preliminary Geologic Evaluation, *U.S. Geol. Surv. Prof. Pap.*, 1–35.

Hall, D. K. (1988), Assessment of Polar Climate Change using Satellite Technology, *Rev. Geophys.*, *26*(1), 26–39, doi:10.1029/RG026i001p00026.

Hannah, D. M., I. A. Malcolm, and C. Bradley (2009), Seasonal hyporheic temperature dynamics over riffle bedforms, *Hydrol. Process.*, *23*, 2178–2194, doi:10.1002/hyp.7256.

Haschenburger, J. K. (1999), A probability model of scour and fill depths in gravel-bed channels, *Water Resour. Res.*, *35*(9), 2857–2869.

Hinch, S., M. C. Healey, R. Em, K. A. Thornson, R. Hourston, M. A. Henderson, and F. Juanes (1995), Potential effects of climate change on marine growth and survival of Fraser River sockeye salmon, *Can. J. Fish. Aquat. Sci.*, *52*, 2651–2659.

Holtby, L. B. (1988), Effects of Logging on Stream Temperatures in Carnation Creek, British, *Can. J. Fish. Aquat. Sci.*, *45*, 502–515, doi:10.1139/f88-060.

Holtby, L. B., and M. C. Healey (1986), Selection for Adult Size in Female Coho Salmon (Oncorhynchus kisutch), *Can. J. Fish. Aquat. Sci.*, *43*, 1946–1959.

Homer, C. G., J. A. Dewitz, L. Yang, S. Jin, P. Danielson, G. Xian, J. Coulston, N. D. Herold, J. D. Wickham, and K. Megown (2015), Completion of the 2011 National Land Cover Database for the conterminous United States-Representing a decade of land cover change information, *Photogramm. Eng. Remote Sensing*, *81*(5), 345–354.

Jaeger, J. M., C. A. Nittrouer, N. D. Scott, and J. D. Milliman (1998), Sediment accumulation along a glacially impacted mountainous coastline: north-east Gulf of Alaska, *Basin Res.*, *10*(1), 155–173, doi:10.1046/j.1365-2117.1998.00059.x.

Jonsson, N., B. Jonsson, and L. P. Hansen (2005), Does climate during embryonic development influence parr growth and age of seaward migration in Atlantic salmon (Salmo salar)?, *Can. J. Fish. Aquat. Sci.*, *62*(11), 2502–2508, doi:10.1139/F05-154.

Kargel, J. S. et al. (2014), Multispectral image analysis of glaciers and glacier lakes in the Chugach Mountains, Alaska, in *Global Land Ice Measurements from Space*, edited by J. S. Kargel, pp. 297–332, Springer Praxis Books, Berlin Heidelberg.

Kelleher, C., T. Wagener, M. Gooseff, B. McGlynn, K. McGuire, and L. Marshall (2012), Investigating controls on the thermal sensitivity of Pennsylvania streams, *Hydrol.*

Process., *26*(5), 771–785, doi:10.1002/hyp.8186.

Kurylyk, B. L., K. T. B. MacQuarrie, and C. I. Voss (2014), Climate change impacts on the temperature and magnitude of groundwater discharge from shallow, unconfined aquifers, *Water Resour. Res.*, *50*(4), 3253–3274, doi:10.1002/2013WR014588.

Kyle, R. E., and T. P. Brabets (2001), Water Temperature of Streams in the Cook Inlet Basin, Alaska, and Implications of Climate Change, *Wri 01-4109*, 32, doi:Water-Resources Investigations Report 01-4109.

Lamb, M. P., W. E. Dietrich, and J. G. Venditti (2008), Is the critical shields stress for incipient sediment motion dependent on channel-bed slope?, *J. Geophys. Res. Earth Surf.*, *113*(2), 1–20, doi:10.1029/2007JF000831.

Leach, J. A., and R. D. Moore (2010), Above-stream microclimate and stream surface energy exchanges in a wildfire-disturbed riparian zone, *Hydrol. Process.*, *24*(17), 2369–2381, doi:10.1002/hyp.7639.

Leach, J. A., and R. D. Moore (2014), Winter stream temperature in the rain-on-snow zone of the Pacific Northwest: Influences of hillslope runoff and transient snow cover, *Hydrol. Earth Syst. Sci.*, *18*(2), 819–838, doi:10.5194/hess-18-819-2014.

Leppi, J. C., D. J. Rinella, R. R. Wilson, and W. M. Loya (2014), Linking climate change projections for an Alaskan watershed to future coho salmon production, *Glob. Chang. Biol.*, *20*(6), 1808–1820, doi:10.1111/gcb.12492.

Lisi, P. J., D. E. Schindler, K. T. Bentley, and G. R. Pess (2013), Association between geomorphic attributes of watersheds, water temperature, and salmon spawn timing in Alaskan streams, *Geomorphology*, *185*, 78–86, doi:10.1016/j.geomorph.2012.12.013.

Lisi, P. J., D. E. Schindler, T. J. Cline, M. D. Scheuerell, and P. B. Walsh (2015), Watershed geomorphology and snowmelt control stream thermal sensitivity to air temperature, *Geophys. Res. Lett.*, *42*(9), 3380–3388, doi:10.1002/2015GL064083.Received.

Lotspeich, F. B., and B. H. Reid (1980), Tri-tube Freeze-core Procedure for Sampling Stream Gravels, *Progress. Fish-Culturist*, *42*(2), 96–99, doi:10.1577/1548-8659(1980)42.

Luce, C., B. Staab, M. Kramer, S. Wenger, D. Isaak, and C. McConnell (2014), Sensitivity of summer streamtemperatures to climate variability in the Pacific Northwest, *Water Resour. Res.*, *50*, 3428–3443, doi:10.1002/2013WR014329.Received.

Magnusson, J., T. Jonas, and J. W. Kirchner (2012), Temperature dynamics of a proglacial stream: Identifying dominant energy balance components and inferring spatially integrated hydraulic geometry, *Water Resour. Res.*, *48*(6), W06510, doi:10.1029/2011WR011378.

Mann, D. H., A. L. Crowell, T. D. Hamilton, and B. P. . Finney (1998), Holocene Geologic and Climatic History Around The Gulf of Alaska, *Artic Anthropol.*, *35*(1), 112–131.

Mantua, N., I. Tohver, and A. Hamlet (2010), Climate change impacts on streamflow extremes and summertime stream temperature and their possible consequences for freshwater salmon habitat in Washington State, *Clim. Change*, *102*(1-2), 187–223,

doi:10.1007/s10584-010-9845-2.

Mantua, N. J., S. R. Hare, Y. Zhang, J. M. Wallace, and R. C. Francis (1997), A Pacific Interdecadal Climate Oscillation with Impacts on Salmon Production, *Bull. Am. Meteorol. Soc.*, *78*(6), 1069–1079, doi:10.1175/1520-0477(1997)078<1069:APICOW>2.0.CO;2.

May, C. L., B. Pryor, T. E. Lisle, and M. Lang (2009), Coupling hydrodynamic modeling and empirical measures of bed mobility to predict the risk of scour and fill of salmon redds in a large regulated river, *Water Resour. Res.*, *45*(5), doi:10.1029/2007WR006498.

Mayer, T. D. (2012), Controls of summer stream temperature in the Pacific Northwest, *J. Hydrol.*, *475*, 323–335, doi:10.1016/j.jhydrol.2012.10.012.

McAfee, S. A., J. Walsh, and T. S. Rupp (2014), Statistically downscaled projections of snow/rain partitioning for Alaska, *Hydrol. Process.*, *28*(12), 3930–3946, doi:10.1002/hyp.9934.

McCullough, D. A. (1999), *A Review and Synthesis of Effects of Alterations to the Water Temperature Regime on Freshwater Life Stages of Salmonids, with Special Reference to Chinook Salmon, Region 10 Water Resources Assessment Report No. 910-R-99-010,* U.S. Environmental Protection Agency.

McCullough, D. A. et al. (2009), Research in Thermal Biology: Burning Questions for Coldwater Stream Fishes, *Rev. Fish. Sci.*, *17*(1), 90–115, doi:10.1080/10641260802590152.

McKean, J., and D. Tonina (2013), Bed stability in unconfined gravel bed mountain streams: With implications for salmon spawning viability in future climates, *J. Geophys. Res. Earth Surf.*, *118*(3), 1227–1240, doi:10.1002/jgrf.20092.

Milliman, J. D., and R. H. Meade (1983), World-Wide Delivery of River Sediment to the Oceans, *J. Geol.*, *91*(1), 1–21.

Milner, A. M., A. L. Robertson, K. a. Monaghan, A. J. Veal, and E. a. Flory (2008), Colonization and development of an Alaskan stream community over 28 years, *Front. Ecol. Environ.*, *6*(8), 413–419, doi:10.1890/060149.

Mohseni, O., and H. G. Stefan (1999), Stream temperature/air temperature relationship: A physical interpretation, *J. Hydrol.*, *218*(3-4), 128–141, doi:10.1016/S0022-1694(99)00034-7.

Mohseni, O., H. G. Stefan, and T. R. Erickson (1998), A nonlinear regression model for weekly stream temperatures, *Water Resour. Res.*, *34*(10), 2685–2692.

Mohseni, O., H. G. Stefan, and J. G. Eaton (2003), Global Warming and Potential Changes in Fish Habitat, *Environ. Prot.*, *59*(1995), 389–409, doi:10.1023/A:1024847723344.

Montgomery, D. R., J. M. Buffington, N. P. Peterson, D. Schuett-Hames, and T. P. Quinn (1996), Stream-bed scour, egg burial depths, and the influence of salmonid spawning on bed surface mobility and embryo survival, *Can. J. Fish. Aquat. Sci.*, *53*(5), 1061–1070, doi:10.1139/f96-028.

Montgomery, D. R., E. M. Beamer, G. R. Pess, and T. P. Quinn (1999), Channel type and salmonid spawning distribution and abundance, *Can. J. Fish. Aquat. Sci.*, *56*(3), 377–387, doi:10.1139/f98-181.

Moore, R. D., D. L. Spittlehouse, and A. Story (2005), Riparian microclimate and stream temperature response to forest harvesting: A review, *J. Am. Water Resour. Assoc.*, *7*(4), 813–834, doi:10.1111/j.1752-1688.2005.tb04465.x.

Morrill, J., R. Bales, and M. Conklin (2005), Estimating Stream Temperature from Air Temperature: Implications for Future Water Quality, *J. Environ. Eng.*, *131*(1), 139–146, doi:doi:10.1061/(ASCE)0733-9372(2005)131:1(139).

Mote, P. W. et al. (2003), Preparing for climatic change: The water, salmon, and forests of the Pacific Northwest, *Clim. Change*, *61*(1-2), 45–88, doi:10.1023/A:1026302914358.

Murray, C. B., and J. D. McPhail (1988), Effect of incubation temperature on the development of five species of Pacific salmon (Oncorhynchus) embryos and alevins, *Can. J. Zool.*, *66*(1), 266–273, doi:10.1139/z88-038.

Neal, E. G., M. Todd Walter, and C. Coffeen (2002), Linking the pacific decadal oscillation to seasonal stream discharge patterns in Southeast Alaska, *J. Hydrol.*, *263*(1-4), 188–197, doi:10.1016/S0022-1694(02)00058-6.

Neuheimer, A. B., and C. T. Taggart (2007), The growing degree-day and fish size-at-age: the overlooked metric, *Can. J. Fish. Aquat. Sci.*, *64*(2), 375–385, doi:10.1139/f07-003.

Nichols, J. E., D. M. Peteet, C. M. Moy, I. S. Castaneda, A. McGeachy, and M. Perez (2014), Impacts of climate and vegetation change on carbon accumulation in a south-central Alaskan peatland assessed with novel organic geochemical techniques, *The Holocene*, *24*(9), 1146–1155, doi:10.1177/0959683614540729.

O'Driscoll, M. a., and D. R. DeWalle (2006), Stream–air temperature relations to classify stream–ground water interactions in a karst setting, central Pennsylvania, USA, *J. Hydrol.*, *329*(1-2), 140–153, doi:10.1016/j.jhydrol.2006.02.010.

Pitlick, J., E. R. Mueller, C. Segura, R. Cress, and M. Torizzo (2008), Relation between flow, surface-layer armoring and sediment transport in gravel-bed rivers, *Earth Surf. Process. Landforms*, *33*, 1192–1209, doi:10.1002/esp.1607.

Plafker, G. (1990), Regional vertical tectonic displacement of shorelines in south-central Alaska during and between great earthquakes, *Northwest Sci.*, *64*(5), 250–258.

Poole, G. C., and C. H. Berman (2001), An Ecological Perspective on In-Stream Temperature: Natural Heat Dynamics and Mechanisms of Human-Caused Thermal Degradation, *Environ. Manage.*, *27*(6), 787–802, doi:10.1007/s002670010188.

R Core Team (2015), R: A language and environment for statistical computing, R Foundation for Statistical Computing, Vienna, Austria,

Reimnitz, E. (1966), Late Quaternary History and Sedimentation of the Copper River Delta and Vicinity, Alaska. PhD Dissertation, University of California, San Diego.

Romero-Lankao, P., J. B. Smith, D. J. Davidson, N. S. Diffenbaugh, P. L. Kinney, P. Kirshen, P. Kovacs, and L. V. Ruiz (2014), Chpt 26. North America. In: Climate Change 2014: Impacts, Adaptation, and Vulnerability. Part B: Regional Aspects. Contribution of Working Group II to the Fifth Assessment Report of the Intergovernmental Panel on Climate Change, in *Climate Change 2014: Impacts, Adaptation, and Vulnerability. Part B: Regional Aspects. Contribution of Working Group II to the Fifth Assessment Report of the Intergovernmental Panel on Climate Change*, edited by V. R. Barros et al., pp. 1439–1498, Cambridge University Press, Cambridge, United Kingdom and New York, NY, USA.

Schindler, D. E., D. E. Rogers, M. D. Scheuerell, and C. A. Abrey (2013), Effects of Changing Climate on Zooplankton and Juvenile Sockeye Salmon Growth in Southwestern Alaska, *Ecology*, *86*(1), 198–209.

Shanley, C. S., and D. M. Albert (2014), Climate Change Sensitivity Index for Pacific Salmon Habitat in Southeast Alaska, *PLoS One*, *9*(8), e104799, doi:10.1371/journal.pone.0104799.

Shanley, C. S. et al. (2015), Climate change implications in the northern coastal temperate rainforest of North America, *Clim. Change*, *130*(2), 155–170, doi:10.1007/s10584-015-1355-9.

Shepard, B. G., G. F. Hartman, and W. J. Wilson (1986), Relationships between stream and intra-gravel temperatures in coastal drainage, and some implications for fisheries workers, *Can. J. Fish. Aquat. Sci.*, *43*, 1818–1822.

Sinokrot, B. a., and H. G. Stefan (1993), Stream temperature dynamics: measurements and modeling, *Water Resour. Res.*, *29*(7), 2299–2312, doi:10.1029/93WR00540.

Smith, C. T., R. J. Nelson, C. C. Wood, and B. F. Koop (2001), Glacial biogeography of North American coho salmon (Oncorhynchus kisutch)., *Mol. Ecol.*, *10*, 2775–2785, doi:10.1046/j.1365-294X.2001.t01-1-01405.x.

Tague, C., G. Grant, M. Farrell, J. Choate, and A. Jefferson (2008), Deep groundwater mediates streamflow response to climate warming in the Oregon Cascades, *Clim. Change*, *86*(1-2), 189–210, doi:10.1007/s10584-007-9294-8.

Tarr, R. S., and L. Martin (1914), *Alaskan Glacier Studies*, The National Geographic Society, Washington.

Thilenius, J. F. (1990a), Plant Succession on Earthquake Uplifted Coastal Wetlands, Copper River Delta, Alaska, *Northwest Sci.*, *64*(5), 259–262.

Thilenius, J. F. (1990b), Woody plant succession on earthquake-uplifted coastal wetlands of the Copper River Delta, Alaska, *For. Ecol. Manage.*, *33/34*, 439–462.

Tuthill, S. J., and W. M. Laird (1966), Geomorphic Effects of the Earthquake of March 27, 1964 In the Martin-Bering Rivers Area, Alaska, *U.S. Geol. Surv. Prof. Pap.*, *543-B*, 1–28.

U.S. Geological Survey (2013), National Hydrography Geodatabase, *Natl. Map Viewer available World Wide Web (http//viewer.nationalmap.gov/viewer/nhd.html?p=nhd),*

accessed Oct. 2015.

University of Alaska (2015), Scenarios Network for Alaska and Arctic Planning, *www.snap.uaf.edu*.

Waller, R. M. (1966), Effects on Hydrologic Regimen, in *The Alaska Earthquake March 27, 1964: Effects on Hydrologic Regimen*, vol. 544-A, pp. 1–27.

Waples, R. S., T. Beechie, and G. R. Pess (2009), Evolutionary History, Habitat Disturbance Regimes, and Anthropogenic Changes: What Do These Mean for Resilience of Pacific Salmon Populations ?, *Ecol. Soc.*, *14*(1), 18.

Wawrzyniak, V., H. Piégay, P. Allemand, L. Vaudor, and P. Grandjean (2013), Prediction of water temperature heterogeneity of braided rivers using very high resolution thermal infrared (TIR) images, *Int. J. Remote Sens.*, *34*(13), 4812–4831, doi:10.1080/01431161.2013.782113.

Webb, B. W., and F. Nobilis (1997), Long-term perspective on the nature of the air-water temperature relationship: A case study, *Hydrol. Process.*, *11*(2), 137–147, doi:10.1002/(SICI)1099-1085(199702)11:2<137::AID-HYP405>3.0.CO;2-2.

Webb, B. W., and Y. Zhang (1997), Spatial and seasonal variability in the components of the river heat budget, *Hydrol. Process.*, *11*, 79–101, doi:10.1002/(SICI)1099-1085(199701)11:1<79::AID-HYP404>3.3.CO;2-E.

Wiedmer, M., D. R. Montgomery, A. R. Gillespie, and H. Greenberg (2010), Late Quaternary megafloods from Glacial Lake Atna, Southcentral Alaska, U.S.A., *Quat. Res.*, *73*(3), 413–424, doi:10.1016/j.yqres.2010.02.005.

Wilson, F. H., C. P. Hults, K. A. Labay, and N. Shew (2008), Digital data for the reconnaissance geologic map for Prince William Sound and the Kenai Peninsula, Alaska, *U.S. Geol. Surv. Open-File Rep. 2008-1002*.

Winkler, B. G. R., G. Plafker, R. J. Goldfarb, J. E. Case, and D. L. Peck (1992), *The Alaska Mineral Resource Assessment Program : Background Information to Accompany Geologic and Mineral-Resource Maps of the Cordova and Middleton Island Quadrangles , Southern Alaska*.

Wobus, C., R. Prucha, D. Albert, C. Woll, M. Loinaz, and R. Jones (2015), Hydrologic Alterations from Climate Change Inform Assessment of Ecological Risk to Pacific Salmon in Bristol Bay, Alaska, *PLoS One*, *10*(12), e0143905, doi:10.1371/journal.pone.0143905.

Zhang, T., S. A. Bowling, and K. Stamnes (1997), Impact of the atmosphere on surface radiative fluxes and snowmelt in the Artic and Subartic, *J. Geophys. Res.*, *102*(D4), 4287–4303, doi:10.1175/1520-0442(1996)009<2110:IOCOSR>2.0.CO;2.

Zimmerman, C. E., and J. E. Finn (2012), A Simple Method for In Situ Monitoring of Water Temperature in Substrates Used by Spawning Salmonids, *J. Fish Wildl. Manag.*, *3*(2), 288–295, doi:10.3996/032012-JFWM-025.

3.9 Figures

Table 3.1 The locations of the study sites (n=8) and a description of catchment characteristics calculated from 5 m resolution DEM data

Site Information					Catchment Characteristics			
ID	Latitude decimal degrees	Longitude decimal degrees	Lake Upstream?	Primary flowpath	Area (ha)	Elevation (m) Min	Max	Mean
Clear	60.57	-144.78		Groundwater	3504	19	1329	337
ET.Mi	60.46	-145.29		Shallow	188	8	83	33
Ibeck	60.59	-145.47		Groundwater	336	48	109	74
LMart	60.40	-144.61	Y	Shallow	2156	29	547	158
Marti	60.34	-144.52		Shallow	2274	27	986	271
Ot.Ca	60.53	-145.46	Y	Shallow	166	20	214	83
Salmo	60.45	-145.17		Groundwater	2267	11	1257	388
TF.Mi	60.44	-145.12		Groundwater	61	11	42	25

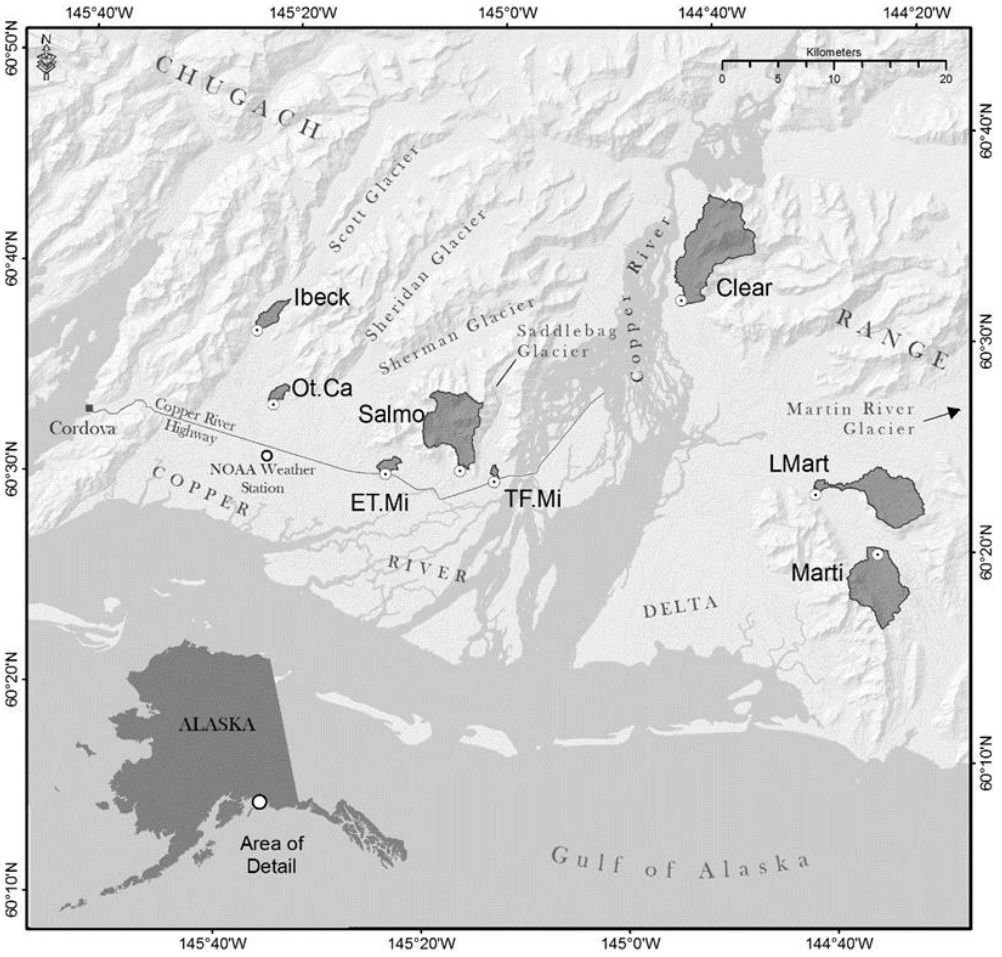

Figure 3.1 Study Sites (n=8) on the Copper River Delta, Alaska

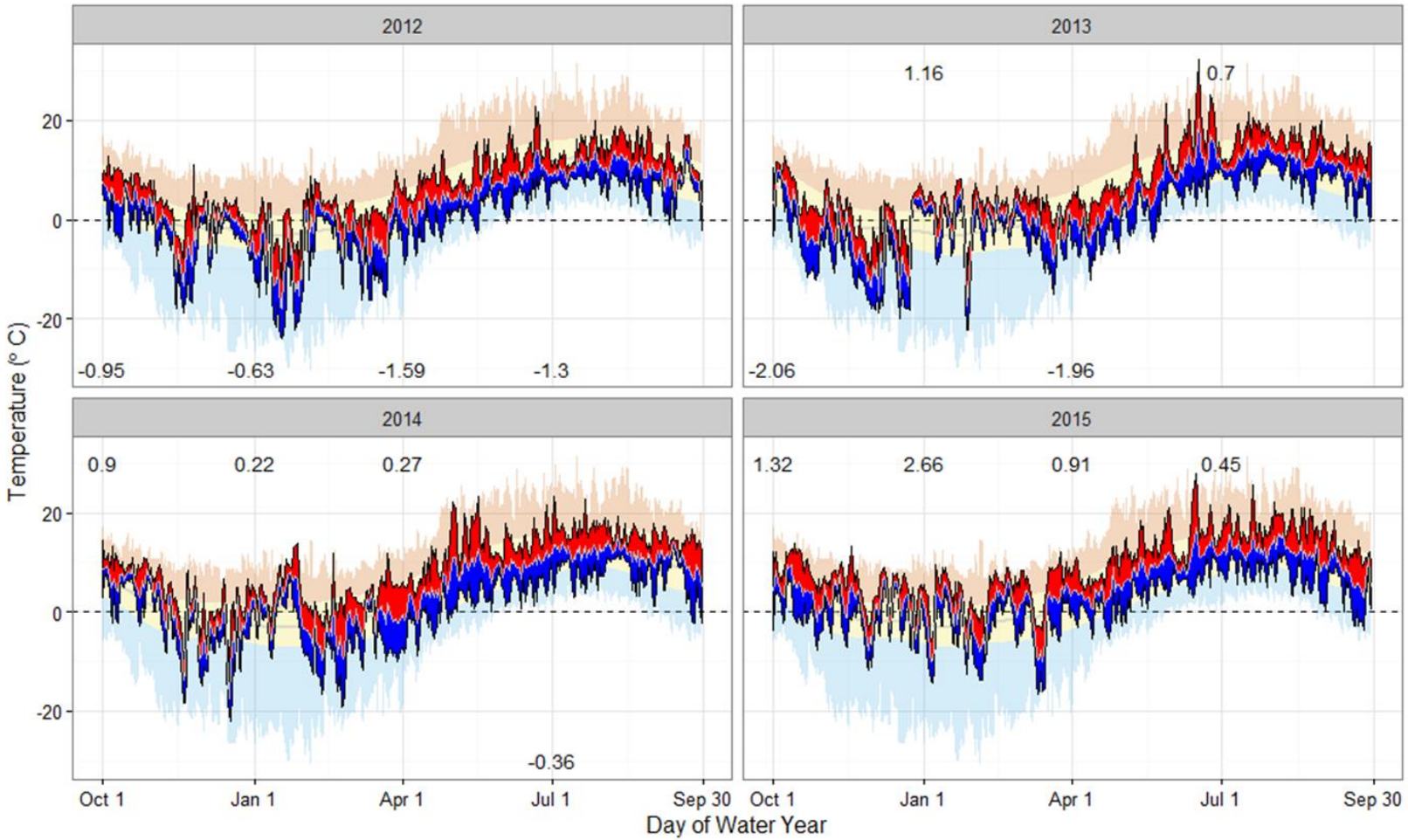

Figure 3.2 Foreground: Daily maximum (top of red ribbon), minimum (bottom of blue ribbon), and mean (gray line) temperatures recorded at M.H. Smith Airport during study period water years (2012-2015). Background shading: Normal daily mean (gray line), normal daily range (yellow ribbon), and daily record low (blue) and high (red) air temperatures based on 31 years of record (1980-2010) at NOAA GHCN station #26410. Text: Seasonal (SON, DJF, MAM, & JJA) temperature anomalies are printed with positive anomalies above and negative anomalies below the plots

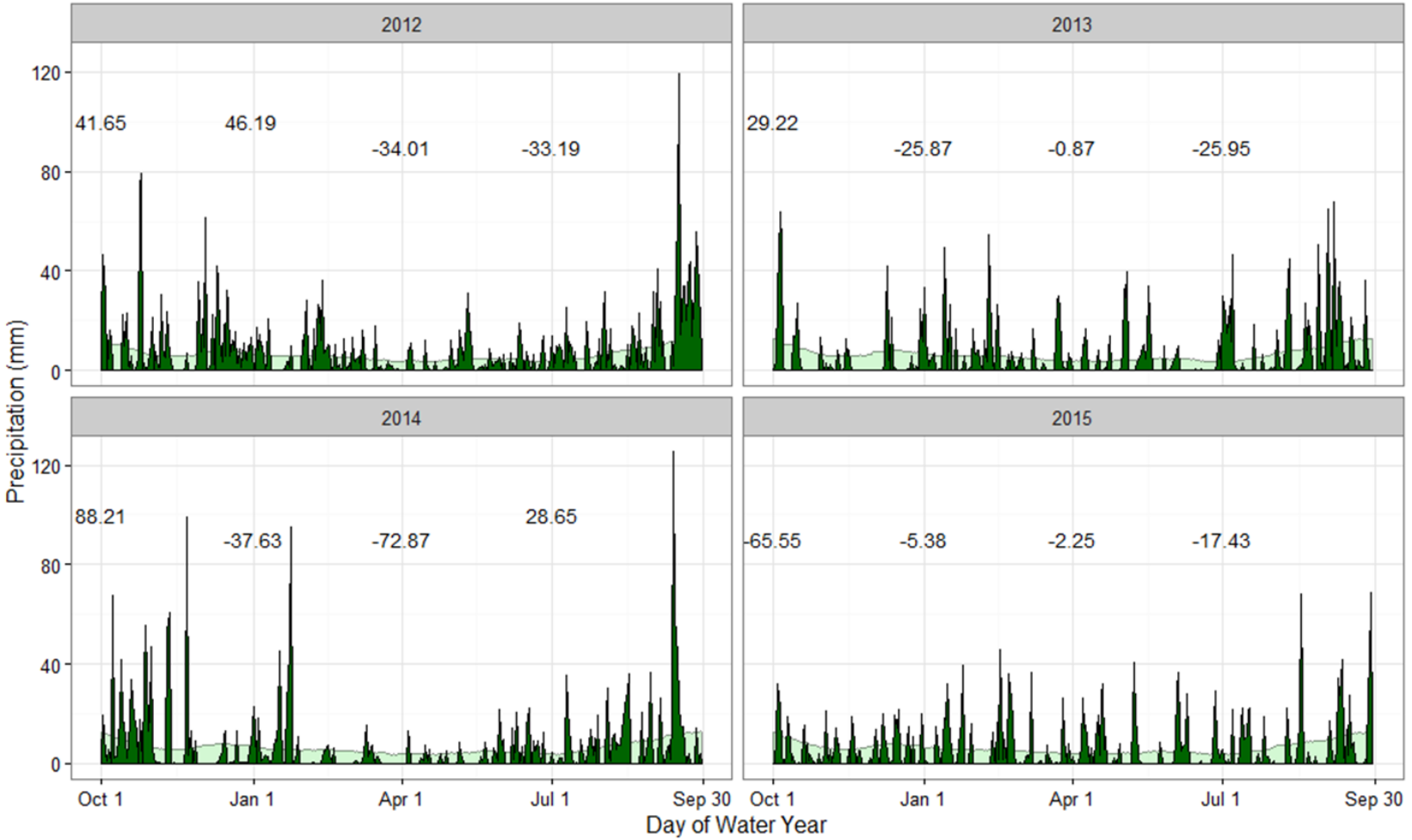

Figure 3.3 Foreground: Daily precipitation (dark green ribbon) recorded at M.H. Smith Airport during study period water years (2012-2015). Background (light green ribbon): Normal daily precipitation based on 31 years of record (1980-2010) at NOAA GHCN station #26410. Text: Seasonal (SON, DJF, MAM, & JJA) precipitation anomalies are printed with positive anomalies offset from negative anomalies above the plots

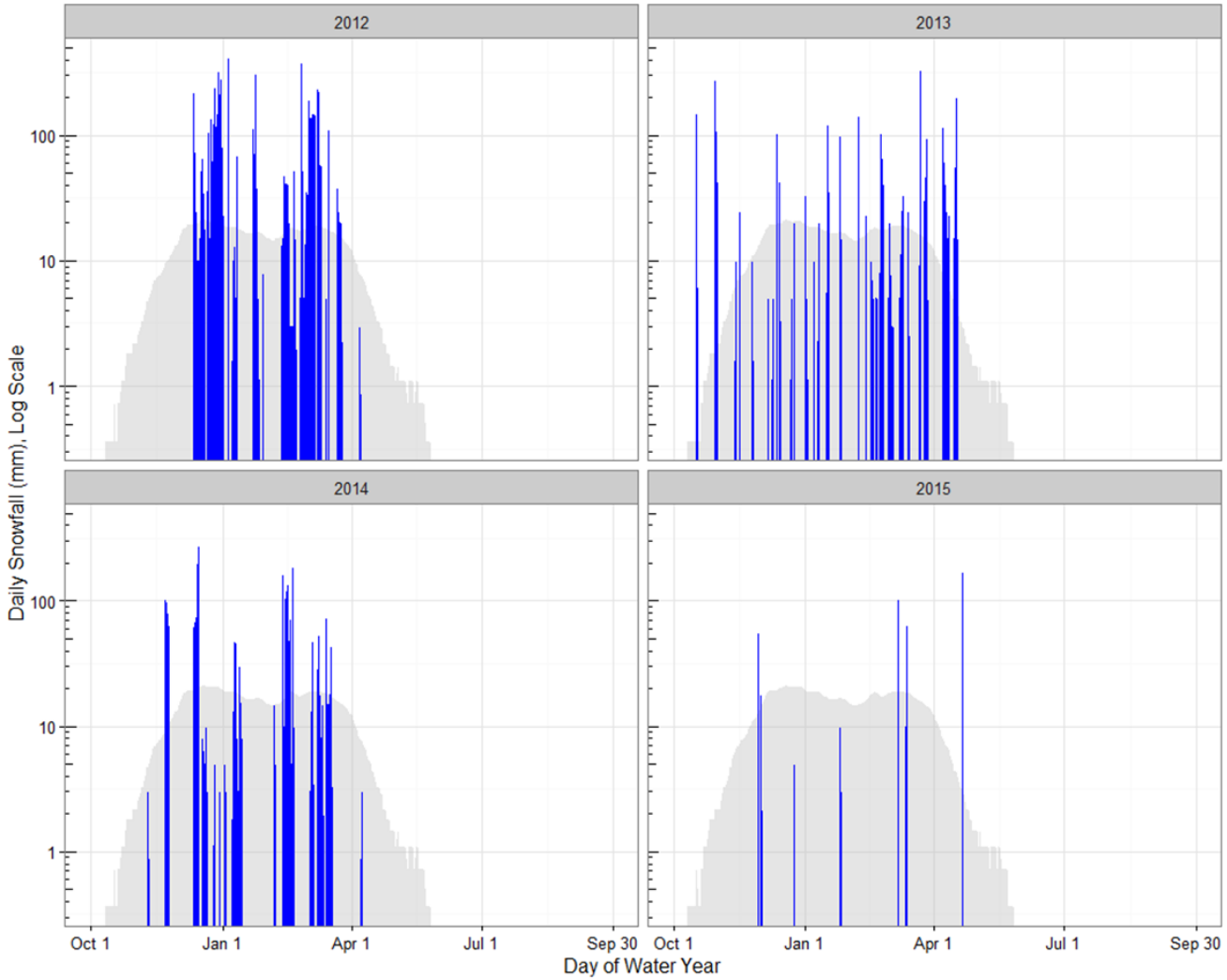

Figure 3.4 Foreground (blue ribbon): Daily snowfall recorded at M.H.Smith Airport during study period water years (2012-2015). Background (gray ribbon): 7 day rolling daily mean snowfall based on 31 years of record (1980-2010) at NOAA GHCN station #26410. Note: Y axis is log scale

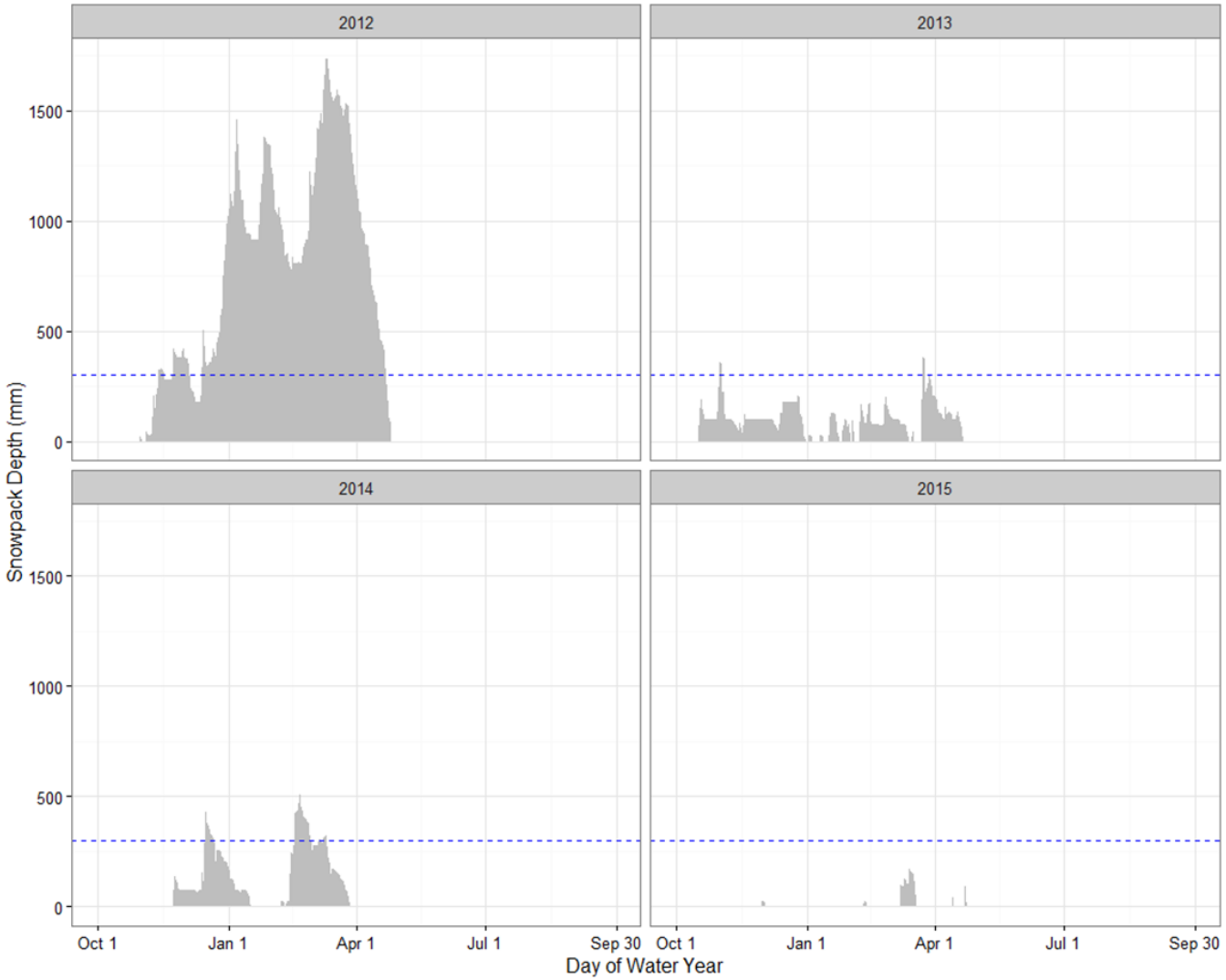

Figure 3.5 Daily mean snowpack depth recorded at M.H. Smith Airport during study period water years (2012-2015). Blue dashed line at 300mm denotes suspected mean winter (DJF) snowpack based on historical documents

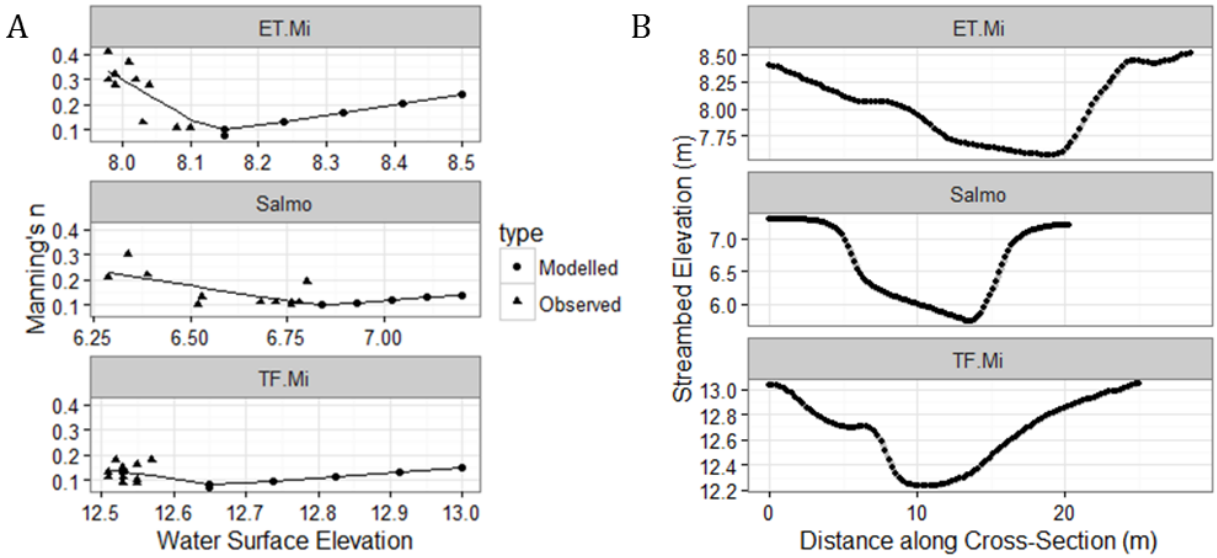

Figure 3.6 A) Model utilized to fit Manning's n to water surface elevation based on observed and tabled n values. B) Cross-sectional profiles at the three gauging sites denoted by interpolated points (black dots) and model of fit (gray line). Note the free y axes

Table 3.2 Gauge and bankfull elevations, count of discharge measurements, and rating curve equations for each gauging site

Site	Pressure Transducer Elevation (m)	Count of discharge measurements	Rating Curve Equation
ET-Mi	7.47	16	$x = e^{\frac{y-8.173}{0.165}}$
Salmo	5.93	15	$x = e^{\frac{y-6.543}{0.296}}$
TF-Mi	11.95	17	$x = e^{\frac{y-12.853}{0.229}}$

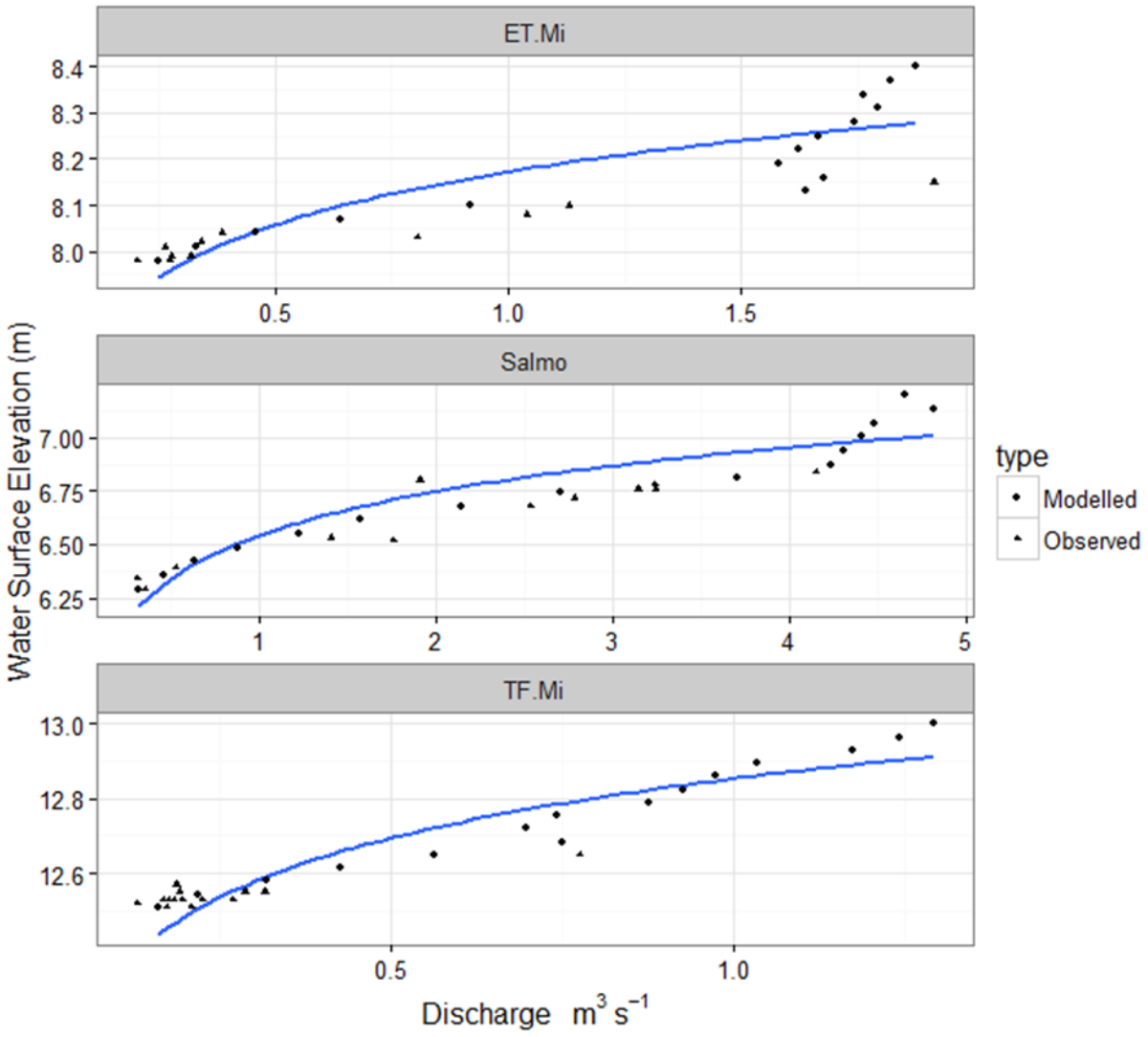

Figure 3.7 Rating curve used to generate hourly discharge estimates. The solid line was fitted to modelled (dots) and measured (triangles) data points

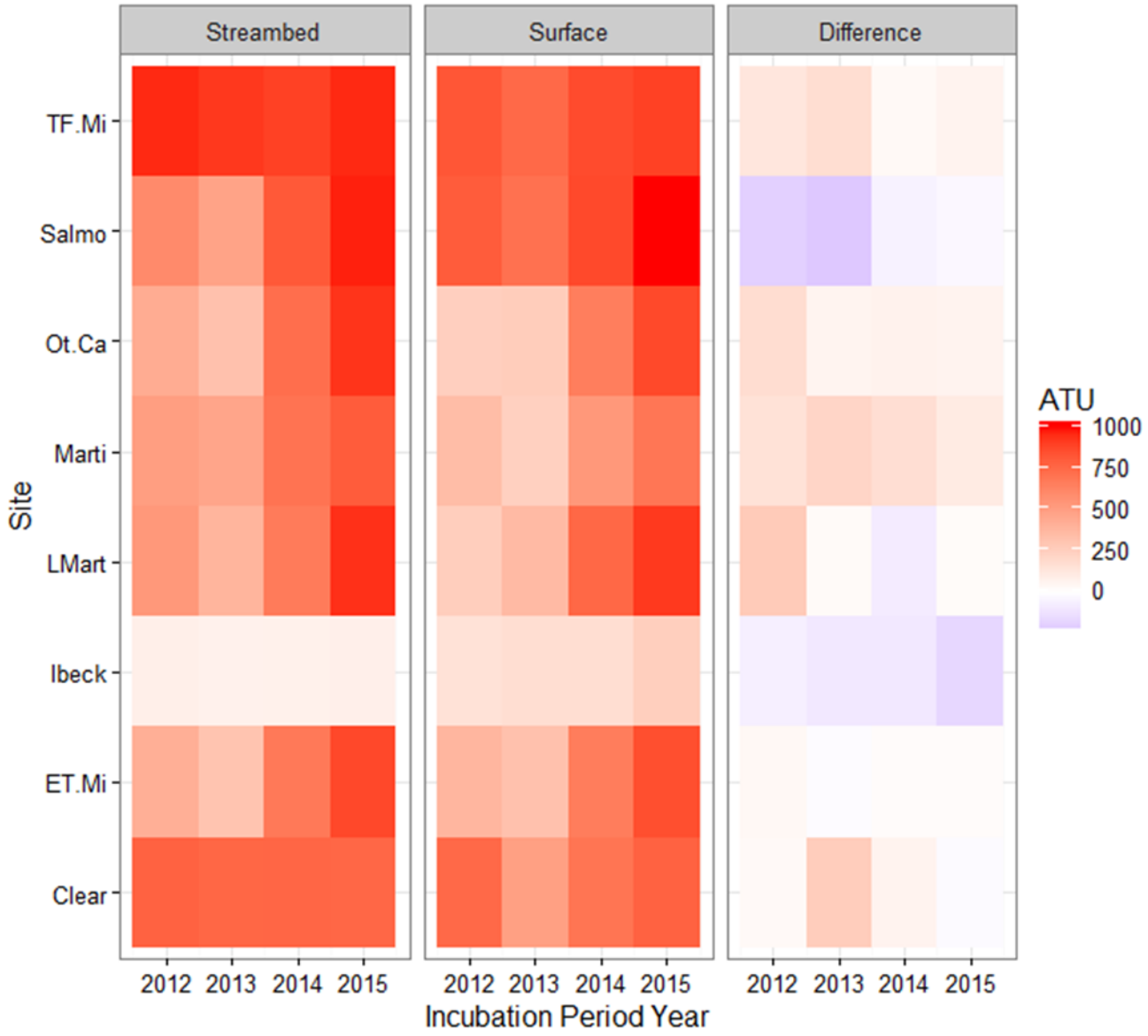

Figure 3.8 Total accumulated thermal units (ATU) in streambed (first column) and surface (second column) water and the difference between streambed and surface water total ATU (third column) during the coho salmon incubation period (defined as Oct 1 to May 31) by year and by study site

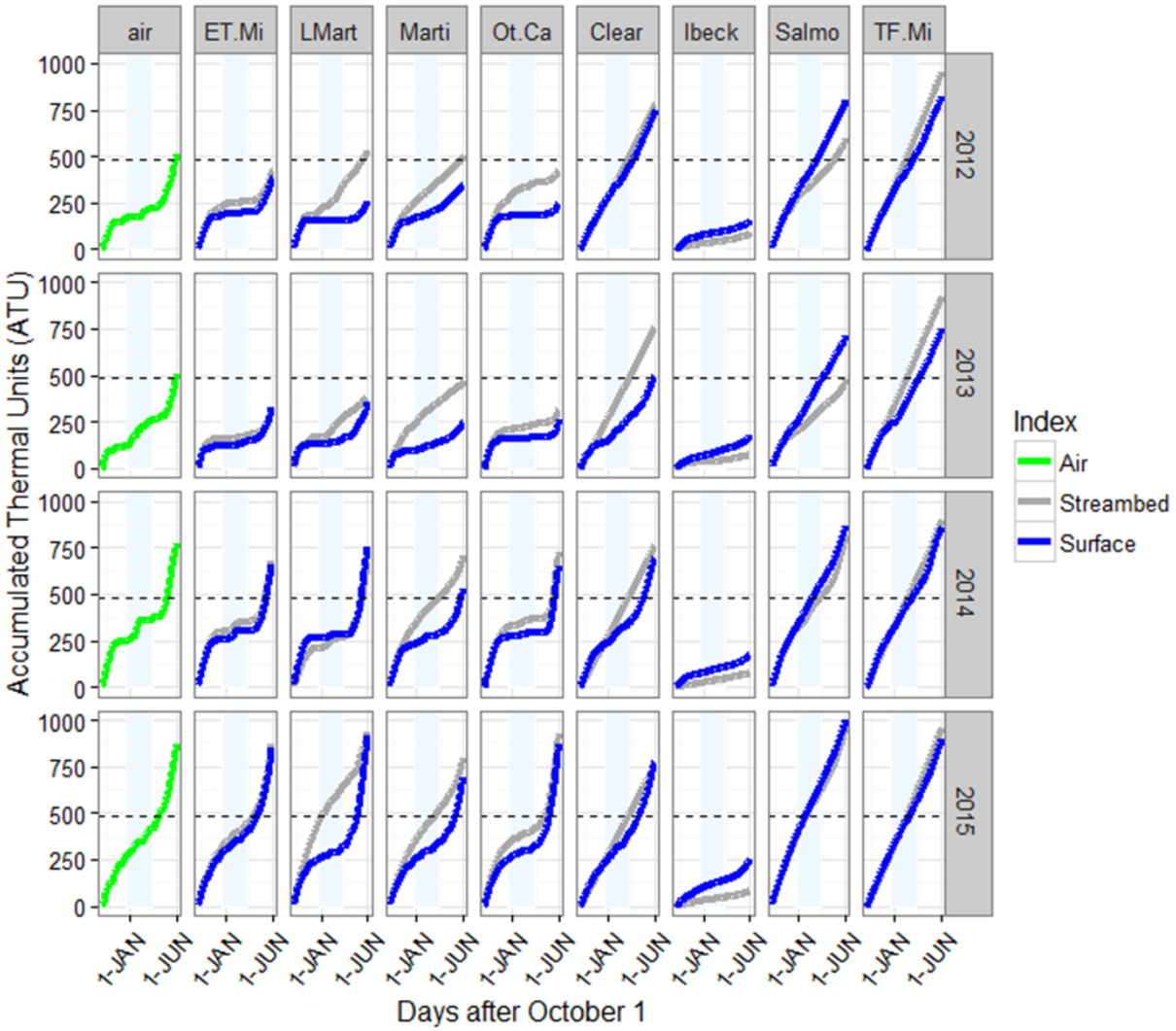

Figure 3.9 Accumulated thermal units (ATU) over the 243 day incubation period (Oct 1 – May 31) for based on air temperature and surface and streambed water temperature. ATU are the cumulative sum of the daily mean temperatures greater than 0 °C. Dashed line at 485 denotes a hypothetical incubation threshold for 50% coho salmon emergence. Light blue region indicates the mid incubation period (Dec 21 – Mar 11)

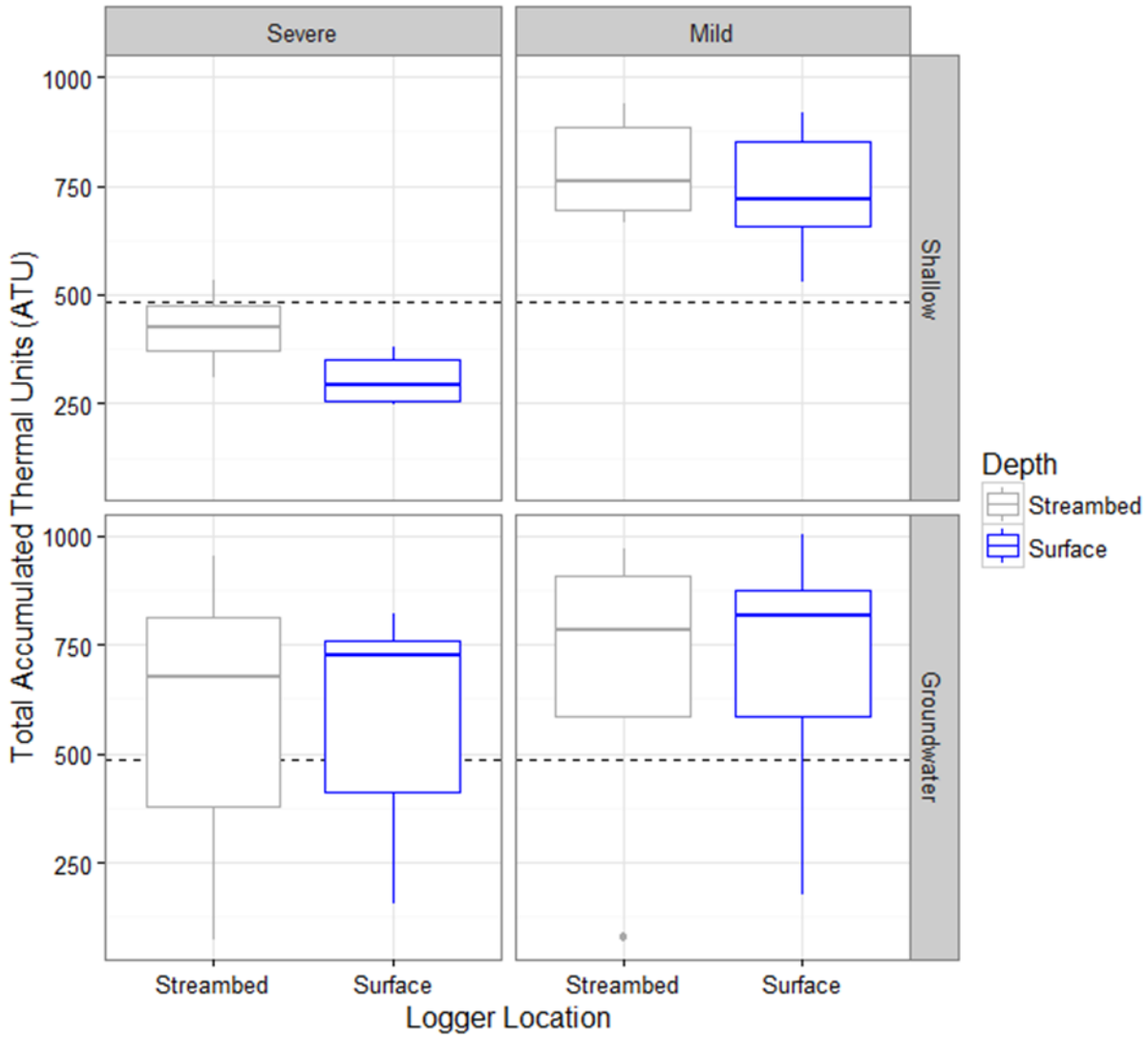

Figure 3.10 Total incubation period ATU by winter severity and sensor depth at shallow flowpath (top) and groundwater flowpath (bottom) sites. Dashed line at 485 denotes a hypothetical Coho Salmon incubation threshold for 50% emergence

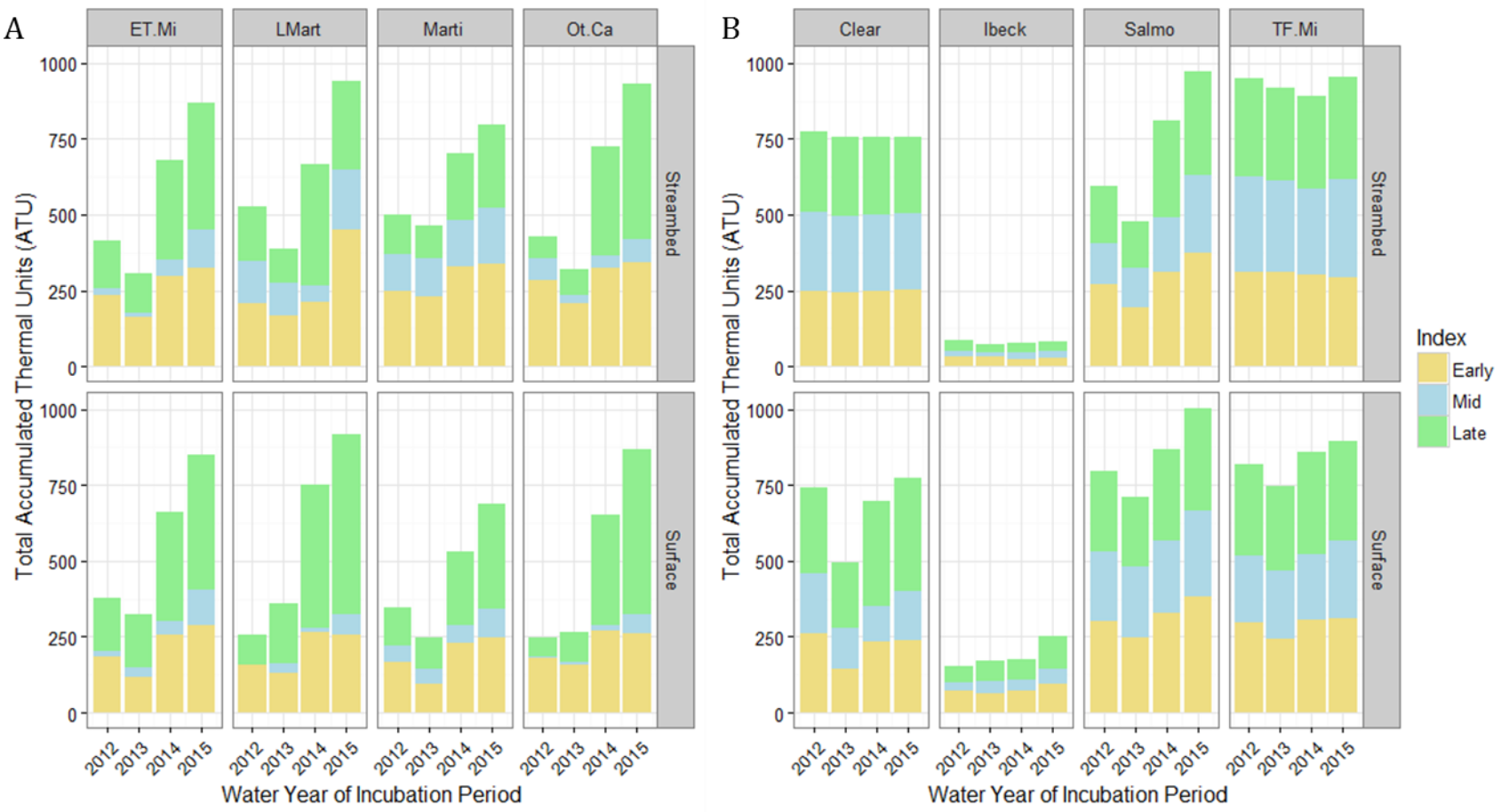

Figure 3.11 Accumulated Thermal Units (ATU) calculated with streambed (top) and surface (bottom) water temperature data at A) shallow flowpath and B) upwelling groundwater sites. Color-coding denotes equal 81 day-long sub-periods ("Early" is Oct 1-Dec 20, "Mid" is Dec 21-Mar 11, and "Late" is Mar 12-May 31)

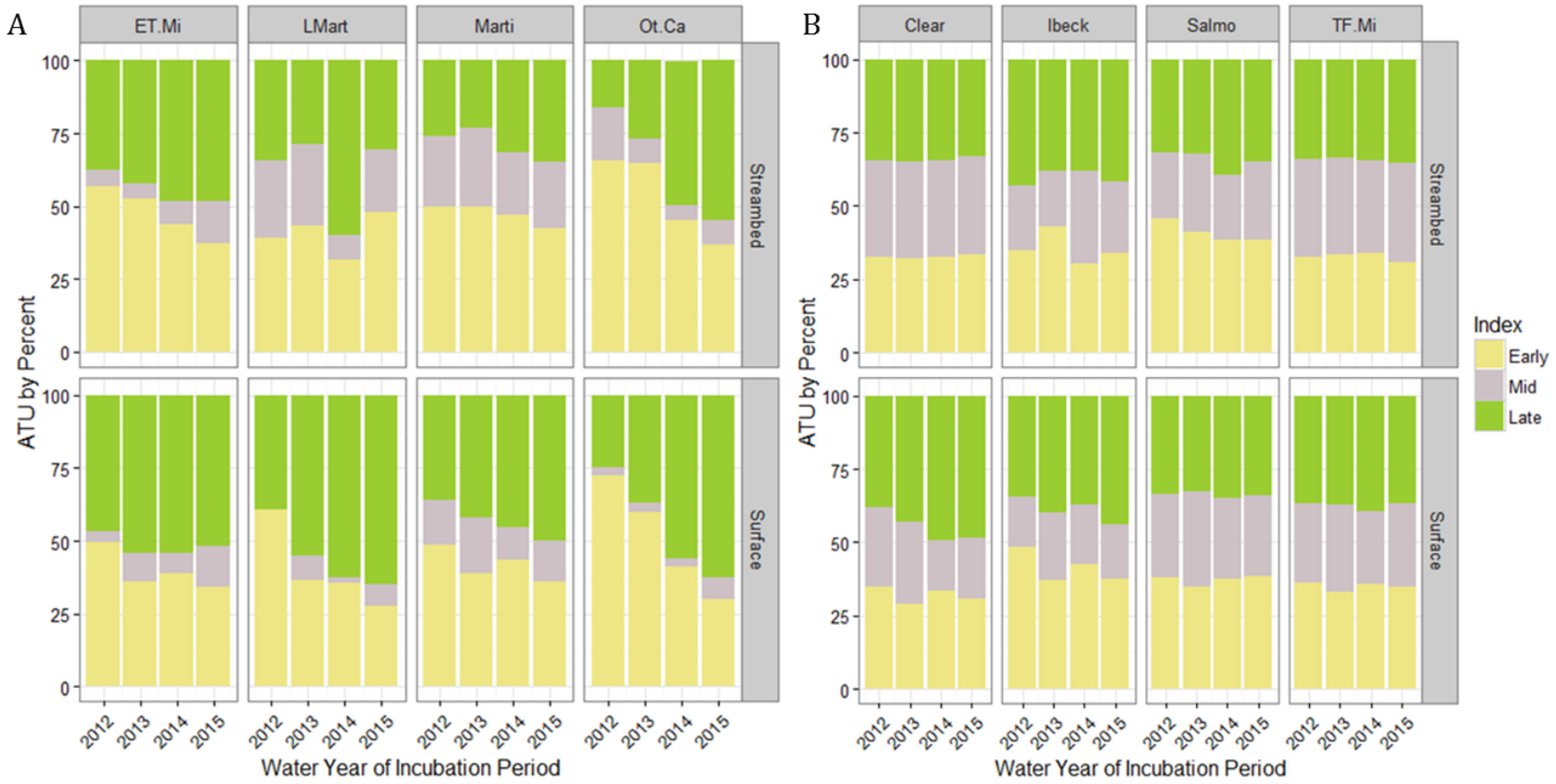

Figure 3.12 Percentage of total accumulated thermal units by season for streambed (top) and surface (bottom) water temperature loggers at A) shallow flowpath and B) groundwater flowpath sites. Color-coding denotes equal 81 day-long sub-periods ("Early" is Oct 1-Dec 20, "Mid" is Dec 21-Mar 11, and "Late" is Mar 12-May 31)

Table 3.3 Discharge statistics by site calculated from daily mean discharge records between April 1, 2014 and September 30, 2015

Site	Daily Discharge				S.D.	Mean Daily Specific Discharge	Max Daily Specific Discharge
	Mean	Max	Min	Bankfull			
	$m^3 s^{-1}$					$mm\ hr^{-1}$	$m^3 s^{-1}$
ET.Mi	0.41	5.63	0.17	4.0	0.31	0.79	10.78
Salmo	1.63	82.63	0.38	9.2	4.19	0.26	13.12
TF.Mi	0.23	0.36	0.13	2.9	0.04	1.36	2.10

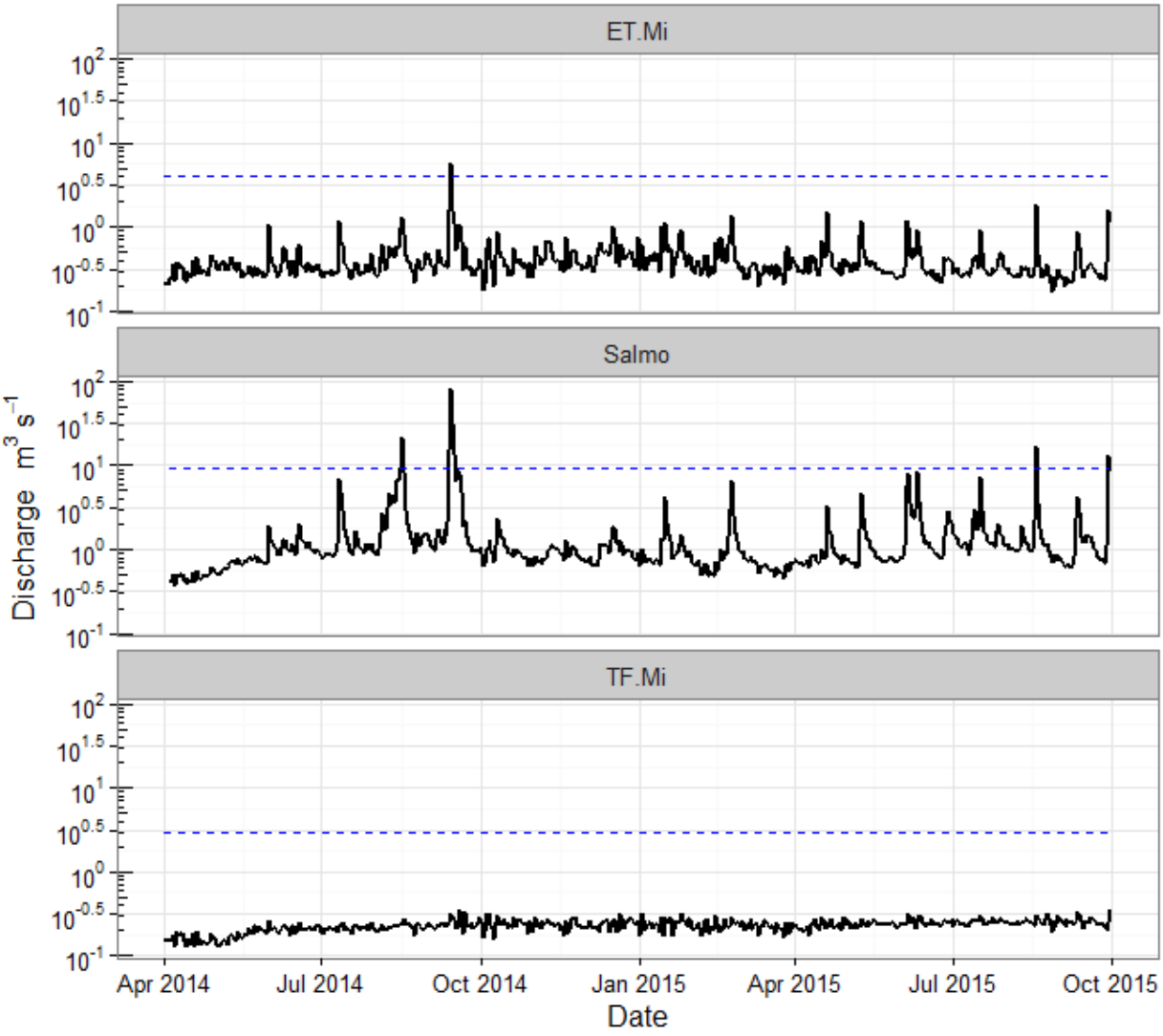

Figure 3.13 Daily discharge between April 1, 2014 and September 30, 2015. Blue dotted line denotes bankfull discharge

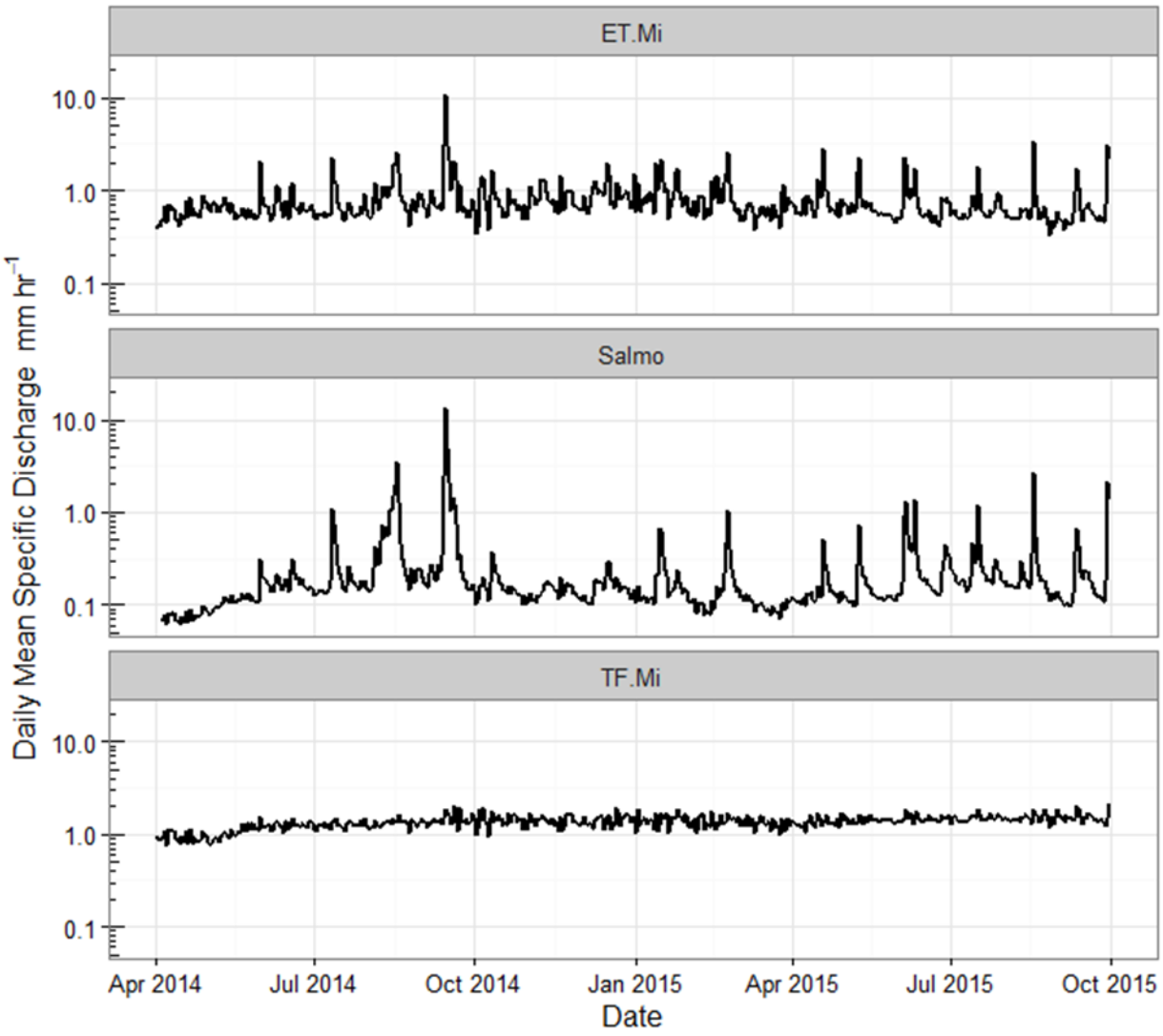

Figure 3.14 Daily specific discharge (mm hr^{-1}) between Apri1 1, 2014 and September 30, 2015. Note that the y axis is log-scale

Table 3.4 Shear Stresses and bed scour depth were calculated for bankfull discharge (second column) using slope, depth, and D50 measurements from each site

Site	Bankfull Water Surface Elevation (m)	Discharge (m^3 $s^{-1)}$	Channel Slope (m/m)	Hydraulic Radius (m)	D50 (mm)	Calculated Dimensionless Shear Stress	Range of Critical Dimensionless Shear Stress	Range of Scour Depth (cm)
ET.Mi	8.4	4	0.003	0.47	15.8	0.054	0.025 - 0.035	3 - 8
Salmo	7.2	9.2	0.002	0.78	12.7	0.071	0.021 - 0.032	11 - 72
TF.Mi	13.1	2.9	0.004	0.37	11.5	0.082	0.028 - 0.038	7 - 19

Table 3.5 Anticipated risks of climate change impacts to spawning gravels at three gauged sites on the CRD

Site	Dominant Flowpath	Increased ATU	Increased Scour
ET.Mi	Shallow	HIGH	LOW
Salmo	Groundwater	MEDIUM	HIGH
TF.Mi	Groundwater	LOW	MEDIUM

4 Conclusions

I investigated climatic and geomorphic controls on year-round water temperature and potential scour depth at salmon spawning and rearing sites on the Copper River Delta (CRD), a large coastal foreland in Southcentral Alaska.

Considerable spatial heterogeneity was observed in year-round water temperatures at the study sites. I attribute this heterogeneity to a mix of water sources (precipitation, melt water, and groundwater), residence times, and flowpaths ("shallow" vs. "deep") across the landscape. Sites with upwelling groundwater were particularly notable. These sites exhibited low sensitivity to changing atmospheric conditions and provided stable thermal environments for salmon.

Weekly temperature maxima were positively correlated with lakes and negatively correlated with catchment elevation and slope. Interestingly, similar correlations were observed for the frequency of freezing conditions during the typical Coho Salmon incubation period (Oct-May), suggesting that catchments with high mean elevation and slope are both the coolest in the summer and the warmest in the winter. Thus, in addition to the upwelling groundwater sites, high-relief, high elevation catchments also exhibited lower thermal sensitivity and are anticipated to be less impacted by projected climatic changes.

Additionally, I documented increases in year-round monthly mean water temperatures during an anomalously warm year, when melt water was greatly reduced. Regression models underestimated the temperature increases, particularly during spring (MAM), suggesting that reduced melt hysteresis contributed to the observed water temperature changes. This finding also suggests that water temperatures projected by regression models may be conservative estimates in catchments were reductions in snowpack are anticipated.

Monthly mean temperatures are highly correlated with accumulated thermal units (^{o}C/day) (ATU), a biologically relevant metric used to model Pacific salmon incubation rates [*Neuheimer and Taggart*, 2007]. Even small increases in incubation period monthly

mean water temperatures will greatly increase total ATU and may accelerate embryo development [*Murray and McPhail*, 1988; *McCullough*, 1999].

Winter severity had little impact on incubation period ATU at upwelling groundwater sites, but this study documented more than two-fold increases in incubation period ATU during mild winters at shallow flowpath sites. Increases in spring (MAM) ATU at shallow flowpath sites were particularly significant when seasonal snow and ice was absent. Because late autumn (ON) ATU has been more significant than MAM ATU under climatological mean conditions, this finding suggests that the seasonality of ATU accumulation will shift if the climate warms and low elevation snowpack is reduced as projected by climate models [*McAfee et al.*, 2014]. To the best of my knowledge, the impacts of this potential shift on salmon embryos and juveniles has not been investigated.

Mid-winter (DJF) freshets contributed relatively little to incubation period ATU, but thaw events that reduce the duration of snow and ice cover may indirectly contribute to significant increases in ATU later in the incubation period, when seasonal snow and ice melt has historically buffered water temperatures under climatological mean conditions.

I did not observe any mid-winter overbank flooding at three gauged sites during an anomalously mild DJF; however, mid-winter floods are projected to occur with increased frequency under future climate scenarios [*Shanley and Albert*, 2014]. I calculated that reach-scale mean scour depth at bankfull discharge varied between 3 and 72 cm at our three gauged sites, suggesting the impacts of scour on egg mortality will be variable across the landscape. I suspect that scour potential is relatively low at salmon spawning and rearing sites on the CRD because the stream channels are generally low-relief and unconfined, but additional research is needed to quantify scour potential across the landscape.

I conclude that the impacts of projected climatic changes on water temperature and potential scour depth are likely to vary in magnitude across the Copper River Delta, even at small spatial scales, due to heterogeneity in climatic and geomorphic controls. Furthermore, the responses of local salmon populations are anticipated to vary due to localized life history adaptations. Understanding both the hydrology and the biology will be

critical to accurately assess the net impact of projected changes on Pacific Salmon production.

Bibliography

Arcement Jr., G. J., and V. R. Schneider (1989), Guide for selecting Manning's roughness coefficients for natural channels and flood plains, *U.S. Geol. Surv. Water-Supply Pap. 2339*.

Arismendi, I., S. L. Johnson, J. B. Dunham, and R. Haggerty (2013), Descriptors of natural thermal regimes in streams and their responsiveness to change in the Pacific Northwest of North America, *Freshw. Biol.*, *58*(5), 880–894, doi:10.1111/fwb.12094.

Arismendi, I., M. Safeeq, J. B. Dunham, and S. L. Johnson (2014), Can air temperature be used to project influences of climate change on stream temperature?, *Environ. Res. Lett.*, *9*(8), 084015, doi:10.1088/1748-9326/9/8/084015.

Barclay, D. J., E. M. Yager, J. Graves, M. Kloczko, and P. E. Calkin (2013), Late Holocene Glacial History of the Copper River Delta, Coastal South-central Alaska, and Controls on Valley Glacier Fluctuations, *Quat. Sci. Rev.*, *81*, 74–89, doi:10.1016/j.quascirev.2013.10.001.

Battin, J., M. W. Wiley, M. H. Ruckelshaus, R. N. Palmer, E. Korb, K. K. Bartz, and H. Imaki (2007), Projected impacts of climate change on salmon habitat restoration., *Proc. Natl. Acad. Sci. U. S. A.*, *104*(16), 6720–5, doi:10.1073/pnas.0701685104.

Baxter, C. V., and F. R. Hauer (2000), Geomorphology, hyporheic exchange, and selection of spawning habitat by bull trout (*Salvelinus confluentus*), *Can. J. Fish. Aquat. Sci.*, *57*(7), 1470–1481, doi:10.1139/cjfas-57-7-1470.

Beacham, T. D., and C. B. Murray (1990), Temperature, Egg Size, and Development of Embryos and Alevins of Five Species of Pacific Salmon: A Comparative Analysis, *Trans. Am. Fish. Soc.*, *119*(6), 927–945.

Beer, W. N., and J. J. Anderson (2011), Sensitivity of juvenile salmonid growth to future climate trends, *River Res. Appl.*, *27*(5), 663–669, doi:10.1002/rra.1390.

Benda, L., T. J. Beechie, R. C. Wissmar, and A. Johnson (1992), Morphology and Evolution of Salmonid Habitats in a Recently Deglaciated River Basin, Washington State, USA, *Can. J. Fish. Aquat. Sci.*, *49*(6), 1246–1256, doi:10.1139/f92-140.

van den Berghe, E. P., and M. R. Gross (1984), Female Size and nest depth in coho salmon (Oncorhynchus kisutch), *Can. J. Fish. Aquat. Sci.*, *41*, 204–206.

Bisson, P. a., J. B. Dunham, and G. H. Reeves (2009), Freshwater ecosystems and resilience of Pacific salmon: habitat management based on natural variability, *Ecol. Soc.*, *14*(1), 45, doi:45.

Boggs, K. (2000), Classification of Community Types, Successional Sequences, and Landscapes of the Copper River Delta, Alaska, *Gen. Tech. Rep. - Pacific Northwest Res. Station. USDA For. Serv.*, (PNW-GTR-469), 244 pp.

Brabets, T. P. (1997), Geomorphology of the lower Copper River, Alaska, *U.S. Geol. Surv. Prof. Pap. #1581*, 89.

Braun, D. C., D. A. Patterson, and J. D. Reynolds (2013), Maternal and environmental influences on egg size and juvenile life-history traits in Pacific salmon, *Ecol. Evol.*, *3*(6), 1727–1740, doi:10.1002/ece3.555.

Bryant, M. D. (1992), The Copper River Delta pulse study: an interdisciplinary survey of the aquatic habitats, *Gen. Tech. Rep. - Pacific Northwest Res. Station. USDA For. Serv.*, *PNW-GTR-28*, 43.

Bryant, M. D. (2009), Global climate change and potential effects on Pacific salmonids in freshwater ecosystems of southeast Alaska, *Clim. Change*, *95*(1-2), 169–193, doi:10.1007/s10584-008-9530-x.

Bunte, K., and S. R. Abt (2001), Sampling Surface and Subsurface Particle-Size Distributions in Wadable Gravel- and Cobble-Bed Streams for Analyses in Sediment Transport , Hydraulics , and Streambed Monitoring, *0*, 450.

Caissie, D. (2006), The thermal regime of rivers: a review, *Freshw. Biol.*, *51*(8), 1389–1406, doi:10.1111/j.1365-2427.2006.01597.x.

Caissie, D., B. L. Kurylyk, A. St-Hilaire, N. El-Jabi, and K. T. B. MacQuarrie (2014), Streambed temperature dynamics and corresponding heat fluxes in small streams experiencing seasonal ice cover, *J. Hydrol.*, *519*, 1441–1452, doi:10.1016/j.jhydrol.2014.09.034.

Caldwell, P., C. Segura, S. Gull Laird, G. Sun, S. G. McNulty, M. Sandercock, J. Boggs, and J. M. Vose (2015), Short-term stream water temperature observations permit rapid assessment of potential climate change impacts, *Hydrol. Process.*, *29*(9), 2196–2211, doi:10.1002/hyp.10358.

Case, J. E., D. F. Barnes, G. Plafker, and S. L. Robbins (1966), Gravity Survey and Regional Geology of the Prince William Sound Epicentral Region, Alaska, in *The Alaska Earthquake, March 27, 1964: Regional Effects*, United States Government Printing Office.

Christensen, H. H. (2000), *Alaska's Copper River: Humankind in a Changing World*, U.S. Dept. of Agriculture, Forest Service, Pacific Northwest Research Station GTR 480.

Cooper, E. E. (2007), Beaver Ecology on the West Copper River Delta, Alaska., Oregon State University.

Crozier, L. G., and R. W. Zabel (2006), Climate impacts at multiple scales: Evidence for differential population responses in juvenile Chinook salmon, *J. Anim. Ecol.*, *75*(5), 1100–1109, doi:10.1111/j.1365-2656.2006.01130.x.

Crozier, L. G., A. P. Hendry, P. W. Lawson, T. P. Quinn, N. J. Mantua, J. Battin, R. G. Shaw, and R. B. Huey (2008), PERSPECTIVE: Potential responses to climate change in organisms with complex life histories: evolution and plasticity in Pacific salmon, *Evol. Appl.*, *1*(2), 252–270, doi:10.1111/j.1752-4571.2008.00033.x.

DeVries, P. (1997), Riverine salmonid egg burial depths: review of published data and implications for scour studies, *Can. J. Fish. Aquat. Sci.*, *54*(8), 1685–1698, doi:10.1139/cjfas-54-8-1685.

Dingman, S. L. (2002), *Physical Hydrology*, 2nd ed., Waveland Press, Inc, Long Grove, IL.

Dorava, J. M., and J. M. Sokup (1994), Overview of Environmental and Hydrogeologic Conditions at the Merle K. "Mudhole" Smith Airport, Near Cordova Alaska, *U.S. Geol. Surv. Open-File Rep. 94-328*, 1–15.

Everest, F. H., C. E. McLemore, and W. J.F. (1980), An improved tritube cryogenic gravel sampler., *Res. Note PNW-350. USDA For. Serv. Northwest For. Range Exp. Station. Portland, Or .*

Fellman, J. B., S. Nagorski, S. Pyare, A. W. Vermilyea, D. Scott, and E. Hood (2014), Stream temperature response to variable glacier coverage in coastal watersheds of Southeast Alaska, *Hydrol. Process.*, *28*(4), 2062–2073, doi:10.1002/hyp.9742.

Fleming, I. A., and M. R. Gross (1990), Latitudinal Clines : A Trade-Off between Egg Number and Size in Pacific Salmon, *Ecology*, *71*(1), 1–11.

Galloway, W. E. (1976), Copper River Fan-Delta, *J. Sediment. Petrol.*, *46*(3), 726–737.

Gariglio, F. P., D. Tonina, and C. H. Luce (2013), Spatiotemporal variability of hyporheic exchange through a pool-riffle-pool sequence, *Water Resour. Res.*, *49*(11), 7185–7204, doi:10.1002/wrcr.20419.

Goode, J. R., J. M. Buffington, D. Tonina, D. J. Isaak, R. F. Thurow, S. Wenger, D. Nagel, C. Luce, D. Tetzlaff, and C. Soulsby (2013), Potential effects of climate change on streambed scour and risks to salmonid survival in snow-dominated mountain basins, *Hydrol. Process.*, *27*(5), 750–765, doi:10.1002/hyp.9728.

Grantz, A., G. Plafker, and R. Kachadoorian (1964), Alaska's Good Friday earthquake, March 27, 1964: A Preliminary Geologic Evaluation, *U.S. Geol. Surv. Prof. Pap.*, 1–35.

Hall, D. K. (1988), Assessment of Polar Climate Change using Satellite Technology, *Rev. Geophys.*, *26*(1), 26–39, doi:10.1029/RG026i001p00026.

Hannah, D. M., I. A. Malcolm, and C. Bradley (2009), Seasonal hyporheic temperature dynamics over riffle bedforms, *Hydrol. Process.*, *23*, 2178–2194, doi:10.1002/hyp.7256.

Haschenburger, J. K. (1999), A probability model of scour and fill depths in gravel-bed channels, *Water Resour. Res.*, *35*(9), 2857–2869.

Hinch, S., M. C. Healey, R. Em, K. A. Thornson, R. Hourston, M. A. Henderson, and F. Juanes (1995), Potential effects of climate change on marine growth and survival of Fraser River sockeye salmon, *Can. J. Fish. Aquat. Sci.*, *52*, 2651–2659.

Holtby, L. B. (1988), Effects of Logging on Stream Temperatures in Carnation Creek, British, *Can. J. Fish. Aquat. Sci.*, *45*, 502–515, doi:10.1139/f88-060.

Holtby, L. B., and M. C. Healey (1986), Selection for Adult Size in Female Coho Salmon (Oncorhynchus kisutch), *Can. J. Fish. Aquat. Sci.*, *43*, 1946–1959.

Homer, C. G., J. A. Dewitz, L. Yang, S. Jin, P. Danielson, G. Xian, J. Coulston, N. D. Herold, J. D. Wickham, and K. Megown (2015), Completion of the 2011 National Land Cover Database for the conterminous United States-Representing a decade of land cover

change information, *Photogramm. Eng. Remote Sensing*, *81*(5), 345–354.

Jaeger, J. M., C. A. Nittrouer, N. D. Scott, and J. D. Milliman (1998), Sediment accumulation along a glacially impacted mountainous coastline: north-east Gulf of Alaska, *Basin Res.*, *10*(1), 155–173, doi:10.1046/j.1365-2117.1998.00059.x.

Jonsson, N., B. Jonsson, and L. P. Hansen (2005), Does climate during embryonic development influence parr growth and age of seaward migration in Atlantic salmon (Salmo salar)?, *Can. J. Fish. Aquat. Sci.*, *62*(11), 2502–2508, doi:10.1139/F05-154.

Kargel, J. S. et al. (2014), Multispectral image analysis of glaciers and glacier lakes in the Chugach Mountains, Alaska, in *Global Land Ice Measurements from Space*, edited by J. S. Kargel, pp. 297–332, Springer Praxis Books, Berlin Heidelberg.

Kelleher, C., T. Wagener, M. Gooseff, B. McGlynn, K. McGuire, and L. Marshall (2012), Investigating controls on the thermal sensitivity of Pennsylvania streams, *Hydrol. Process.*, *26*(5), 771–785, doi:10.1002/hyp.8186.

Kurylyk, B. L., K. T. B. MacQuarrie, and C. I. Voss (2014), Climate change impacts on the temperature and magnitude of groundwater discharge from shallow, unconfined aquifers, *Water Resour. Res.*, *50*(4), 3253–3274, doi:10.1002/2013WR014588.

Kyle, R. E., and T. P. Brabets (2001), Water Temperature of Streams in the Cook Inlet Basin, Alaska, and Implications of Climate Change, *Wri 01-4109*, 32, doi:Water-Resources Investigations Report 01-4109.

Lamb, M. P., W. E. Dietrich, and J. G. Venditti (2008), Is the critical shields stress for incipient sediment motion dependent on channel-bed slope?, *J. Geophys. Res. Earth Surf.*, *113*(2), 1–20, doi:10.1029/2007JF000831.

Leach, J. A., and R. D. Moore (2010), Above-stream microclimate and stream surface energy exchanges in a wildfire-disturbed riparian zone, *Hydrol. Process.*, *24*(17), 2369–2381, doi:10.1002/hyp.7639.

Leach, J. A., and R. D. Moore (2014), Winter stream temperature in the rain-on-snow zone of the Pacific Northwest: Influences of hillslope runoff and transient snow cover, *Hydrol. Earth Syst. Sci.*, *18*(2), 819–838, doi:10.5194/hess-18-819-2014.

Leppi, J. C., D. J. Rinella, R. R. Wilson, and W. M. Loya (2014), Linking climate change projections for an Alaskan watershed to future coho salmon production, *Glob. Chang. Biol.*, *20*(6), 1808–1820, doi:10.1111/gcb.12492.

Lisi, P. J., D. E. Schindler, K. T. Bentley, and G. R. Pess (2013), Association between geomorphic attributes of watersheds, water temperature, and salmon spawn timing in Alaskan streams, *Geomorphology*, *185*, 78–86, doi:10.1016/j.geomorph.2012.12.013.

Lisi, P. J., D. E. Schindler, T. J. Cline, M. D. Scheuerell, and P. B. Walsh (2015), Watershed geomorphology and snowmelt control stream thermal sensitivity to air temperature, *Geophys. Res. Lett.*, *42*(9), 3380–3388, doi:10.1002/2015GL064083.Received.

Lotspeich, F. B., and B. H. Reid (1980), Tri-tube Freeze-core Procedure for Sampling Stream Gravels, *Progress. Fish-Culturist*, *42*(2), 96–99, doi:10.1577/1548-8659(1980)42.

Luce, C., B. Staab, M. Kramer, S. Wenger, D. Isaak, and C. McConnell (2014), Sensitivity of summer streamtemperatures to climate variability in the Pacific Northwest, *Water Resour. Res.*, *50*, 3428–3443, doi:10.1002/2013WR014329.Received.

Magnusson, J., T. Jonas, and J. W. Kirchner (2012), Temperature dynamics of a proglacial stream: Identifying dominant energy balance components and inferring spatially integrated hydraulic geometry, *Water Resour. Res.*, *48*(6), W06510, doi:10.1029/2011WR011378.

Mann, D. H., A. L. Crowell, T. D. Hamilton, and B. P. . Finney (1998), Holocene Geologic and Climatic History Around The Gulf of Alaska, *Artic Anthropol.*, *35*(1), 112–131.

Mantua, N., I. Tohver, and A. Hamlet (2010), Climate change impacts on streamflow extremes and summertime stream temperature and their possible consequences for freshwater salmon habitat in Washington State, *Clim. Change*, *102*(1-2), 187–223, doi:10.1007/s10584-010-9845-2.

Mantua, N. J., S. R. Hare, Y. Zhang, J. M. Wallace, and R. C. Francis (1997), A Pacific Interdecadal Climate Oscillation with Impacts on Salmon Production, *Bull. Am. Meteorol. Soc.*, *78*(6), 1069–1079, doi:10.1175/1520-0477(1997)078<1069:APICOW>2.0.CO;2.

May, C. L., B. Pryor, T. E. Lisle, and M. Lang (2009), Coupling hydrodynamic modeling and empirical measures of bed mobility to predict the risk of scour and fill of salmon redds in a large regulated river, *Water Resour. Res.*, *45*(5), doi:10.1029/2007WR006498.

Mayer, T. D. (2012), Controls of summer stream temperature in the Pacific Northwest, *J. Hydrol.*, *475*, 323–335, doi:10.1016/j.jhydrol.2012.10.012.

McAfee, S. A., J. Walsh, and T. S. Rupp (2014), Statistically downscaled projections of snow/rain partitioning for Alaska, *Hydrol. Process.*, *28*(12), 3930–3946, doi:10.1002/hyp.9934.

McCullough, D. A. (1999), *A Review and Synthesis of Effects of Alterations to the Water Temperature Regime on Freshwater Life Stages of Salmonids, with Special Reference to Chinook Salmon, Region 10 Water Resources Assessment Report No. 910-R-99-010,* U.S. Environmental Protection Agency.

McCullough, D. A. et al. (2009), Research in Thermal Biology: Burning Questions for Coldwater Stream Fishes, *Rev. Fish. Sci.*, *17*(1), 90–115, doi:10.1080/10641260802590152.

McKean, J., and D. Tonina (2013), Bed stability in unconfined gravel bed mountain streams: With implications for salmon spawning viability in future climates, *J. Geophys. Res. Earth Surf.*, *118*(3), 1227–1240, doi:10.1002/jgrf.20092.

Milliman, J. D., and R. H. Meade (1983), World-Wide Delivery of River Sediment to the Oceans, *J. Geol.*, *91*(1), 1–21.

Milner, A. M., A. L. Robertson, K. a. Monaghan, A. J. Veal, and E. a. Flory (2008), Colonization and development of an Alaskan stream community over 28 years, *Front. Ecol. Environ.*,

6(8), 413–419, doi:10.1890/060149.

Mohseni, O., and H. G. Stefan (1999), Stream temperature/air temperature relationship: A physical interpretation, *J. Hydrol.*, *218*(3-4), 128–141, doi:10.1016/S0022-1694(99)00034-7.

Mohseni, O., H. G. Stefan, and T. R. Erickson (1998), A nonlinear regression model for weekly stream temperatures, *Water Resour. Res.*, *34*(10), 2685–2692.

Mohseni, O., H. G. Stefan, and J. G. Eaton (2003), Global Warming and Potential Changes in Fish Habitat, *Environ. Prot.*, *59*(1995), 389–409, doi:10.1023/A:1024847723344.

Montgomery, D. R., J. M. Buffington, N. P. Peterson, D. Schuett-Hames, and T. P. Quinn (1996), Stream-bed scour, egg burial depths, and the influence of salmonid spawning on bed surface mobility and embryo survival, *Can. J. Fish. Aquat. Sci.*, *53*(5), 1061–1070, doi:10.1139/f96-028.

Montgomery, D. R., E. M. Beamer, G. R. Pess, and T. P. Quinn (1999), Channel type and salmonid spawning distribution and abundance, *Can. J. Fish. Aquat. Sci.*, *56*(3), 377–387, doi:10.1139/f98-181.

Moore, R. D., D. L. Spittlehouse, and A. Story (2005), Riparian microclimate and stream temperature response to forest harvesting: A review, *J. Am. Water Resour. Assoc.*, *7*(4), 813–834, doi:10.1111/j.1752-1688.2005.tb04465.x.

Morrill, J., R. Bales, and M. Conklin (2005), Estimating Stream Temperature from Air Temperature: Implications for Future Water Quality, *J. Environ. Eng.*, *131*(1), 139–146, doi:doi:10.1061/(ASCE)0733-9372(2005)131:1(139).

Mote, P. W. et al. (2003), Preparing for climatic change: The water, salmon, and forests of the Pacific Northwest, *Clim. Change*, *61*(1-2), 45–88, doi:10.1023/A:1026302914358.

Murray, C. B., and J. D. McPhail (1988), Effect of incubation temperature on the development of five species of Pacific salmon (Oncorhynchus) embryos and alevins, *Can. J. Zool.*, *66*(1), 266–273, doi:10.1139/z88-038.

Neal, E. G., M. Todd Walter, and C. Coffeen (2002), Linking the pacific decadal oscillation to seasonal stream discharge patterns in Southeast Alaska, *J. Hydrol.*, *263*(1-4), 188–197, doi:10.1016/S0022-1694(02)00058-6.

Neuheimer, A. B., and C. T. Taggart (2007), The growing degree-day and fish size-at-age: the overlooked metric, *Can. J. Fish. Aquat. Sci.*, *64*(2), 375–385, doi:10.1139/f07-003.

Nichols, J. E., D. M. Peteet, C. M. Moy, I. S. Castaneda, A. McGeachy, and M. Perez (2014), Impacts of climate and vegetation change on carbon accumulation in a south-central Alaskan peatland assessed with novel organic geochemical techniques, *The Holocene*, *24*(9), 1146–1155, doi:10.1177/0959683614540729.

O'Driscoll, M. a., and D. R. DeWalle (2006), Stream–air temperature relations to classify stream–ground water interactions in a karst setting, central Pennsylvania, USA, *J. Hydrol.*, *329*(1-2), 140–153, doi:10.1016/j.jhydrol.2006.02.010.

Pitlick, J., E. R. Mueller, C. Segura, R. Cress, and M. Torizzo (2008), Relation between flow, surface-layer armoring and sediment transport in gravel-bed rivers, *Earth Surf. Process. Landforms*, *33*, 1192–1209, doi:10.1002/esp.1607.

Plafker, G. (1990), Regional vertical tectonic displacement of shorelines in south-central Alaska during and between great earthquakes, *Northwest Sci.*, *64*(5), 250–258.

Poole, G. C., and C. H. Berman (2001), An Ecological Perspective on In-Stream Temperature: Natural Heat Dynamics and Mechanisms of Human-Caused Thermal Degradation, *Environ. Manage.*, *27*(6), 787–802, doi:10.1007/s002670010188.

R Core Team (2015), R: A language and environment for statistical computing, R Foundation for Statistical Computing, Vienna, Austria,

Reimnitz, E. (1966), Late Quaternary History and Sedimentation of the Copper River Delta and Vicinity, Alaska. PhD Dissertation, University of California, San Diego.

Romero-Lankao, P., J. B. Smith, D. J. Davidson, N. S. Diffenbaugh, P. L. Kinney, P. Kirshen, P. Kovacs, and L. V. Ruiz (2014), Chpt 26. North America. In: Climate Change 2014: Impacts, Adaptation, and Vulnerability. Part B: Regional Aspects. Contribution of Working Group II to the Fifth Assessment Report of the Intergovernmental Panel on Climate Change, in *Climate Change 2014: Impacts, Adaptation, and Vulnerability. Part B: Regional Aspects. Contribution of Working Group II to the Fifth Assessment Report of the Intergovernmental Panel on Climate Change*, edited by V. R. Barros et al., pp. 1439–1498, Cambridge University Press, Cambridge, United Kingdom and New York, NY, USA.

Schindler, D. E., D. E. Rogers, M. D. Scheuerell, and C. A. Abrey (2013), Effects of Changing Climate on Zooplankton and Juvenile Sockeye Salmon Growth in Southwestern Alaska, *Ecology*, *86*(1), 198–209.

Shanley, C. S., and D. M. Albert (2014), Climate Change Sensitivity Index for Pacific Salmon Habitat in Southeast Alaska, *PLoS One*, *9*(8), e104799, doi:10.1371/journal.pone.0104799.

Shanley, C. S. et al. (2015), Climate change implications in the northern coastal temperate rainforest of North America, *Clim. Change*, *130*(2), 155–170, doi:10.1007/s10584-015-1355-9.

Shepard, B. G., G. F. Hartman, and W. J. Wilson (1986), Relationships between stream and intra-gravel temperatures in coastal drainage, and some implications for fisheries workers, *Can. J. Fish. Aquat. Sci.*, *43*, 1818–1822.

Sinokrot, B. a., and H. G. Stefan (1993), Stream temperature dynamics: measurements and modeling, *Water Resour. Res.*, *29*(7), 2299–2312, doi:10.1029/93WR00540.

Smith, C. T., R. J. Nelson, C. C. Wood, and B. F. Koop (2001), Glacial biogeography of North American coho salmon (Oncorhynchus kisutch)., *Mol. Ecol.*, *10*, 2775–2785, doi:10.1046/j.1365-294X.2001.t01-1-01405.x.

Tague, C., G. Grant, M. Farrell, J. Choate, and A. Jefferson (2008), Deep groundwater

mediates streamflow response to climate warming in the Oregon Cascades, *Clim. Change*, *86*(1-2), 189–210, doi:10.1007/s10584-007-9294-8.

Tarr, R. S., and L. Martin (1914), *Alaskan Glacier Studies*, The National Geographic Society, Washington.

Thilenius, J. F. (1990a), Plant Succession on Earthquake Uplifted Coastal Wetlands, Copper River Delta, Alaska, *Northwest Sci.*, *64*(5), 259–262.

Thilenius, J. F. (1990b), Woody plant succession on earthquake-uplifted coastal wetlands of the Copper River Delta, Alaska, *For. Ecol. Manage.*, *33/34*, 439–462.

Tuthill, S. J., and W. M. Laird (1966), Geomorphic Effects of the Earthquake of March 27, 1964 In the Martin-Bering Rivers Area, Alaska, *U.S. Geol. Surv. Prof. Pap.*, *543-B*, 1–28.

U.S. Geological Survey (2013), National Hydrography Geodatabase, *Natl. Map Viewer available World Wide Web (http//viewer.nationalmap.gov/viewer/nhd.html?p=nhd), accessed Oct. 2015.*

University of Alaska (2015), Scenarios Network for Alaska and Arctic Planning, *www.snap.uaf.edu*.

Waller, R. M. (1966), Effects on Hydrologic Regimen, in *The Alaska Earthquake March 27, 1964: Effects on Hydrologic Regimen*, vol. 544-A, pp. 1–27.

Waples, R. S., T. Beechie, and G. R. Pess (2009), Evolutionary History, Habitat Disturbance Regimes, and Anthropogenic Changes: What Do These Mean for Resilience of Pacific Salmon Populations ?, *Ecol. Soc.*, *14*(1), 18.

Wawrzyniak, V., H. Piégay, P. Allemand, L. Vaudor, and P. Grandjean (2013), Prediction of water temperature heterogeneity of braided rivers using very high resolution thermal infrared (TIR) images, *Int. J. Remote Sens.*, *34*(13), 4812–4831, doi:10.1080/01431161.2013.782113.

Webb, B. W., and F. Nobilis (1997), Long-term perspective on the nature of the air-water temperature relationship: A case study, *Hydrol. Process.*, *11*(2), 137–147, doi:10.1002/(SICI)1099-1085(199702)11:2<137::AID-HYP405>3.0.CO;2-2.

Webb, B. W., and Y. Zhang (1997), Spatial and seasonal variability in the components of the river heat budget, *Hydrol. Process.*, *11*, 79–101, doi:10.1002/(SICI)1099-1085(199701)11:1<79::AID-HYP404>3.3.CO;2-E.

Wiedmer, M., D. R. Montgomery, A. R. Gillespie, and H. Greenberg (2010), Late Quaternary megafloods from Glacial Lake Atna, Southcentral Alaska, U.S.A., *Quat. Res.*, *73*(3), 413–424, doi:10.1016/j.yqres.2010.02.005.

Wilson, F. H., C. P. Hults, K. A. Labay, and N. Shew (2008), Digital data for the reconnaissance geologic map for Prince William Sound and the Kenai Peninsula, Alaska, *U.S. Geol. Surv. Open-File Rep. 2008-1002*.

Winkler, B. G. R., G. Plafker, R. J. Goldfarb, J. E. Case, and D. L. Peck (1992), *The Alaska Mineral Resource Assessment Program : Background Information to Accompany*

Geologic and Mineral-Resource Maps of the Cordova and Middleton Island Quadrangles , Southern Alaska.

Wobus, C., R. Prucha, D. Albert, C. Woll, M. Loinaz, and R. Jones (2015), Hydrologic Alterations from Climate Change Inform Assessment of Ecological Risk to Pacific Salmon in Bristol Bay, Alaska, *PLoS One*, *10*(12), e0143905, doi:10.1371/journal.pone.0143905.

Zhang, T., S. A. Bowling, and K. Stamnes (1997), Impact of the atmosphere on surface radiative fluxes and snowmelt in the Artic and Subartic, *J. Geophys. Res.*, *102*(D4), 4287–4303, doi:10.1175/1520-0442(1996)009<2110:IOCOSR>2.0.CO;2.

Zimmerman, C. E., and J. E. Finn (2012), A Simple Method for In Situ Monitoring of Water Temperature in Substrates Used by Spawning Salmonids, *J. Fish Wildl. Manag.*, *3*(2), 288–295, doi:10.3996/032012-JFWM-025.

Appendix A- Study Catchment Descriptions

To better understand changing thermal conditions within Pacific salmon spawning habitats, the U.S.D.A. Forest Service (USFS) is monitoring surface (stream) water temperature year-round at 20 salmon spawning locations in 19 catchments across the CRD. Streambed water temperatures are monitored year-round at 15 of these sites in 14 catchments (Figure 7). All study sites are spawning and rearing habitat for Coho Salmon (*O. kisutch*) and 9 of the sites are also utilized by Sockeye Salmon (*O. nerka*).

The study sites are located between 5 and 48 m a.s.l, and are generally located along the slope break between the Chugach piedmont and the deltaic plain where substrate particle sizes are most suitable for spawning (Figure 8). The study catchments vary in total area (61 to 5426 ha), mean elevation (21 to 622 m a.s.l.), and mean slope (1 to 28 degrees) but these catchment characteristics are generally positively correlated (Table 6).

Catchment lake and ice coverage were calculated with NHD data. Maximum lake and ice cover is 15.4% and 12.7% of total catchment area respectively. Land cover statistics were calculated from NLC data. Development is non-existent in most catchments, although gravel roads are present in in some catchments (<2% of total catchment area). The most impacted site (Power Creek) is downstream from a run-of –the-river micro-hydropower facility. The impacts of this facility on stream temperature are assumed to be negligible. Study catchments are generally heavily vegetated with trees, shrubs, and woody wetlands (Table 7). High elevation land surfaces are barren or perennially covered with snow and ice. Much like the CRD as a whole, surficial geology within the study catchments is variable. While marine deposited sediments are common on the CRD, salmon prefer to spawn in the more coarse deposits on the outwash plain and quaternary deposits within the study catchments are generally composed of glaciofluvial drift. Catchments with high percentages of drift are located on glacial outwashes while catchments without abundant drift are located in regions of the piedmont less impacted by the large proximal glaciers.

Appendix A Figures

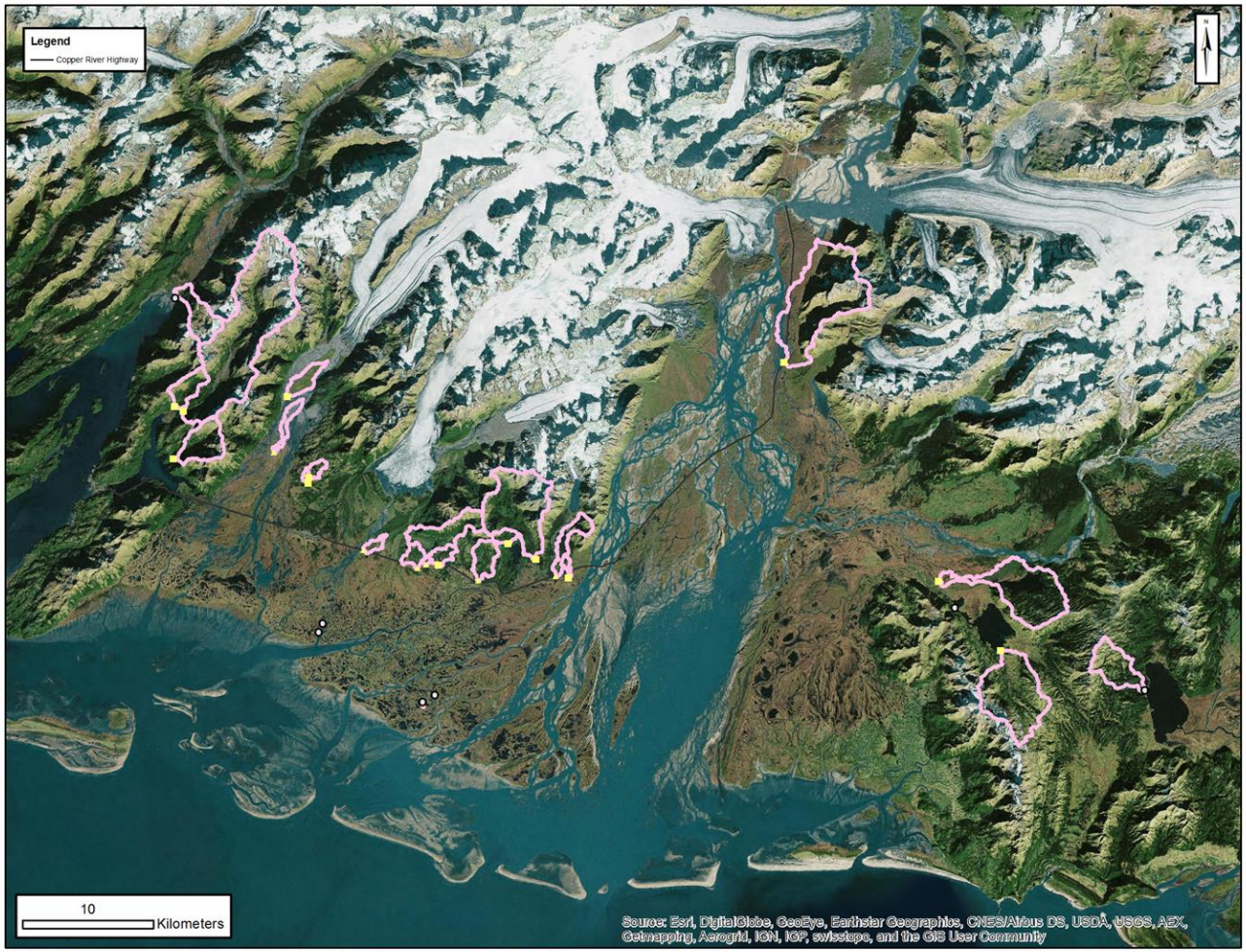

Figure A.1 Study Site locations (yellow points) and catchments (pink polygons) on the Copper River Delta.

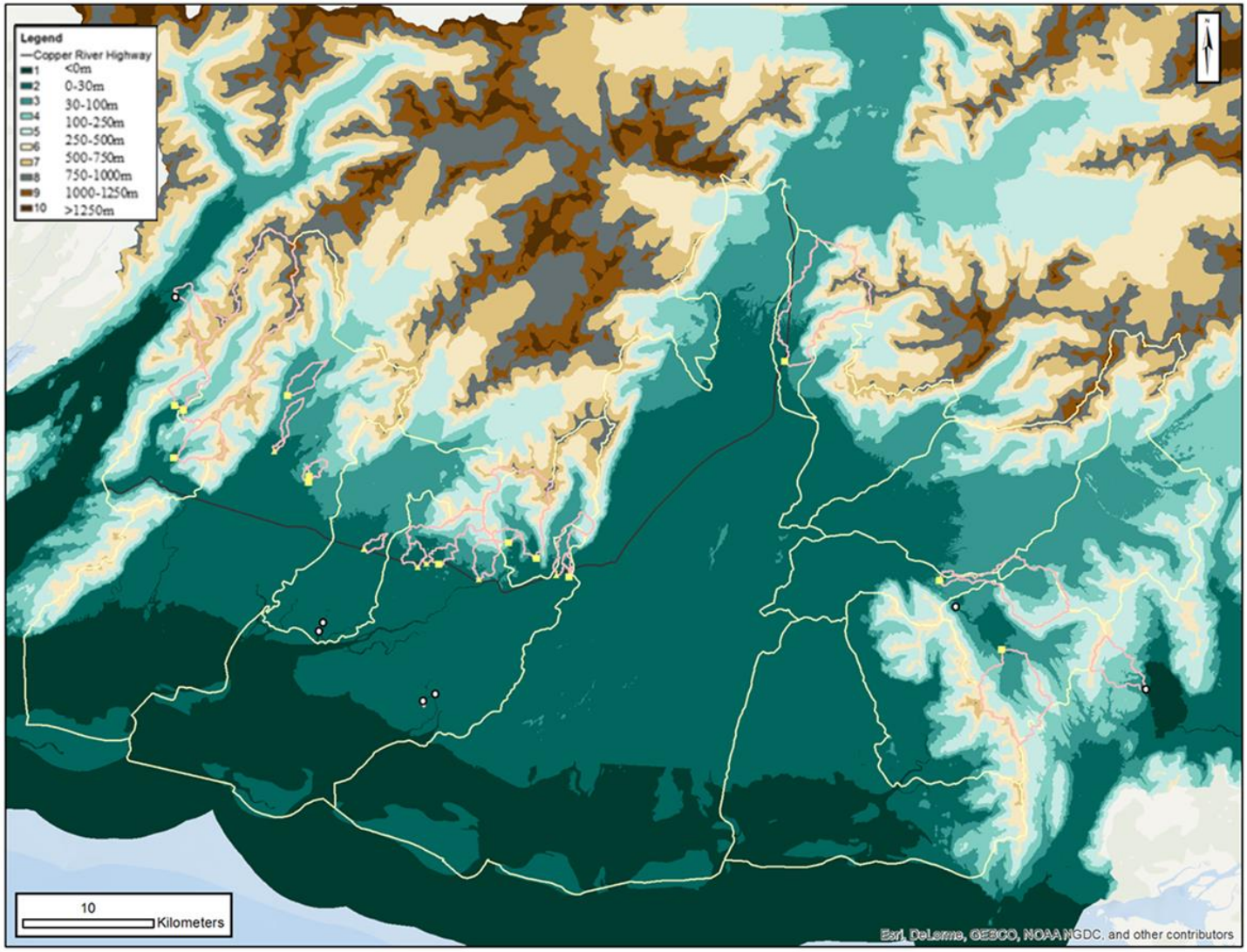

Figure A.2 Elevations within the study catchments calculated from 5m IFSAR DEM data.

Table A.1 Study site location, description, and catchment statistics for all USFS monitored sites (n=19)

Site Information							Catchment Information Zone Statistics						
Type	Name	ID	Latitude (decimal degrees)	Longitude (decimal degrees)	Installation Date	Salmon Sp. Present	Area (ha)	Elevation (m) Min	Elevation (m) Max	Elevation (m) Mean	Slope (deg) Range	Slope (deg) Mean	Slope (deg) SD
Surface & Streambed	Blackhole Creek	Black	60.45	-145.24	21-Sep-2013	Coho	424	8	715	118	69	14	13
	Clear Creek	Clear	60.57	-144.78	19-Oct-2010	Sockeye, coho	3504	19	1329	337	83	23	20
	18 Mile East Fork	ET.Mi	60.46	-145.29	13-Nov-2009	Coho	188	8	83	33	36	7	5
	Middle Arm Eyak Trib.	EyakL	60.56	-145.64	19-Oct-2010	Sockeye, coho	792	5	962	433	76	28	13
	Hatchery Creek	Hatch	60.59	-145.64	19-Sep-2011	Sockeye, coho	454	8	886	308	75	24	13
	Ibeck Trib- High	Ibeck	60.59	-145.47	18-Jun-2011	Coho	336	48	109	74	32	3	2
	Cabin Lake Inlet Ck.	In.Ca	60.53	-145.46	26-Jul-2011	Coho	129	32	214	90	58	11	7
	L. Martin River	LMart	60.40	-144.61	20-Oct-2010	Sockeye, coho	2156	29	547	158	67	11	11
	Martin Lake- Inlet	Marti	60.34	-144.52	20-Oct-2010	Sockeye, coho	2274	27	986	271	76	20	14
	McKinley Lake - Inlet	McKin	60.47	-145.19	13-Nov-2009	Sockeye, coho	155	9	715	224	64	24	12
	Cabin Lake Outlet Ck.	Ot.Ca	60.53	-145.46	26-Jul-2011	Coho	166	20	214	83	58	11	7
	Power Creek	Power	60.59	-145.62	13-Nov-2009	Sockeye, coho	5426	16	1468	622	80	27	14
	Salmon Creek	Salmo	60.45	-145.17	13-Nov-2009	Sockeye, coho	2267	11	1257	388	81	26	15
	25 Mile Creek	TF.Mi	60.44	-145.12	19-Oct-2010	Sockeye, coho	61	11	42	25	18	3	2
Surface only	18 Mile Middle Fork	ET.MF	60.46	-145.31	19-Sep-2012	Coho	955	9	908	212	81	19	16
	18 Mile West Fork	ET.WF	60.46	-145.32	17-Apr-2013	Coho	201	9	115	23	55	5	8
	Ibeck Trib-Low	LoIbe	60.55	-145.50	1-Oct-2012	Coho	202	21	61	40	11	1	1
	24.9 Mile Creek	S.Bag	60.44	-145.14	4-Oct-2012	Coho	418	12	676	160	72	13	13
	Sheridan Trib	Sheri	60.48	-145.40	4-Oct-2012	Coho	110	16	34	21	16	2	2

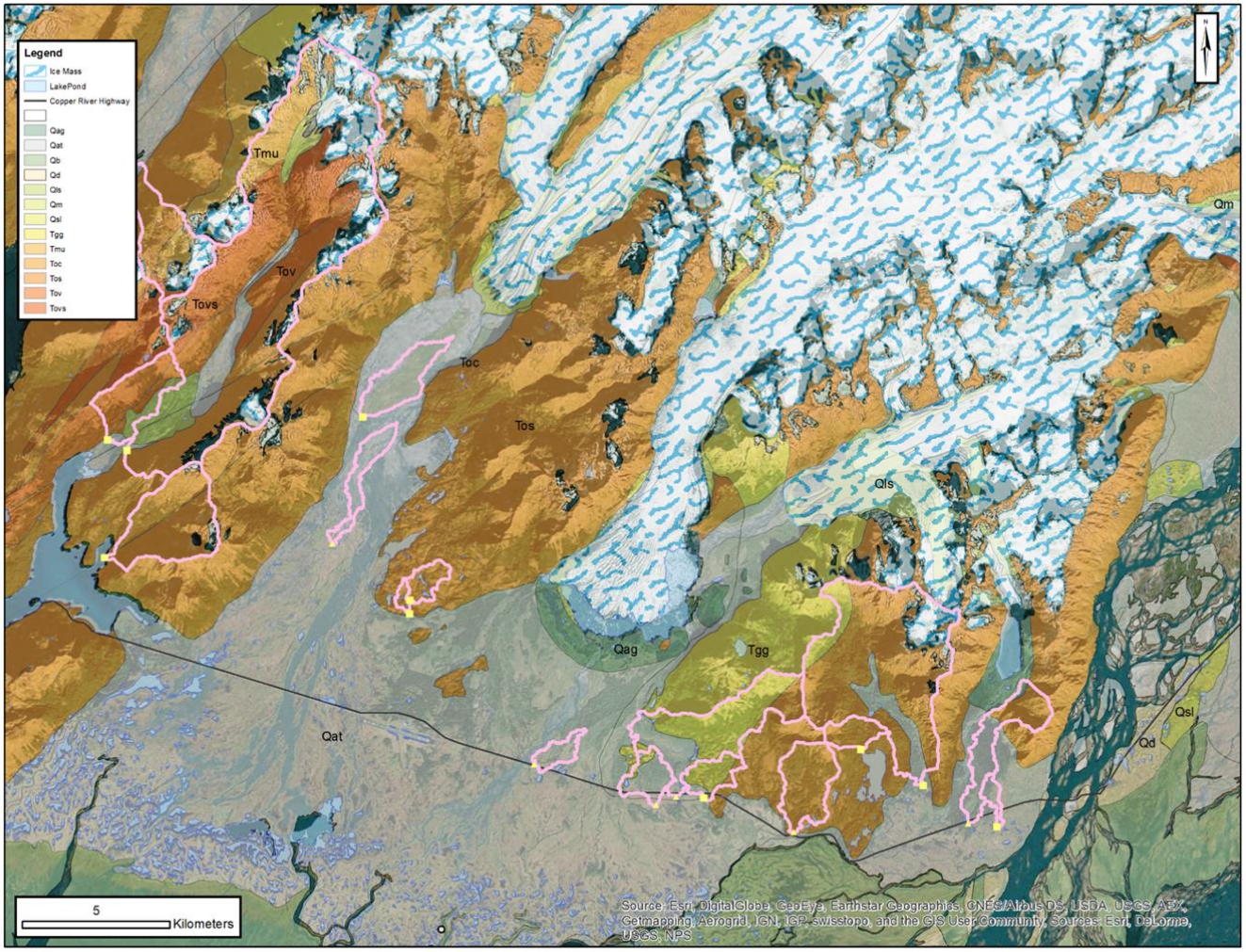

Figure A.3 Surficial geology within the study catchments. Glaciofluvial drift materials denoted with gray, marine sediments denoted with green, sedimentary rocks denoted with orange, granitic intrusions denoted with yellow, and basaltic rocks denoted with red

Table A.2 Land cover statistics calculated with National Hydrography Dataset (NHD), National Land Cover (NLC), and U.S. Geological Survey data for all 19 USFS temperature monitoring sites

Site Information		Percent of Catchment Area													
		NHD Waterbody		NLC Land Cover							USGS Surficial Geology				
											Quaternary Deposits		Tertiary Bedrock		
Type	ID	Lake	Ice	Developed-light	Barren	Forested	Shrub/ Grassland	Herb-acious	Woody Wetland	Emergent Wetland	Till, Marine, Lacustrine	Drift & Colluvium	Intrusive	Sedimentary	Volcanic
Surface & Streambed	Black	0.6	0.0	0.0	0.0	47.1	34.7	0.1	18.0	0.0	0.0	0.0	0.0	98.0	0.0
	Clear	0.3	1.8	0.4	20.2	35.6	35.2	0.7	0.8	0.0	7.7	35.0	0.0	53.3	0.6
	ET.Mi	0.0	0.0	0.5	0.0	56.8	10.1	0.0	30.4	0.4	0.0	13.0	70.6	16.0	0.0
	EyakL	0.0	0.0	0.0	18.2	42.5	34.2	0.1	0.0	0.0	0.0	0.0	0.0	95.4	0.0
	Hatch	0.0	0.0	0.8	0.7	51.2	45.5	1.2	0.0	0.0	0.0	23.0	0.0	0.0	77.2
	Ibeck	0.0	0.0	0.0	12.7	3.6	60.1	7.0	16.4	0.0	0.0	100.0	0.0	0.0	0.0
	In.Ca	7.8	0.0	0.0	0.0	45.1	40.0	0.0	13.5	0.0	0.0	0.0	0.0	98.9	0.0
	LMart	15.4	0.0	0.0	0.6	46.8	20.4	1.1	16.1	0.0	0.0	24.6	0.0	60.1	0.0
	Marti	1.3	0.0	0.0	8.8	28.3	49.7	0.9	8.4	0.7	8.0	21.0	0.0	46.2	21.4
	McKin	0.0	0.0	0.0	1.3	74.6	23.2	0.3	0.6	0.0	0.0	0.0	0.0	100.0	0.0
	Ot.Ca	6.7	0.0	0.0	0.0	49.0	37.6	0.0	11.5	0.0	0.0	0.0	0.0	99.7	0.0
	Power	0.0	12.7	0.2	33.2	23.1	25.7	0.4	0.3	0.0	2.0	12.0	7.3	16.8	38.0
	Salmo	0.1	7.2	0.0	15.2	45.6	31.2	0.2	0.3	0.0	0.0	9.8	7.2	71.6	0.0
	TF.Mi	0.0	0.0	0.9	0.0	43.5	16.7	0.3	38.5	0.0	0.0	100.0	0.0	0.0	0.0
Surface only	ET.MF	0.5	0.0	0.1	0.4	46.4	35.9	0.3	15.4	0.0	0.0	25.2	62.6	12.1	0.0
	ET.WF	1.2	0.0	2.2	0.0	30.9	15.4	0.0	50.7	0.0	0.0	87.2	14.9	0.0	0.0
	LoIbe	0.0	0.0	0.0	86.1	0.0	0.2	0.0	12.0	0.2	0.0	100.0	0.0	0.0	0.0
	S.Bag	0.0	0.0	1.5	1.3	69.7	22.2	1.6	3.8	0.0	4.8	54.5	0.0	41.3	0.0
	Sheri	0.0	0.0	1.2	0.0	2.0	0.1	0.0	96.1	0.2	0.0	100.0	0.0	0.0	0.0

.

Appendix B- Water Temperature Sampling Methods

All data loggers were manufactured by the Onset Computer Corporation and have manufacturer reported ± 0.2 °C sensor accuracy. Surface water temperature is recorded with a HOBO Pro v2 data logger housed in a 15 cm long section of 4.1 cm internal diameter galvanized steel pipe. The housing protects the sensor from physical damage and direct solar radiation. The data loggers sit at the bottom of the water column, on the streambed surface and are cabled to fixed anchors to minimize loss. Data logger placement is somewhat subjective, but the sensors are generally placed near the bank in 50 to 80 cm deep water. Some of the study sites have high width-to-depth ratio and the water is shallow throughout the study reach (<100 m in length). In these situations, the data logger is placed as deeply as possible, always more than 25 cm deep. The surface water at each study reach is assumed to be well-mixed vertically, laterally, and longitudinally by turbulent forces. If the logger is persistently buried in sediments, it is relocated within the immediate study reach; however, most loggers have stayed in the same location throughout the monitoring period.

Streambed water temperature is measured 50-70 cm into the substrate using HOBO Pro v2 and TidbiT v2 data loggers. The Pro v2 loggers are suspended near the bottom of a 101 cm long piezometer constructed from 4.1 cm internal diameter galvanized steel pipe. The data logger sits in a 10 cm long ported section (screen) above a tapered 10 cm driving point that also serves as a sediment trap. A foam baffle minimizes vertical water flux within the piezometer. Piezometers are capped with PVC to prevent rainwater from entering and are secured with a cable and earth anchor to minimize loss. TidbiT v2 data loggers are installed directly into the substrate using a custom-made portable percussion drilling device. The device consists of a heavy 4.3 cm inside diameter steel pipe with a removeable steel center rod and strike plate. To install a data logger, the center rod is placed into the pipe and the strike plate is placed on top. A sledge hammer is used to drive the pipe and center rod 50 cm into the substrate. The center rod is removed and the temperature logger is attached to a stainless steel cable and is inserted and held at the bottom of the hole as the

pipe is removed from the gravel. The cable is attached to an earth anchor to minimize loss during the event of streambed scour. Each site has 2 to 4 streambed loggers using one or both deployment method. Initial logger placement is subjective. Generally, two streambed data loggers are installed at each site, one near the bank and one near mid channel. All data loggers record hourly. Each site is downloaded 1-2 times each year. If the data logger can be retrieved, it is redeployed in the same location throughout the study period. The depth of each data logger is measured at each download.

Data loggers are replaced every 3-5 years as recommended by the manufacturer. The data are reviewed for errors in Microsoft Excel using the USFS Natural Resource Manager add-in tool and erroneous hourly values are removed. Data are stored in the USFS Aquatic Surveys ("AqS") database. Data from surface loggers buried in sediment are excluded.